ΕΘΝΙΚΟ ΜΕΤΣΟΒΙΟ ΠΟΛΥΤΕΧΝΕΙΟ

ΣΧΟΛΗ ΧΗΜΙΚΩΝ ΜΗΧΑΝΙΚΩΝ

ΔΠΜΣ ΥΠΟΛΟΓΙΣΤΙΚΗ ΜΗΧΑΝΙΚΗ

ΜΕΤΑΠΤΥΧΙΑΚΗ ΕΡΓΑΣΙΑ

Σχολή Πολιτικών Μηχανικών

Εργαστήριο Στατικής και Αντισεισμικών Ερευνών

ROCKING RESPONSE OF RIGID BLOCKS

ΕΚΠΟΝΗΣΗ: ΑΡΙΘΜΟΣ ΜΗΤΡΩΟΥ: chm11004

ΕΠΙΒΛΕΠΩΝ ΚΑΘΗΓΗΤΗΣ: ΠΑΠΑΔΟΠΟΥΛΟΣ ΒΗΣΣΑΡΙΩΝ

ΑΘΗΝΑ 2018

ACKNOWLEDGMENTS

Thanks to my supervisors Vasileios Merevis and prof Vissarion Papadopoulos

Contents

1.1 Contact Surfaces

1.1.1 Finite Element Formulation of Contact Problems

In Body Interactions, contact elements cannot penetrate into the target surface while the target elements can penetrate into the contact elements. Target x is projected onto the piecewise linear segments of the master segment with xc (x = xc) as the projected point. If the measured gap g= $(x-x_1)e_n \geq 0$ there is no contact.

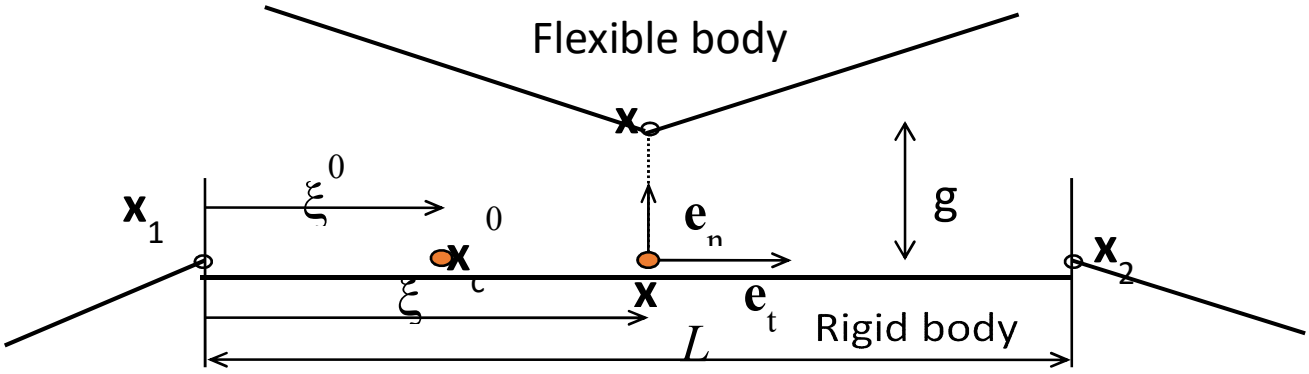

Figure 1: Node projection

$$\mathbf{e}_t = \frac{\mathbf{x}_2 - \mathbf{x}_1}{L}, \qquad \mathbf{e}_n = \mathbf{e}_3 \times \mathbf{e}_t \tag{1}$$

$$\xi_c = \frac{1}{L}(\mathbf{x} - \mathbf{x}_1)^T \mathbf{e}_t$$

(2)

$$g_n = (\mathbf{x} - \mathbf{x}_1)^T \mathbf{e}_n \geq 0$$ is the gap function (3)

$$P = \frac{1}{2}\sum_{I=1}^{NC}\left(\omega \langle g \rangle_-^2\right)_I$$

is the penalty function (4)

Virtual work done by contact force through normal virtual displacement:

$$b_N(\mathbf{u},\bar{\mathbf{u}}) = \sum_{I=1}^{NC}\left(\omega\langle g_n\rangle_- \bar{\mathbf{d}}^T\mathbf{e}_n\right)_I = \{\bar{\mathbf{d}}\}^T\{\mathbf{f}^c\} \tag{5}$$

where (ωgn) is contact force

Linearization

$$\Delta\langle g_n\rangle_- = H(-g_n)\mathbf{e}_n^T\Delta\mathbf{u} = H(-g_n)\mathbf{e}_n^T\Delta\mathbf{d} \tag{6}$$

$$b_N^*(\mathbf{u};\Delta\mathbf{u},\bar{\mathbf{u}}) = \sum_{I=1}^{NC}\left(\omega H(-g_n)\bar{\mathbf{d}}^T\mathbf{e}_n\mathbf{e}_n^T\Delta\mathbf{d}\right)_I = \{\bar{\mathbf{d}}\}^T\sum_{I=1}^{NC}\left(\omega H(-g_n)\mathbf{e}_n\mathbf{e}_n^T\right)_I\{\Delta\mathbf{d}\}$$
$$= \{\bar{\mathbf{d}}\}^T[\mathbf{K}_c]\{\Delta\mathbf{d}\} \tag{7}$$

Global finite element matrix equation for increment

$$\{\bar{\mathbf{d}}\}^T[\mathbf{K}_T + \mathbf{K}_c]\{\Delta\mathbf{d}\} = \{\bar{\mathbf{d}}\}^T\{\mathbf{f}^{ext} - \mathbf{f}^{int} - \mathbf{f}^c\} \tag{9}$$

A similar approach can be used for flexible-flexible body contact.

Frictional slip

$$g_t = l^0(\xi_c - \xi_c^0) \tag{10}$$

Friction force and tangent stiffness (stick condition)

$$\mathbf{f}_t^c = -\omega_t g_t \mathbf{e}_t \tag{11}$$
$$\mathbf{k}_t^c = \omega_t \mathbf{e}_t\mathbf{e}_t^T$$

Friction force and tangent stiffness (slip condition)

$$\mathbf{f}_t^c = \mu\omega_n\, sgn(g_t)g_n\mathbf{e}_t, \qquad if\ \left|\omega_t g_t\right| \geq \left|\mu\omega_n g_n\right| \tag{12}$$
$$\mathbf{k}_t^c = \mu\omega_n\, sgn(g_t)\mathbf{e}_t\mathbf{e}_n^T$$

1.1.2 Contact Analysis & Modelling

Contact condition is a rough boundary nonlinearity due to discontinuous contact force and unknown contact region. Both force and displacement on the contact boundary are unknown. Contact search is necessary at each iteration.

The choice of which surface is designated contact or target can cause a different amount of penetration and thus affect the solution accuracy. For rigid-to-flexible contact, the designation is obvious: the target surface is always the rigid surface and the contact surface is always the deformable surface. For flexible-to-flexible contact, the following guidelines are considered:

- If a convex surface is expected to come into contact with a flat or concave surface, the flat/concave surface should be the target surface.
- If one surface has a fine surface mesh and, in comparison, the other has a coarse mesh, the fine mesh should be the contact surface and the coarse mesh should be the target surface.
- If one surface is stiffer than the other, the softer surface should be the contact surface and the stiffer surface should be the target surface.
- If higher-order elements underlay one of the external surfaces and lower-order elements underlay the other surface, the surface with the underlying higher-order elements should be the contact surface and the other surface should be the target. However, for 3-D node-to-surface contact, the lower-order elements should be the contact surface. The higher-order elements should be the target surface.
- If one surface is markedly larger than the other surface, such as in the instance where one surface surrounds the other surface, the larger surface should be the target surface.

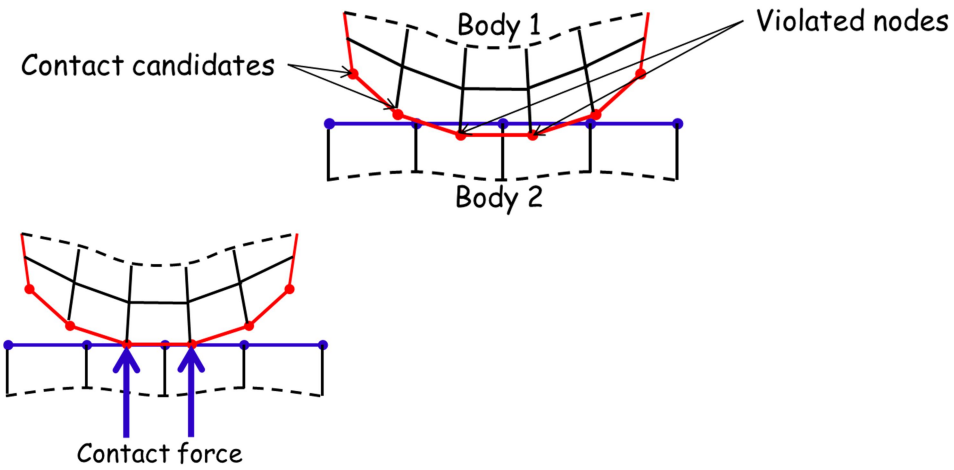

Figure 2: Contact Force

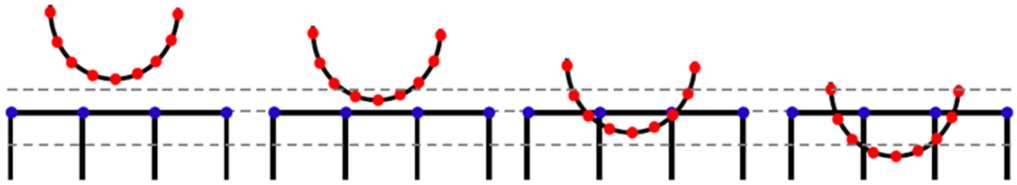

Figure 3:Body Interactions

Contact elements are constrained against penetrating the target surface. However, target elements can penetrate through the contact surface. For the contacting pairs, penetration needs to be corrected by applying the contact force. The higher the penetration the bigger the contact force needs to be applied. Contact is detected by the trajectory as shown in figure 1. The trajectory of nodes and faces included in frictional or frictionless contact are tracked during the computation cycle. If the trajectory of a node and a face intersects during the cycle a contact event is detected. The trajectory contact algorithm is the default and recommended option in most cases for contact in Explicit Dynamics analyses. Contacting nodes/faces can be initially separated or coincident at the start of the analysis. Trajectory based contact detection does not impose any constraint on the analysis time step and therefore often provides the most efficient solution. If contact is detected, a local penalty force is calculated to push the node involved in the contact event back to the face. Equal and opposite forces are calculated on the nodes of the face in order to conserve linear and angular momentum.

Penalty method or Lagrange multiplier method can be used to represent the contact constraint. Penalty-based contact force depends on the material stiffness of the two bodies. The higher the penetration the higher the contact force. The penalty parameter Kn method allows a small penetration ($g < 0$) but easy to implement.. Large contact stiffness reduces penetration, but can cause problem in convergence. The Lagrange multiplier method can impose contact condition exactly as the contact force is calculated from penetration. The additional conditions (2) & (3) need to be satisfied. The stiffness matrix (4) is a positive semi definite and the contact force is applied in the normal direction to the master segment. Lagrange multiplier method can impose contact condition accurately, but requires additional variables and the matrix become positive semi-definite

$$F_C = K_n \langle -g \rangle \qquad K_n = SF \cdot E \qquad SF \approx 1.0 \tag{13}$$

$$F_C \langle -g \rangle = 0 \tag{14}$$

$$\begin{aligned} \langle -g \rangle &= 0 \quad F_C > 0 \quad \text{contact} \\ \langle -g \rangle &> 0 \quad F_C = 0 \quad \text{no contact} \end{aligned} \tag{15}$$

$$\begin{bmatrix} K & A \\ A^T & 0 \end{bmatrix} \begin{Bmatrix} d \\ F_C \end{Bmatrix} = \begin{Bmatrix} F \\ 0 \end{Bmatrix} \tag{16}$$

$$\mathbf{F} = \sum_{i=1}^{N_p} p_{ci} = \sum_{i=1}^{N_q} q_{ci}$$

(17)

$$[K]\{d\} = \{F\} - \{F_C(d)\} \quad (18)$$

$$[K + K_C]\{\Delta d\} = \{F\} - \{F_C(d)\} - [K]\{d\} \quad (19)$$

$$[K_C] = \left[\frac{\partial F_C}{\partial d}\right] \quad (20)$$

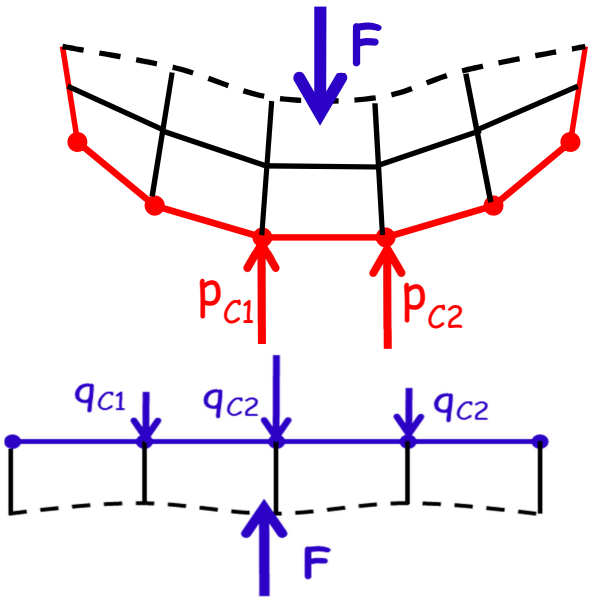

Figure 4: Forces acting in contact elements

Friction force is produced by a relative motion in the interface and is applied to the parallel direction. It depends on load history in comparison with contact force which is independent of load path.

$$F_f < \mu F_C \quad \text{Stick}$$
$$= \mu F_C \quad \text{Slip} \quad (21)$$

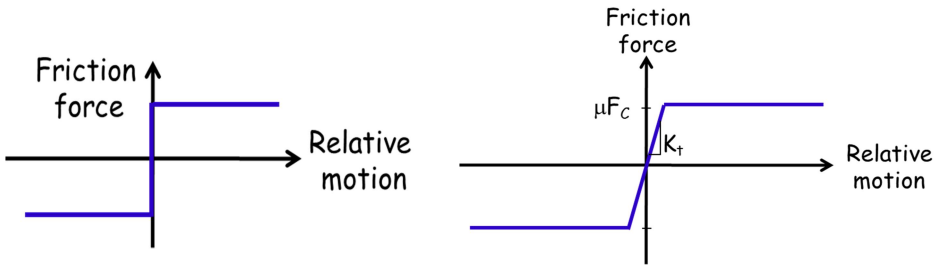

Figure 5: Coulomb and regularised friction force

$$F_f = K_t s \quad \text{Stick}$$
$$= \mu F_C \quad \text{Slip} \qquad (22)$$

In general, the tangential or sliding behavior of two contacting bodies may be frictionless or involve friction. Coulomb friction force is indeterminate when two bodies are stick so the regularised friction model is used instead. In reality, there is a small elastic deformation before slip. Tangential stiffness K_t determines the stick case and is related to shear strength of the material. Contact surface with a large Kt behaves like a rigid body. Contact surface with small Kt have elastic stick condition too long.

Time Step Controls offers an additional layer of convergence enhancement that allows bisections and adjustments to time step size based on changes in contact behavior. By default, changes in contact behavior do not influence automatic time stepping. This is appropriate for most analyses when bisections triggered by contact status change might be a detriment to overall run time efficiency. Contact behavior is reviewed at the end of each substep to determine whether excessive penetration or drastic changes in contact status have occurred. If so, the current sub step is re-evaluated using a “bisected” time increment (reduced by half).

1.2 Earthquake pulses

We have to conclude to a displacement equation through an acceleration one. The idea is to integrate twice the equation which described the acceleration during the 1995 Aigion, Greece earthquake:

$$\ddot{u_g} = a_p \left(1 - 2\frac{\pi^2 t^2}{T_p^2}\right) e^{-\frac{\frac{1}{2}2\pi^2 t^2}{T_p^2}}$$

$$\dot{u_g} = \int a_p \left(1 - 2\frac{\pi^2 t^2}{T_p^2}\right) e^{-\frac{\frac{1}{2}2\pi^2 t^2}{T_p^2}} dt = a\, t\, e^{-\frac{\pi^2 t^2}{T_p^2}} + c_1$$

$$u_g = \int \left(a\, t\, e^{-\frac{\pi^2 t^2}{T_p^2}} + c_1\right) dt = -\frac{a_p T_p^2 e^{-\frac{(\pi^2 t^2)}{T_p^2}}}{2\,\pi^2} + c_1 t + c_2$$

Initial conditions for t=0:

$$\dot{u_g} = 0 \rightarrow c_1 = 0$$

$$u_g = 0 \rightarrow c_2 = \frac{a_p T_p^2}{2\,\pi^2} \qquad (23)$$

Finally we conclude to the displacement equation of the aforementioned earthquake:

$$u_g(t) = \frac{a_p T_p^2}{2\,\pi^2} + \frac{a_p T_p^2 e^{-\frac{(\pi^2 t^2)}{T_p^2}}}{2\,\pi^2} \qquad (24)$$

To better understand the above equations we decided to graphical imprint them. Starting with the acceleration function and assuming acceleration amplitude $\mathbf{a_p = 0.5\ g = 5m/s^2}$ and $\mathbf{T_p = 1\ sec}$ we conclude to:

$$\ddot{u_g} = 5\left(1 - 2\frac{\pi^2 t^2}{1}\right) e^{-\frac{\frac{1}{2}2\pi^2 t^2}{1}} \qquad (25)$$

Of which the graphical representation **for t=-1 to t=1** (the domain equals two periods) is:

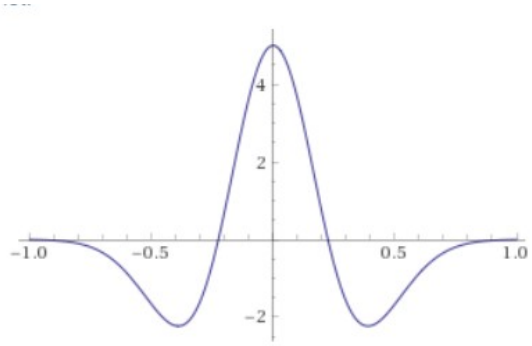

Figure 6: Aigion peak acceleration

Because the time domain in which we have calculated all values of acceleration it does not relate to an actual time domain we have to move the function in positive half space by Tp. In order to achieve this we need to assume the replace t for t-Tp. Which in our case is t-1 so we get for t=0 to t=2 (again the domain equals two periods):

$$\ddot{u_g} = 5\left(1 - 2\frac{\pi^2 (t-1)^2}{1}\right) e^{-\frac{\frac{1}{2}2\pi^2 (t-1)^2}{1}} \qquad (26)$$

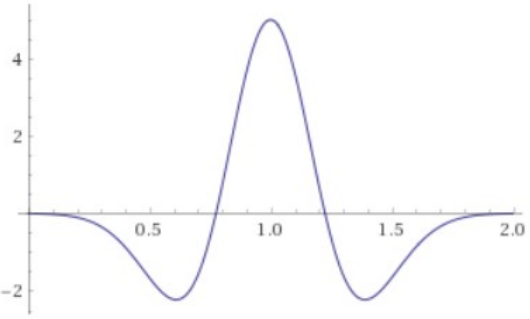

Figure 7 : Acceleration peak for T=1s and a=0.5g

Or a more generalized approach based on the initial acceleration function could be:

$$\ddot{u_g} = a_p \left(1 - 2\frac{\pi^2(t-T_p)^2}{T_p^2}\right) e^{-\frac{\frac{1}{2}2\pi^2(t-T_p)^2}{T_p^2}} \qquad (27)$$

The same procedure follows for the displacement function. Initially assuming the same values and time domain as in our first approach regarding the acceleration equation (**a_p = 0.5 g = 5m/s^2** and **T_p = 1 sec for t=-1 to t=1**) we get:

$$u_g(t) = \frac{5}{2\,\pi^2} + \frac{5e^{-\frac{(\pi^2 t^2)}{1}}}{2\,\pi^2} \qquad (28)$$

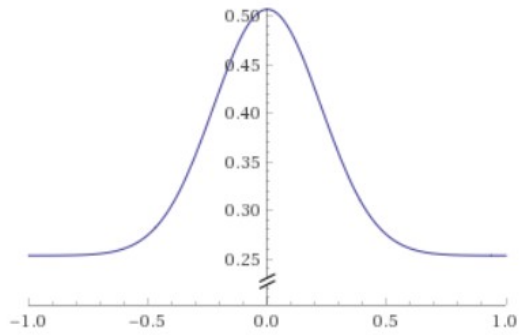

Figure 8 : Displacement for Aigion earthquake

In the same way we need to transfer the whole function into a more physical and realistic time domain. So we need to move it by T_p which in the specified case is **1 sec for the time domain t=0 to t=2:**

$$u_g(t) = \frac{5}{2\,\pi^2} + \frac{5e^{-\frac{(\pi^2(t-1)^2)}{1}}}{2\,\pi^2} \qquad (29)$$

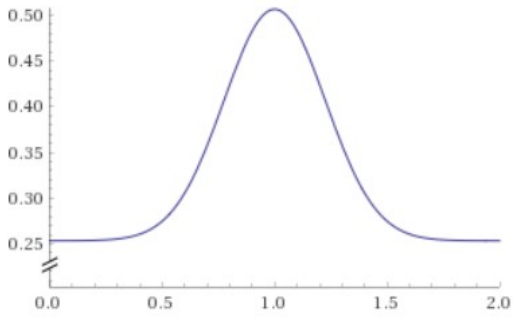

Figure 9 : Displacement for Aigion earthquake for T=1sec and a=0.5g

And of course a more generalized approach for a variety of a_p and T_p values is:

$$u_g(t) = \frac{a_p T_p^2}{2\,\pi^2} + \frac{a_p T_p^2 e^{-\frac{\left(\pi^2 (t-T_p)^2\right)}{T_p^2}}}{2\,\pi^2} \qquad (30)$$

For time domains **t=0 to t=2*T_p.**

Where for the same time domain (**t=0 to t=2**) and **T_p=1sec** we can graphically imprint all the history when we study various a_p values:

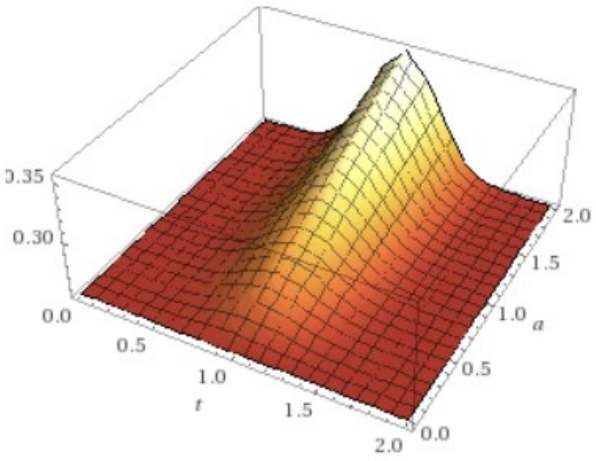

Figure 10 : Graphical representation of acceleration for given period

Or the other way around when we keep **a_p=5m/s^2** as a constant value and vary T_p :

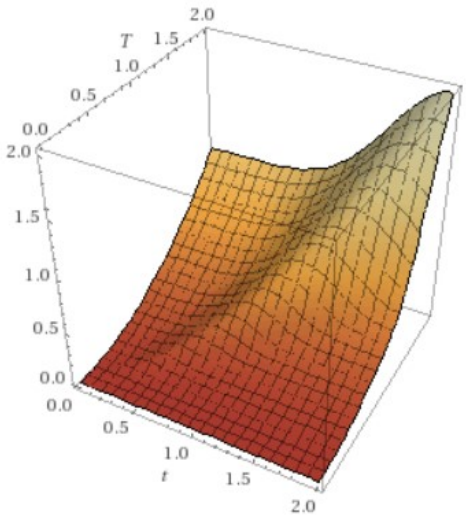

Figure 11 : Graphical representation of period for given acceleration

1.3 Computer simulation for different values of acceleration and time period

1.3.1 Computer Models

In Ansys, two models were considered, a simple free standing column shown in figure 6 and one with base isolators as shown in figure 7. The dimension of the column is 2m high and 0.5 m wide while the base is 1.5m long and 0,5m high. Concrete is set as the material of the column and base. In the meantime,elastomer is used to model the base isolators. The contact surface between the column and the base were simulated by 2D contact and target elements respectively. The model was meshed using quadrilateral elements.

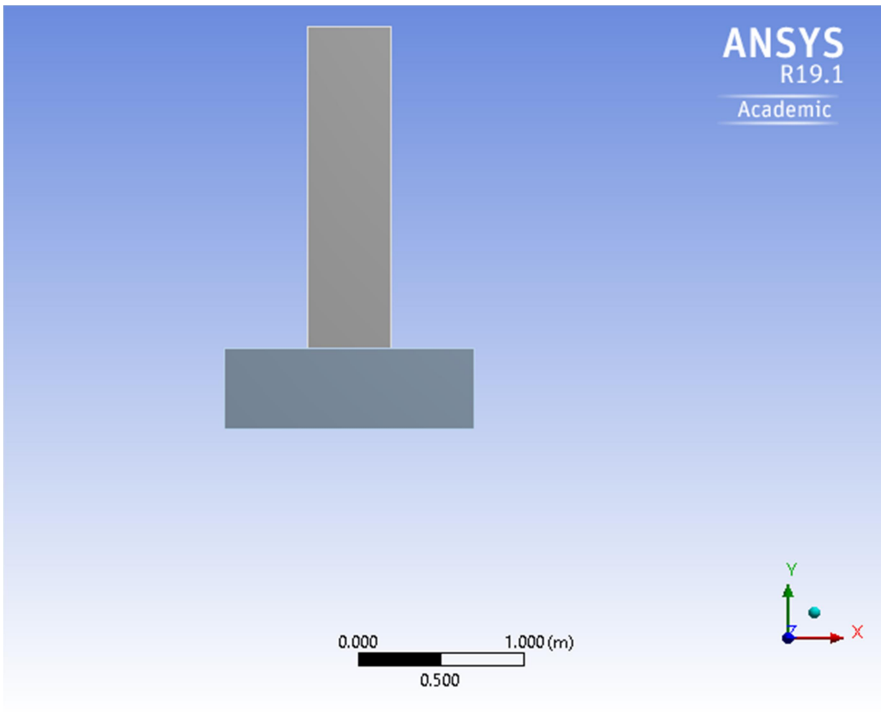

Figure 12: Simple column model

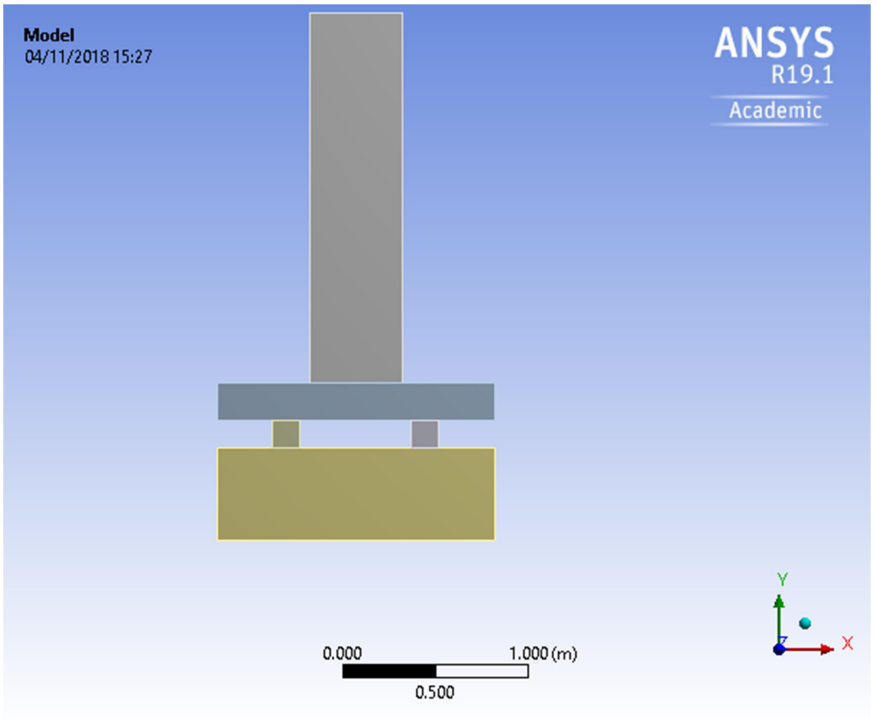

Figure 13 : Base isolated model

The contact surface between the column and the base were simulated by 2D contact and target elements respectively. The model was meshed using quadrilateral elements.

In the base isolated model, the column and the concrete slab consist the upper structure and the contact surface is set between the slab and the base isolators. The base isolators are meshed using 2D target elements while the slab is meshed using 2D contact elements. (figure 8)

The explicit dynamics solver is used to analyze the behavior of both structures as the overall time is small.

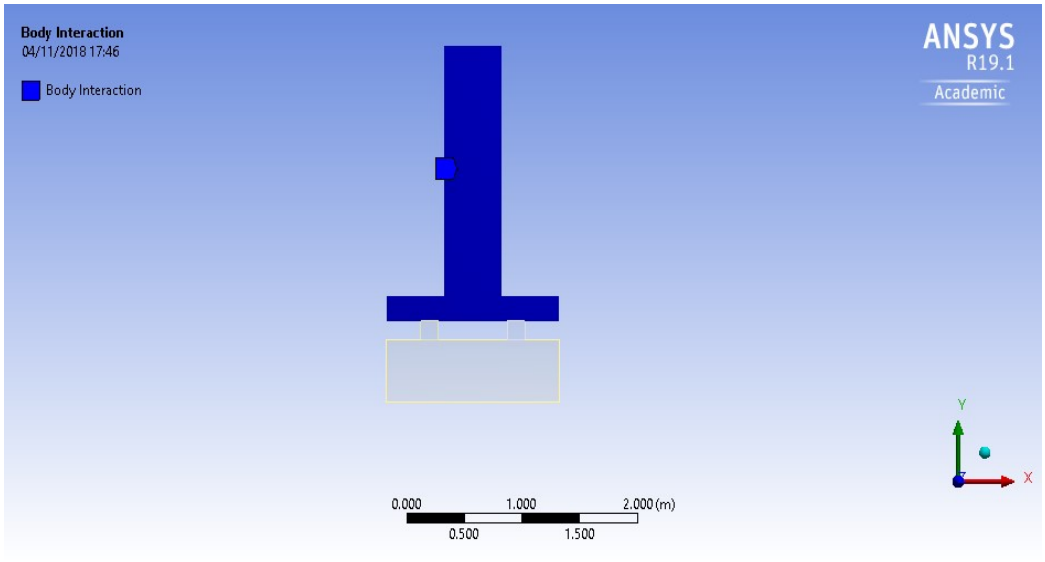

Figure 14: Body interaction in base isolated model

The partial differential equations to be solved in an Explicit Dynamics analysis express the conservation of mass, momentum, and energy in Lagrangian coordinates. These, together with a material model and a set of initial and boundary conditions, define the complete solution of the problem.

For the Lagrangian formulations currently available in the Ansys Explicit Dynamics system, the mesh moves and distorts with the material it models and conservation of mass is automatically satisfied. The density at any time can be determined from the current volume of the zone and its initial mass. The partial differential equations that express the conservation of momentum relate the acceleration to the stress tensor σij.

These equations are solved explicitly for each element in the model, based on input values at the end of the previous time step. Small time increments are used to ensure stability and accuracy of the solution. Note that in Explicit Dynamics we do not seek any form of equilibrium; we simply take results from the previous time point to predict results at the next time point. There is no requirement for iteration.

In a well-posed Explicit Dynamics simulation, mass, momentum, and energy should be conserved. Only mass and momentum conservation is enforced. Energy is accumulated over time and conservation is monitored during the solution. Feedback on the quality of the solution is provided via summaries of momentum and energy conservation (as opposed to convergent tolerances in implicit transient dynamics).

The Explicit Dynamic solver uses a central difference time integration scheme (often referred to as the Leapfrog method).

After forces have been computed at the nodes of the mesh (resulting from internal stress, contact, or boundary conditions), the nodal accelerations are derived by equating acceleration to force divided by mass.

The advantages of using this method for time integration for nonlinear problems are:

- The equations become uncoupled and can be solved directly (explicitly). There is no requirement for iteration during time integration.
- No convergence checks are needed because the equations are uncoupled.
- No inversion of the stiffness matrix is required. All nonlinearities (including contact) are included in the internal force vector.

To ensure stability and accuracy of the solution, the size of the timestep used in Explicit time integration is limited by the CFL (Courant-Friedrichs-Lewy [Courant]) condition. This condition implies that the timestep be limited such that a disturbance (stress wave) cannot travel farther than the smallest characteristic element dimension in the mesh, in a single timestep.

The maximum timestep that can be used in Explicit time integration is inversely proportional to the soundspeed of the material, hence directionally proportional to the square root of the mass of material in an element. By artificially increasing the mass of an element, one can increase the maximum allowable stability timestep, and reduce the number of time increments required to complete a solution. When mass scaling is applied in an Explicit Dynamics system, it is applied only to those elements which have a stability timestep less than a specified value. If the model contains a relatively small number of small elements, this can be a useful mechanism for reducing the number of time steps required to complete an Explicit simulation.

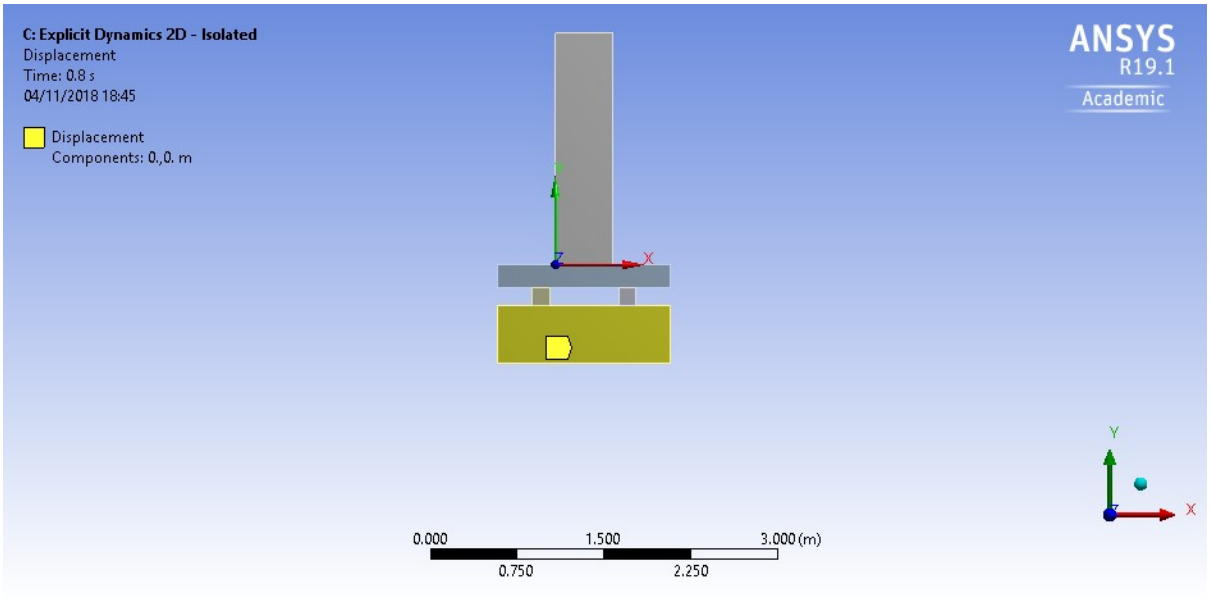

Figure 15: Body interaction in base isolated model

The displacement equation (30) from Aigion Earthquake was introduced at the base of each model for different values of period and acceleration amplitude. The displacement at upper and lower edge was measured (figures 16 and 17), in order to calculate the angle of rotation and check for overturning.

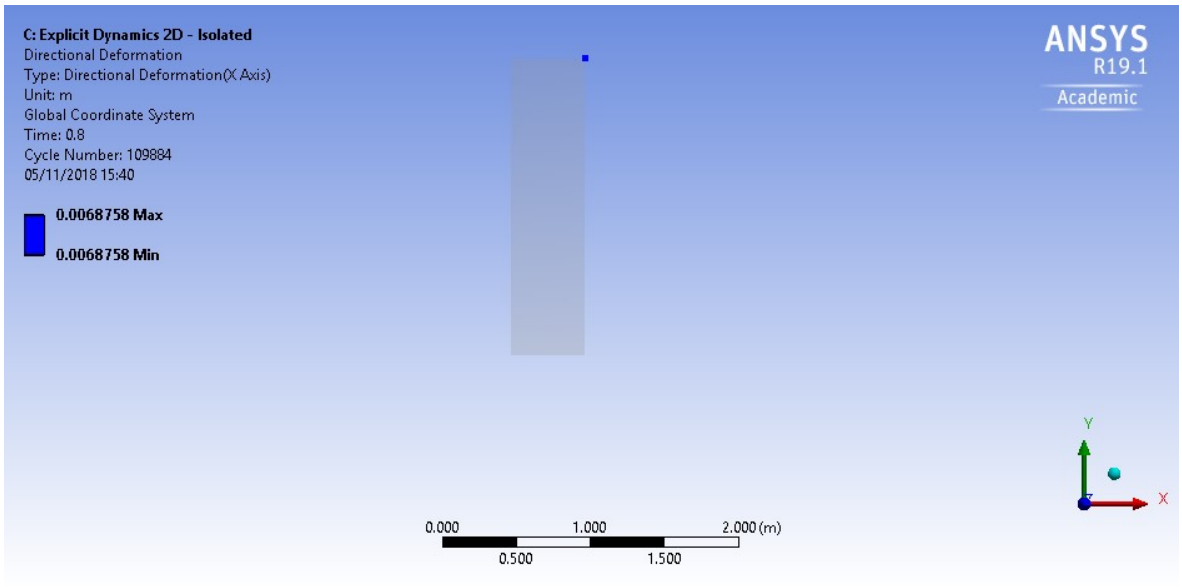

Figure 16: Input displacement for T=0.4s and a=0.3g

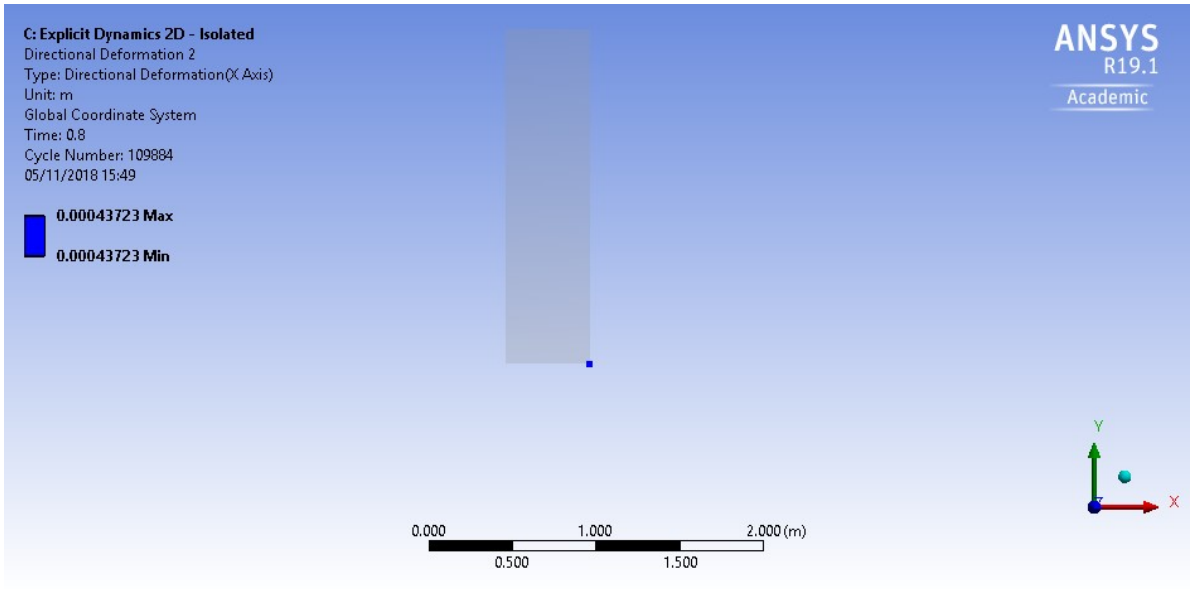

Figure 17: Upper edge nodal directional deformation

1.3.2 Simulation for T= 0.4s and a= 0.3g, 0.5g , 0.8g and 1.2g

Time	Displacement a=0.3g	Displacement a=0.3g	Displacement a=0.5g	Displacement a=0.5g
0	0.023856293	0	0.039760489	0
0.1	0.023947642	9.13485E-05	0.039912736	0.000152248
0.2	0.025878087	0.002021794	0.043130145	0.003369656
0.3	0.036728239	0.012871946	0.061213732	0.021453243
0.4	0.047710119	0.023853826	0.079516865	0.039756376
0.5	0.036728239	0.012871946	0.061213732	0.021453243
0.6	0.025878087	0.002021794	0.043130145	0.003369656
0.7	0.023947642	9.13485E-05	0.039912736	0.000152248
0.8	0.023856293	0	0.039760489	0

Table 1 : Displacement input data for T=0.4 sec

Time	Displacement a=0.8g	Displacement a=0.8g	Displacement a=1.2g	Displacement a=1.2g
0	0.063616782	0	0.095425173	0
0.1	0.063860378	0.000243596	0.095790568	0.000365394
0.2	0.069008232	0.00539145	0.103512349	0.008087175
0.3	0.097941971	0.034325189	0.146912957	0.051487784
0.4	0.127226984	0.063610202	0.190840476	0.095415302
0.5	0.097941971	0.034325189	0.146912957	0.051487784
0.6	0.069008232	0.00539145	0.103512349	0.008087175
0.7	0.063860378	0.000243596	0.095790568	0.000365394
0.8	0.063616782	0	0.095425173	0

Table 2: Displacement input data for T=0.4 sec (continue)

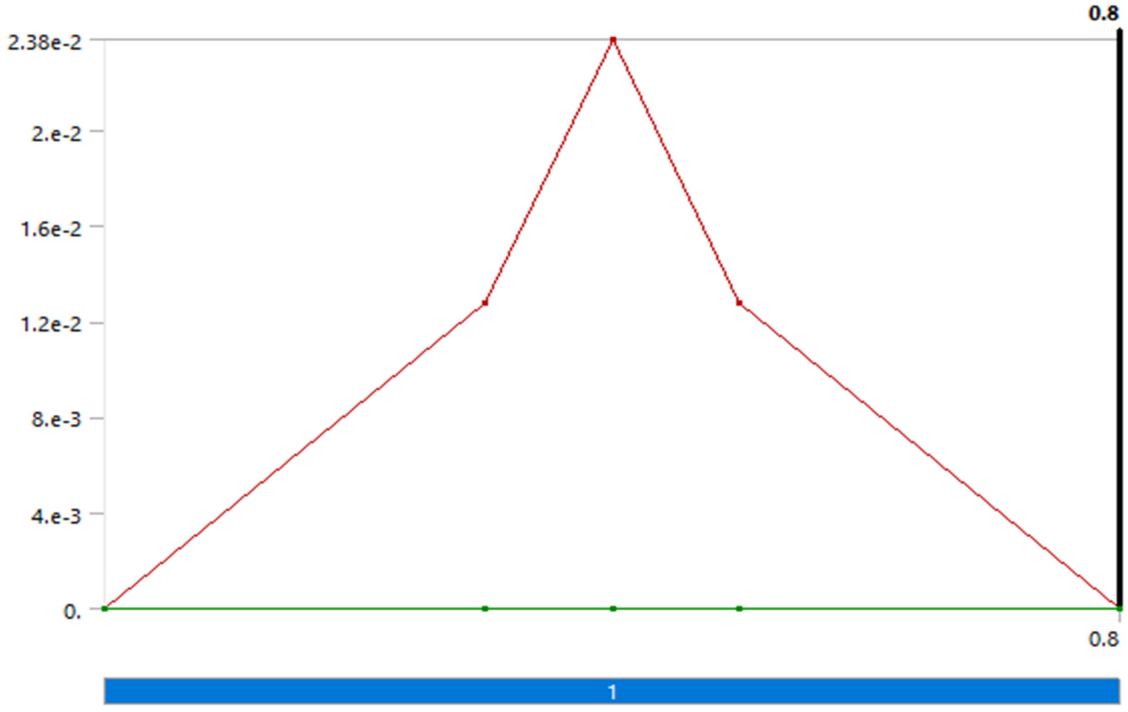

Figure 18: Lower edge nodal directional deformation

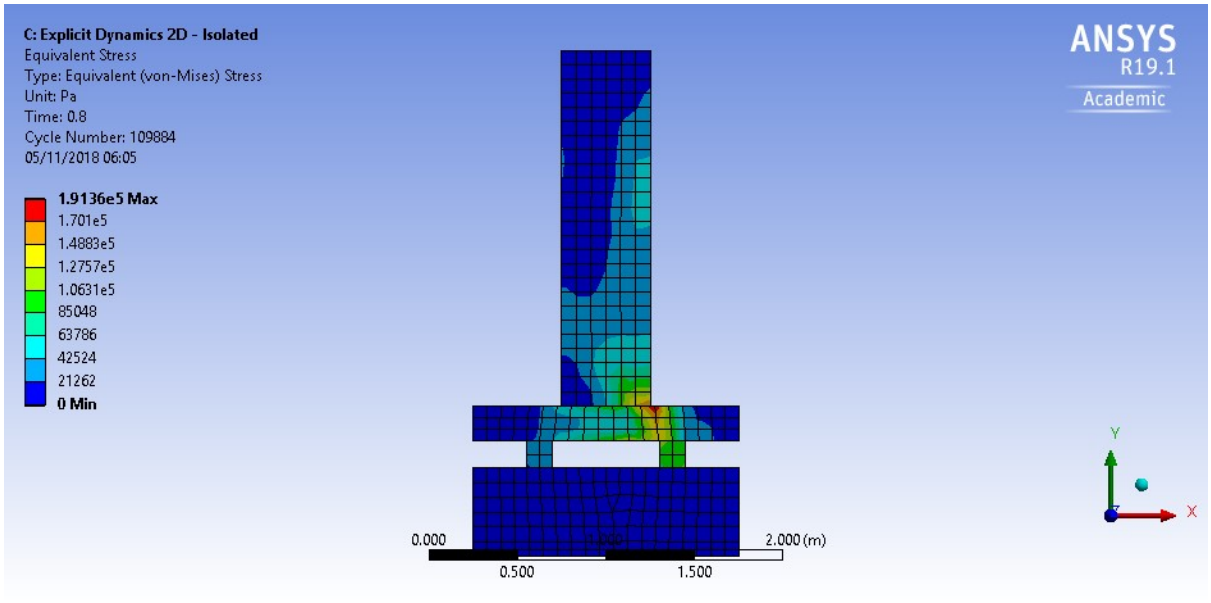

Figure 19: Von-Mises stress distribution (T=0.4s , a =0.3g)

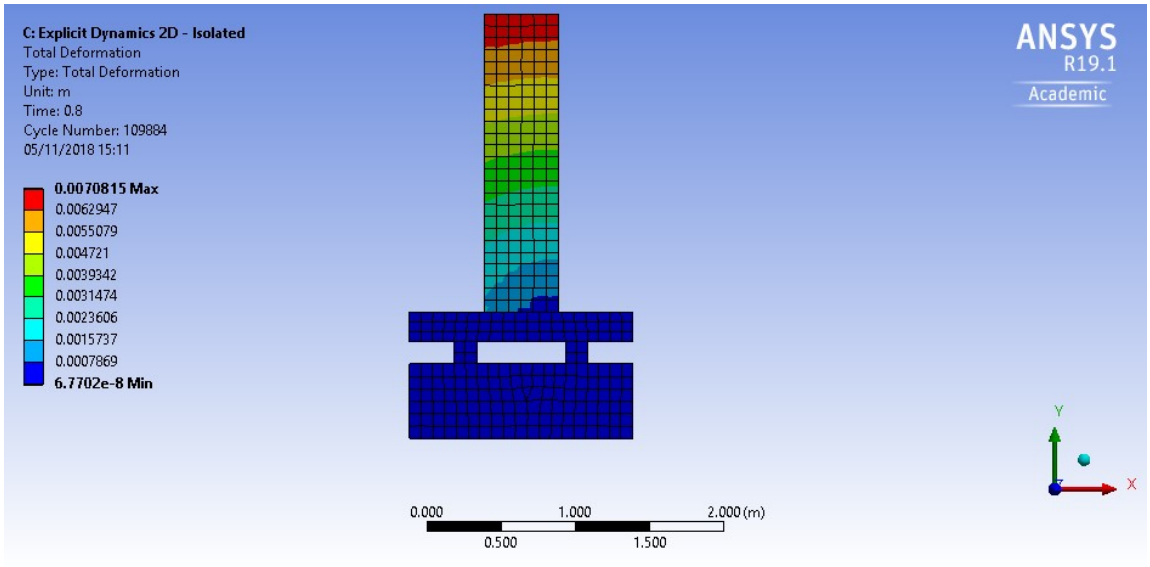

Figure 20: Total Deformation (T=0.4s , a =0.3g)

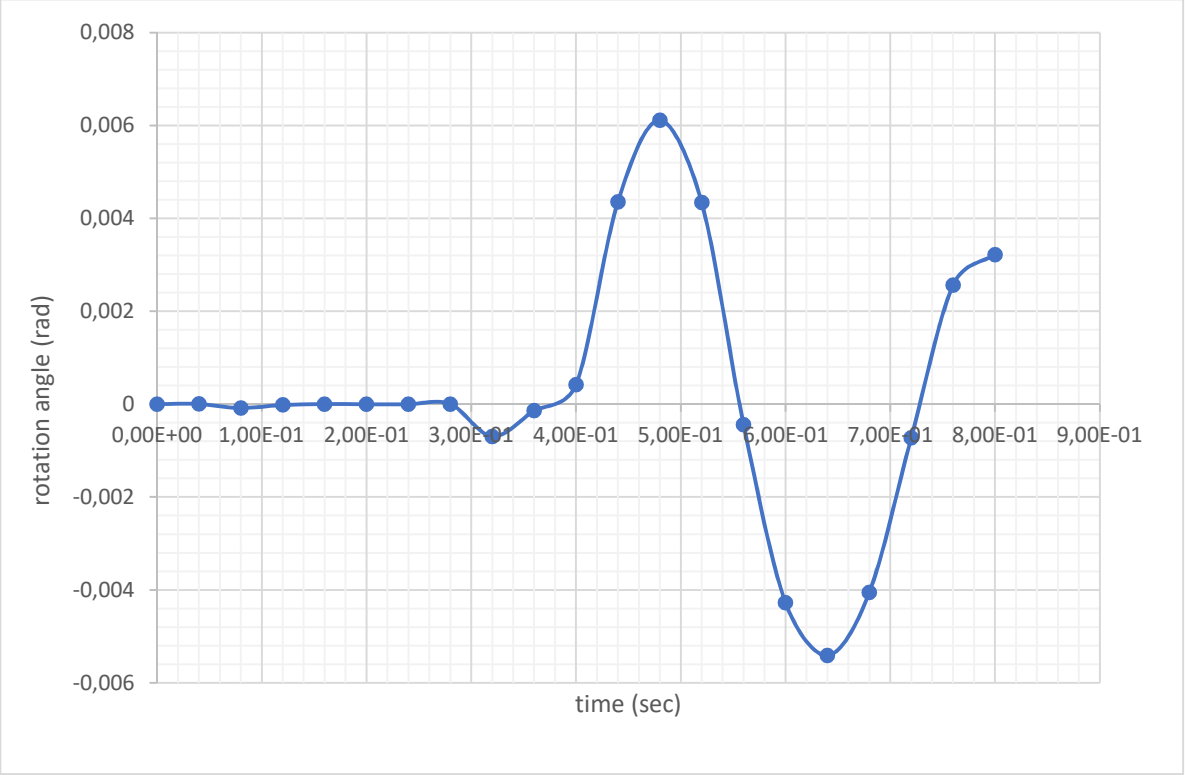

Figure 21: Rotation angle for base isolated model (T=0.4s , a =0.3g)

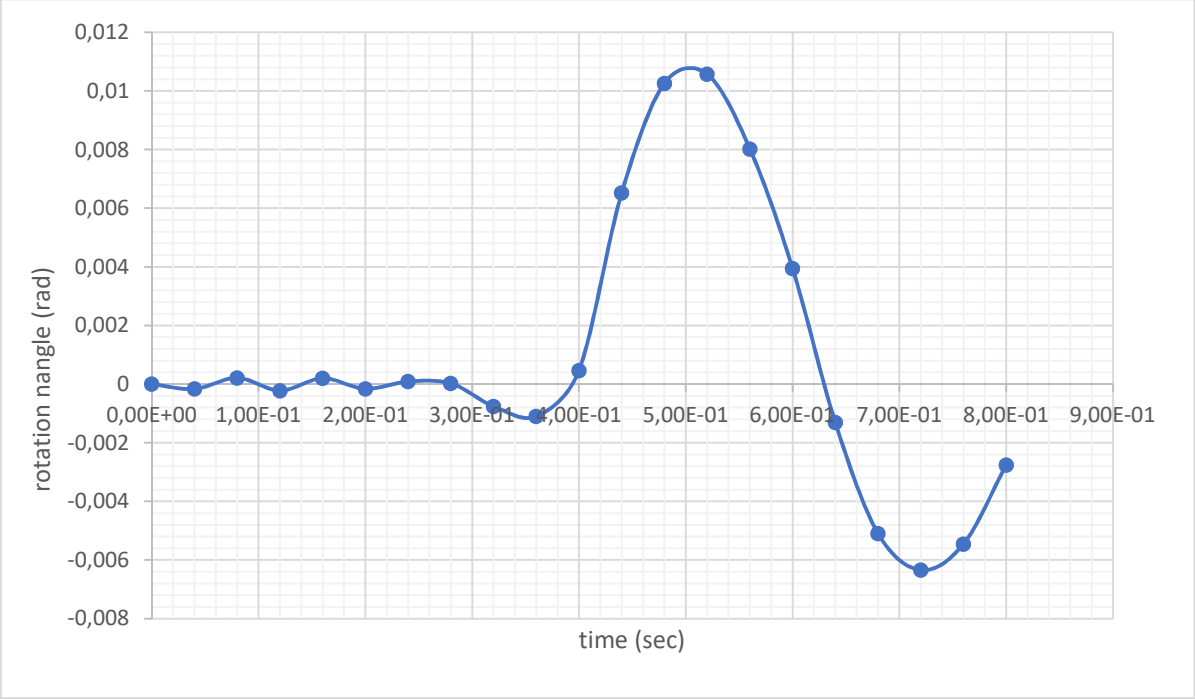

Figure 22: Rotation angle simple column model (T=0.4s , a =0.3g)

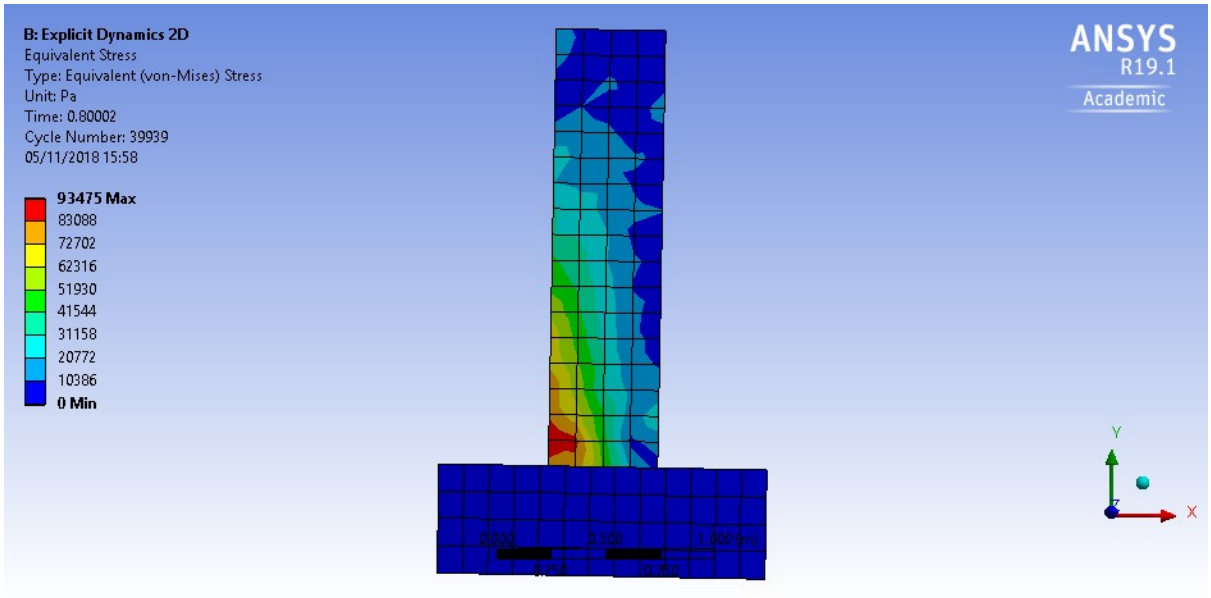

Figure 23: Von Mises stress simple column model (T=0.4s , a =0.3g)

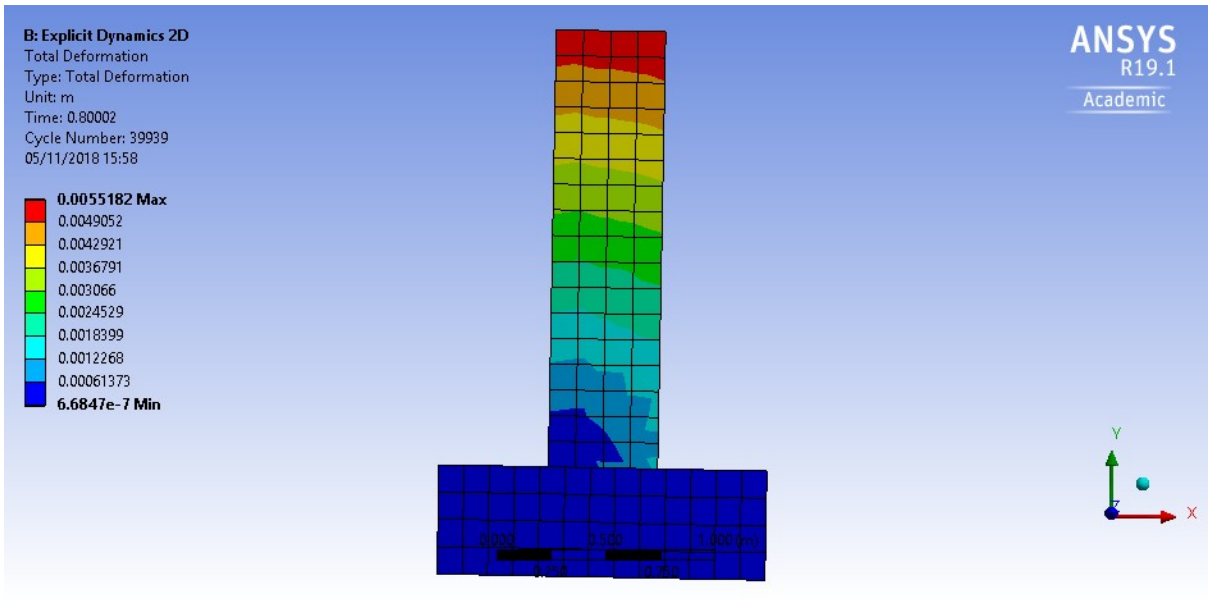

Figure 24: Total Deformation simple column model (T=0.4s , a =0.3g)

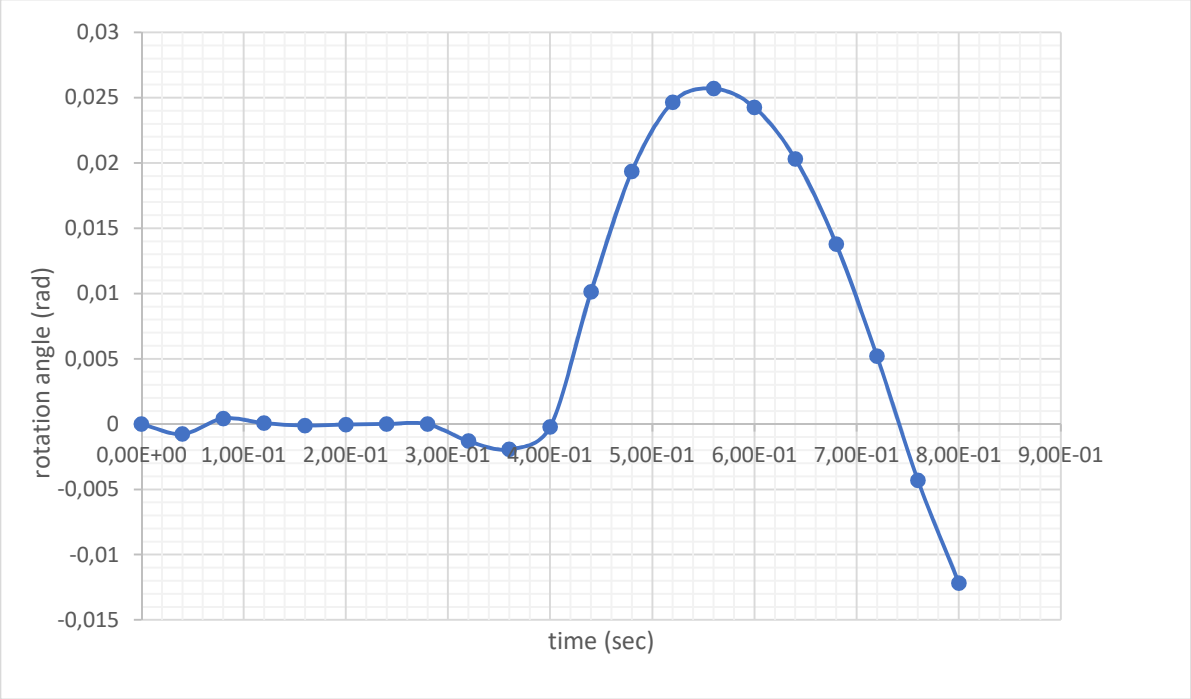

Figure 25: Rotation angle for base isolated model (T=0.4s , a =0.5g)

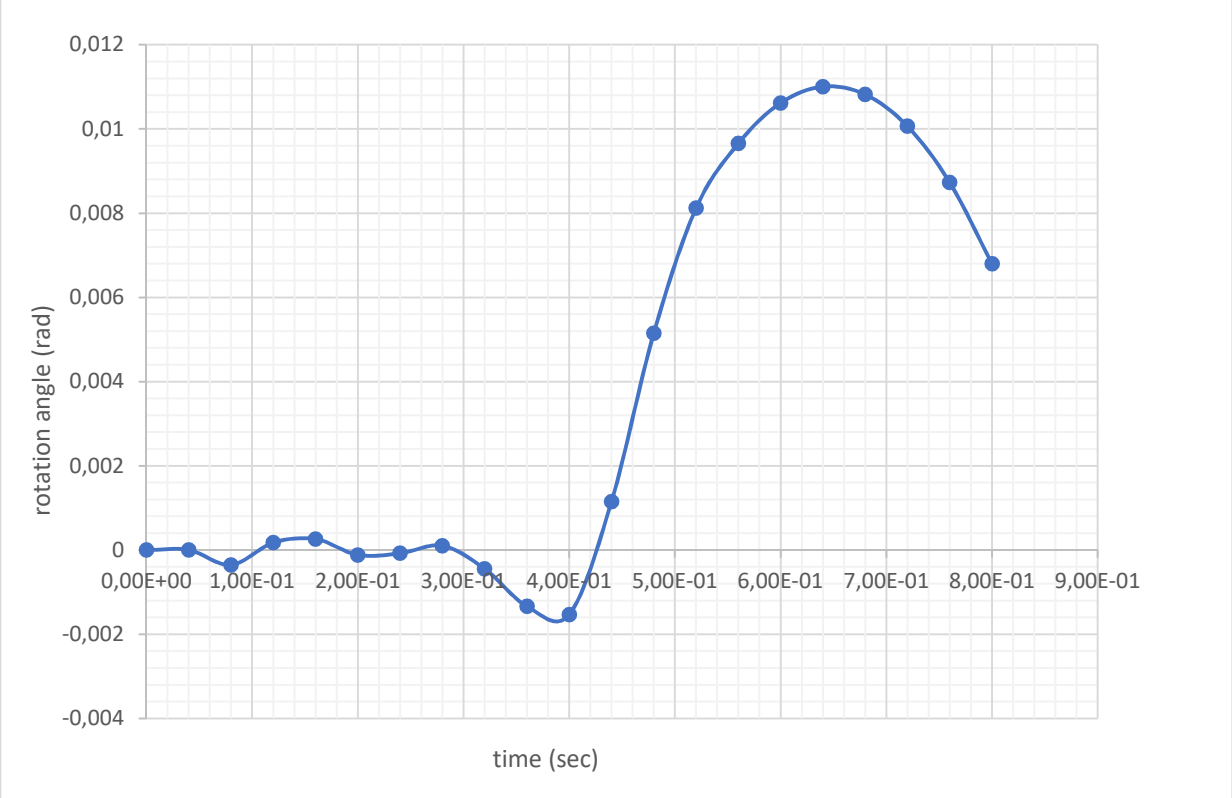

Figure 26: Rotation angle for simple column model (T=0.4s , a =0.5g)

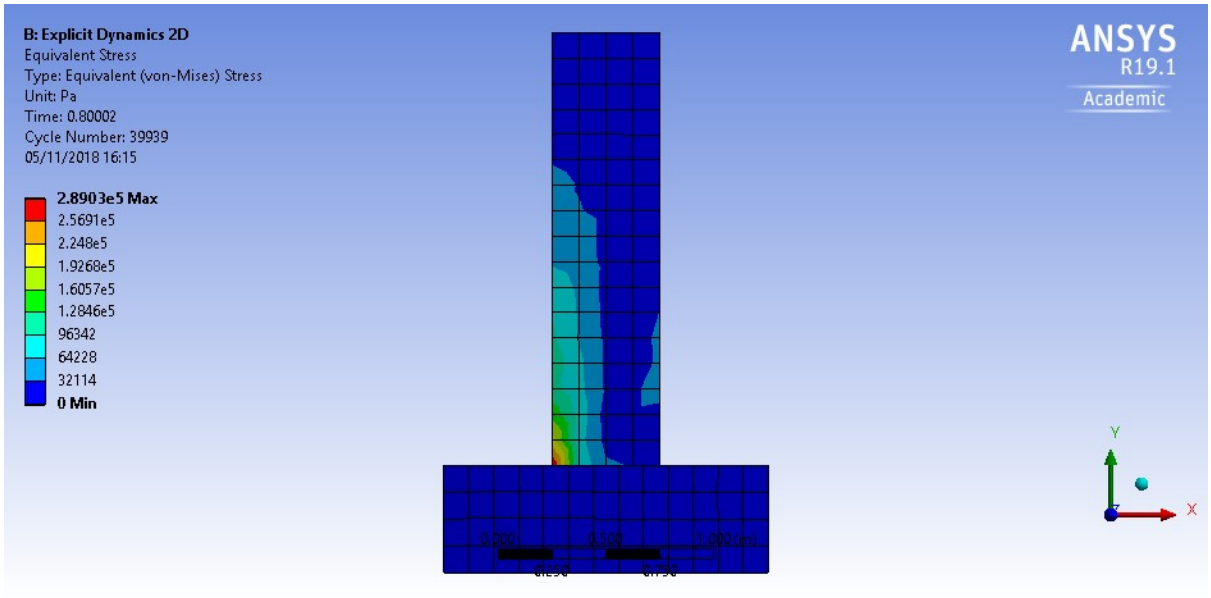

Figure 27: Von Mises stress simple column model (T=0.4s , a =0.5g)

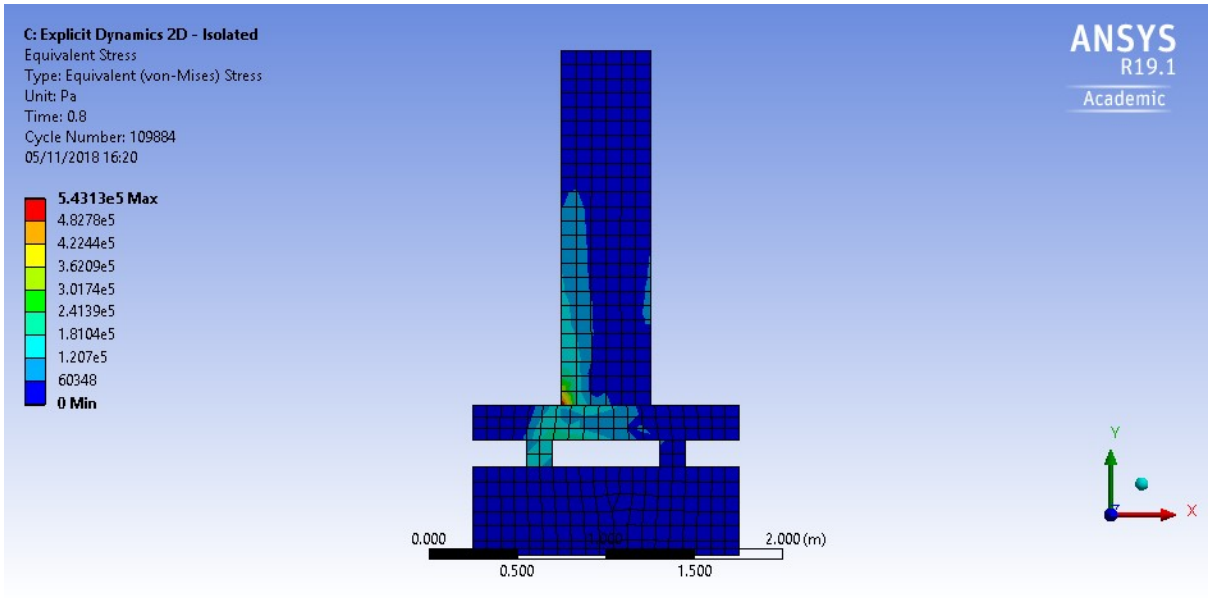

Figure 28: Von-Mises stress distribution (T=0.4s , a =0.5g)

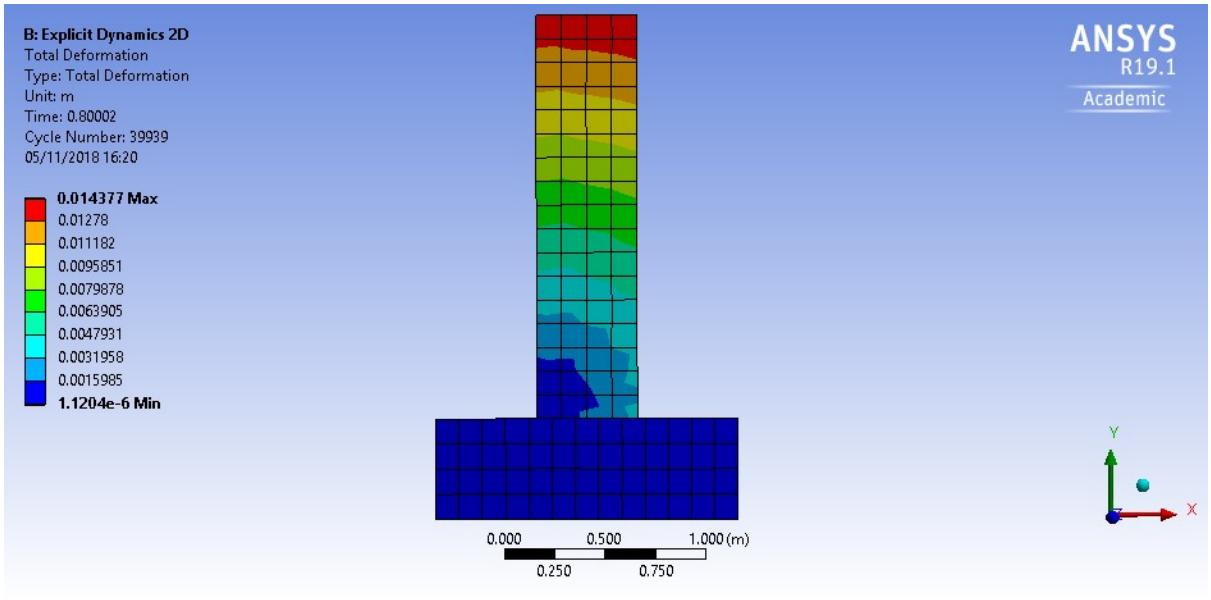

Figure 29 : Total Deformation simple column model (T=0.4s , a =0.3g)

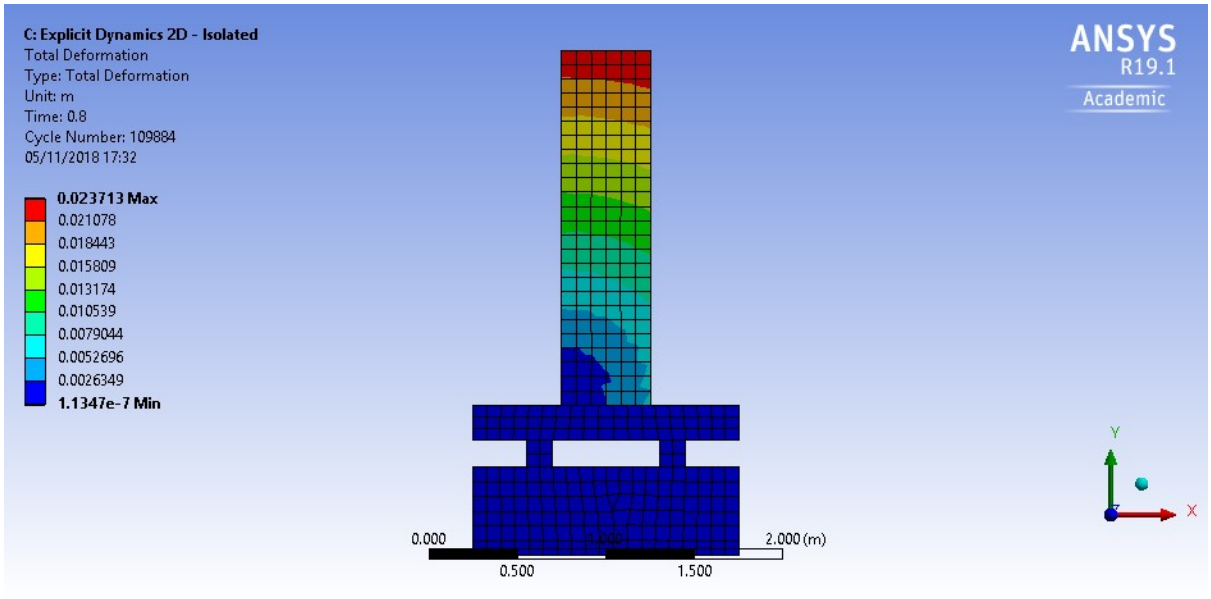

Figure 30 : Total Deformation (T=0.4s , a =0.5g)

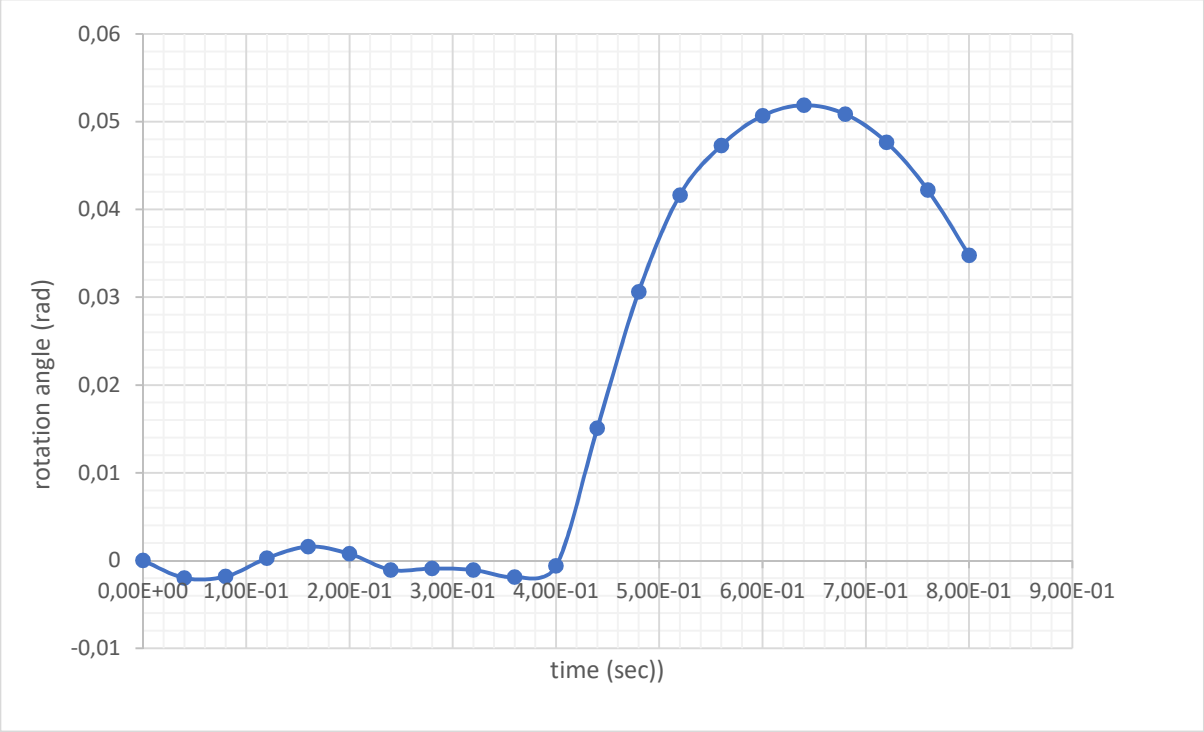

Figure 31 : Rotation angle for base isolated model (T=0.4s , a =0.8g)

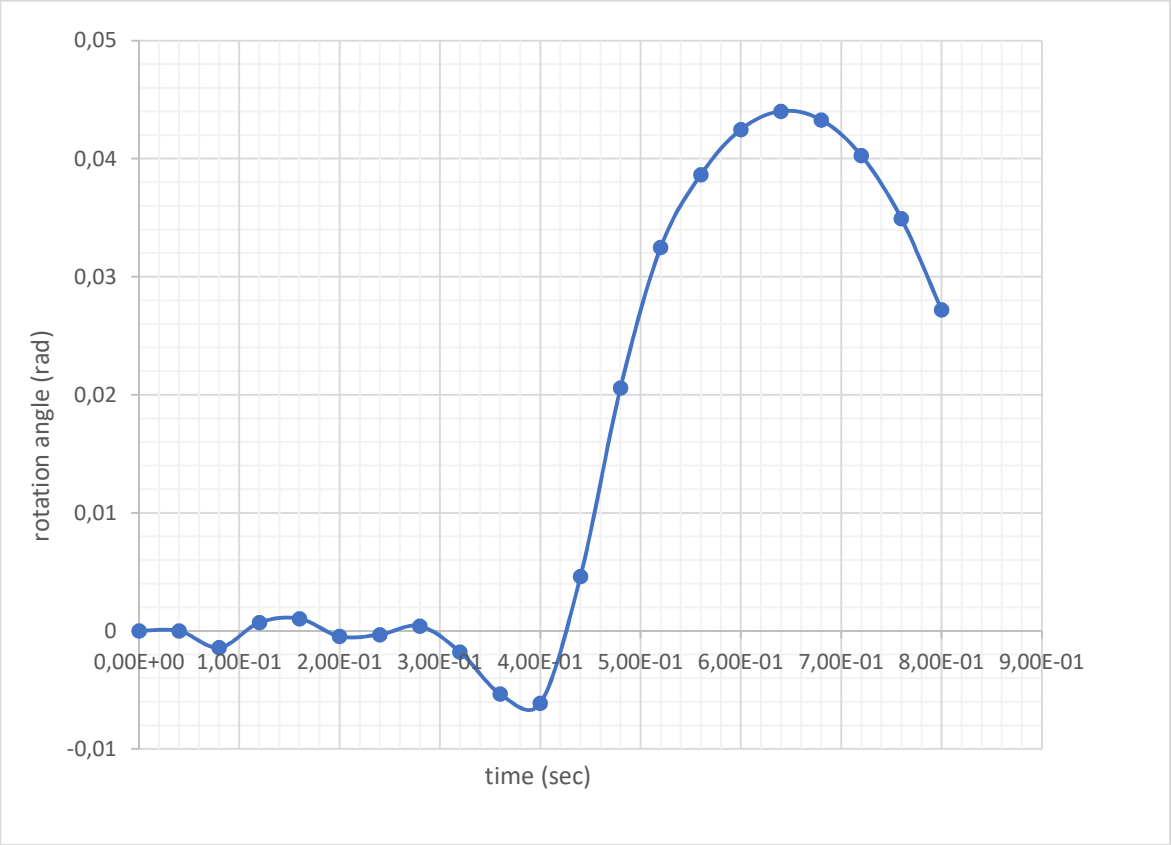

Figure 32 : Rotation angle for simple column model (T=0.4s , a =0.8g)

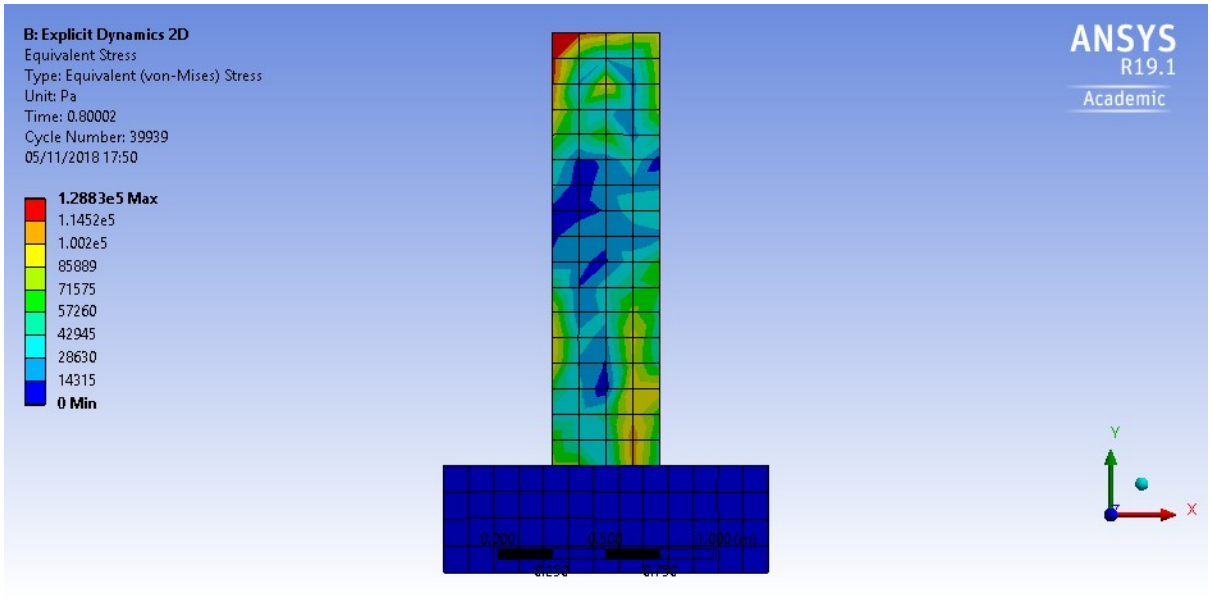

Figure 33 : Von Mises stress simple column model (T=0.4s , a =0.8g)

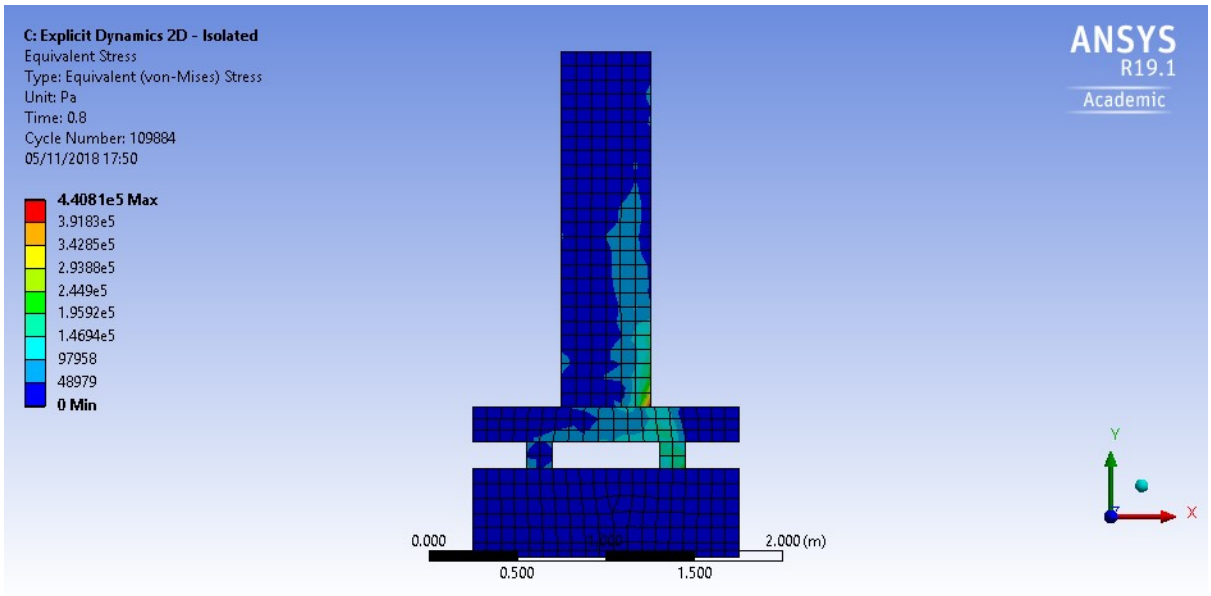

Figure 34 : Von Mises stress distribution for base isolated model (T=0.4s , a =0.8g)

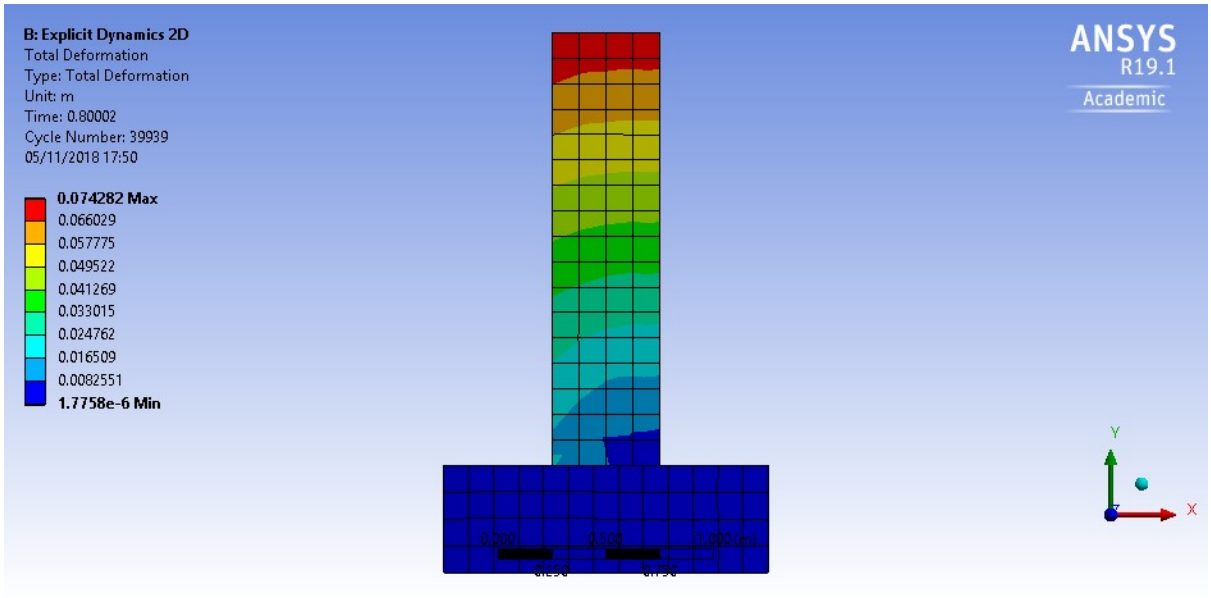

Figure 35 : Total Deformation (T=0.4s , a =0.8g)

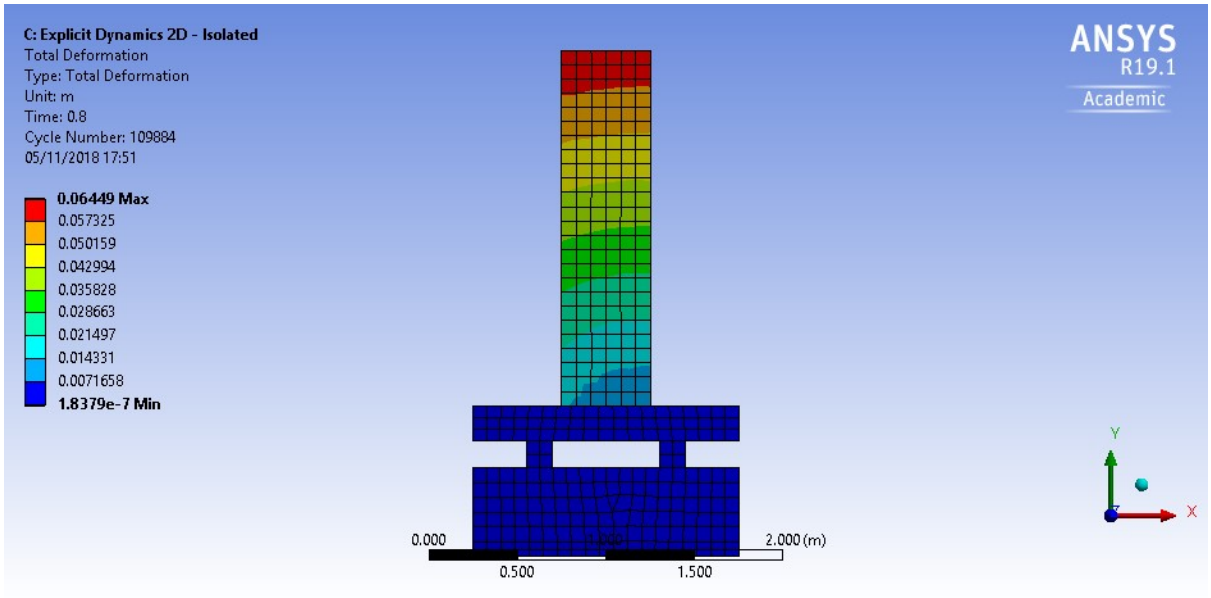

Figure 36: Total Deformation (base isolated, T=0.4s , a =0.8g)

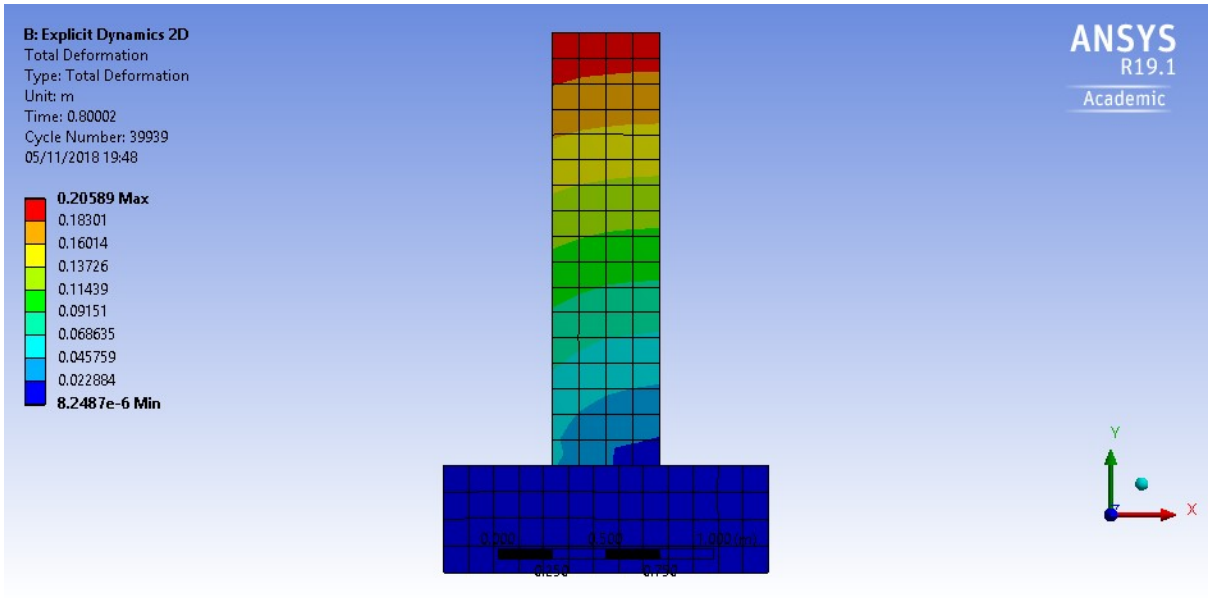

Figure 37 : Total Deformation (T=0.4s , a =1.2g)

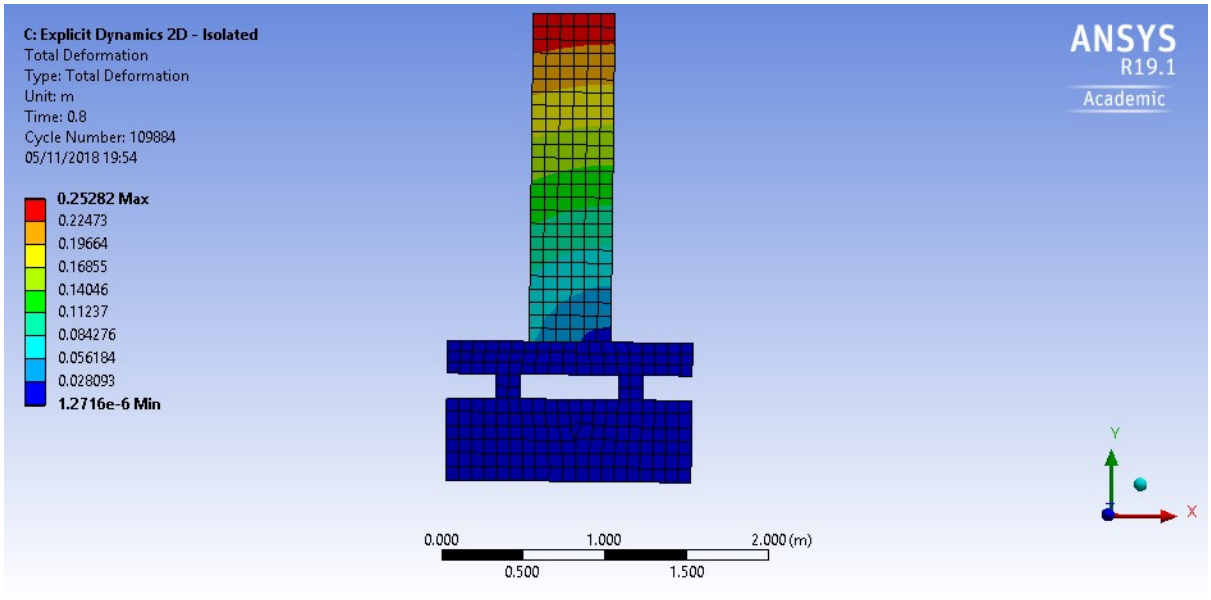

Figure 38 : Total Deformation (base isolated, T=0.4s , a =1.2g)

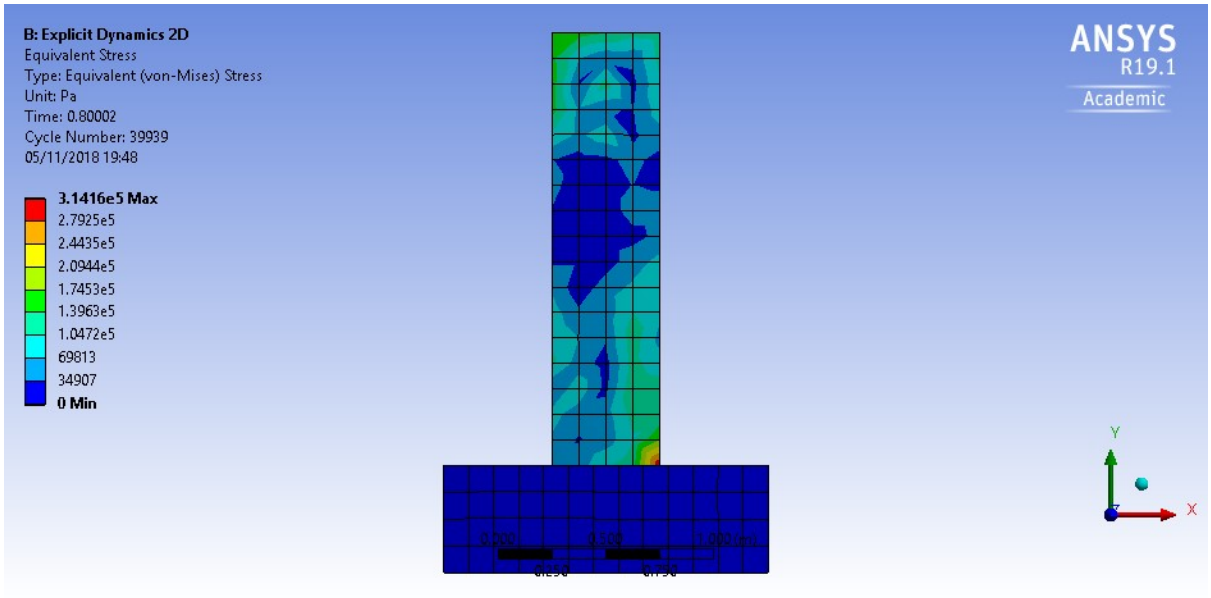

Figure 39 : Von Mises stress simple column model (T=0.4s , a =0.8g)

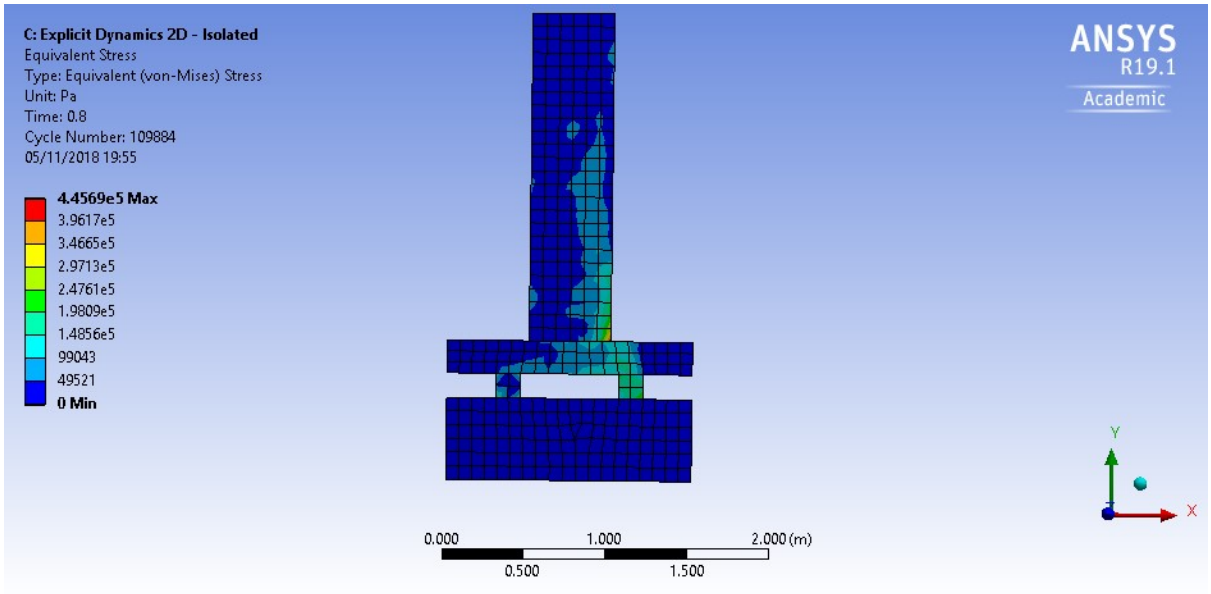

Figure 40: Von Mises stress base isolated model (T=0.4s , a =1.2g)

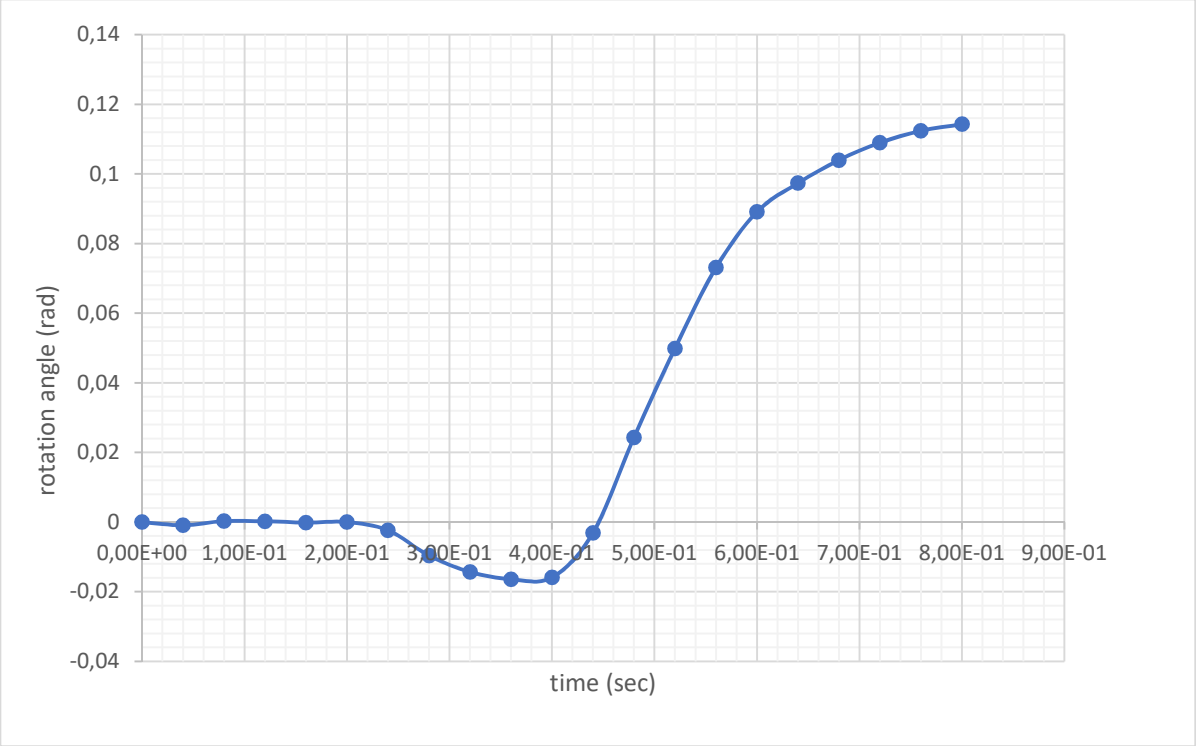

Figure 41: Rotation angle for base isolated model (T=0.4s , a =1.2g)

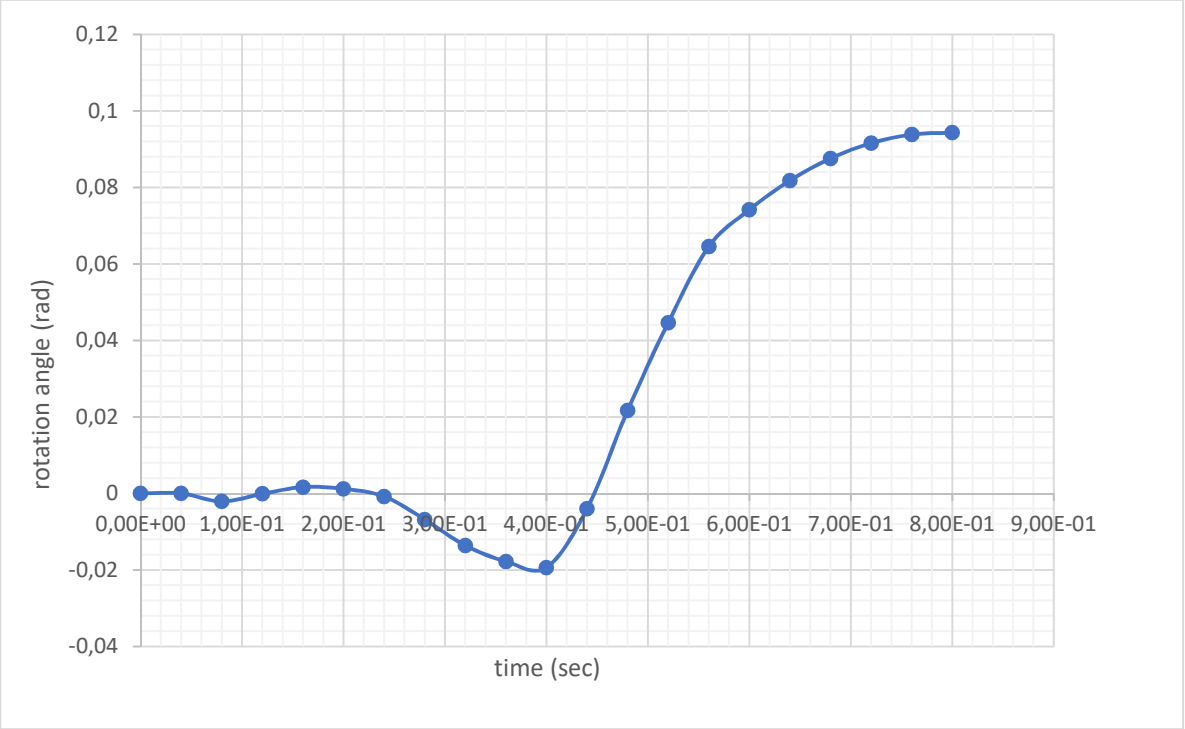

Figure 42: Rotation angle for simple column model (T=0.4s , a =1.2g)

1.3.3 Simulation for T= 0.5s and a= 0.3g, 0.5g , 0.8g and 1.2g

Time	Displacement a=0.5g	Displacement a=0.5g	Displacement a=0.3g	Displacement a=0.3g
0	0.062125764	0	0.037275458	0
0.1	0.062234755	0.000108991	0.037340853	6.53944E-05
0.2	0.063901551	0.001775787	0.038340931	0.001065472
0.3	0.0749293	0.012803537	0.04495758	0.007682122
0.4	0.103982306	0.041856543	0.062389384	0.025113926
0.5	0.124245101	0.062119338	0.074547061	0.037271603
0.6	0.103982306	0.041856543	0.062389384	0.025113926
0.7	0.0749293	0.012803537	0.04495758	0.007682122
0.8	0.063901551	0.001775787	0.038340931	0.001065472
0.9	0.062234755	0.000108991	0.037340853	6.53944E-05
1	0.062125764	0	0.037275458	0

Table 3 : Displacement input data for T=0.5 sec

Time	Displacement a=0.8g	Displacement a=0.8g	Displacement a=1.2g	Displacement a=1.2g
0	0.099401222	0	0.149101833	0
0.1	0.099575607	0.000174385	0.149363411	0.000261578
0.2	0.102242481	0.002841259	0.153363722	0.004261889
0.3	0.119886881	0.020485658	0.179830321	0.030728488
0.4	0.16637169	0.066970468	0.249557536	0.100455702
0.5	0.198792162	0.09939094	0.298188243	0.14908641
0.6	0.16637169	0.066970468	0.249557536	0.100455702
0.7	0.119886881	0.020485658	0.179830321	0.030728488
0.8	0.102242481	0.002841259	0.153363722	0.004261889
0.9	0.099575607	0.000174385	0.149363411	0.000261578
1	0.099401222	0	0.149101833	0

Table 4 : Displacement input data for T=0.5 sec (continue)

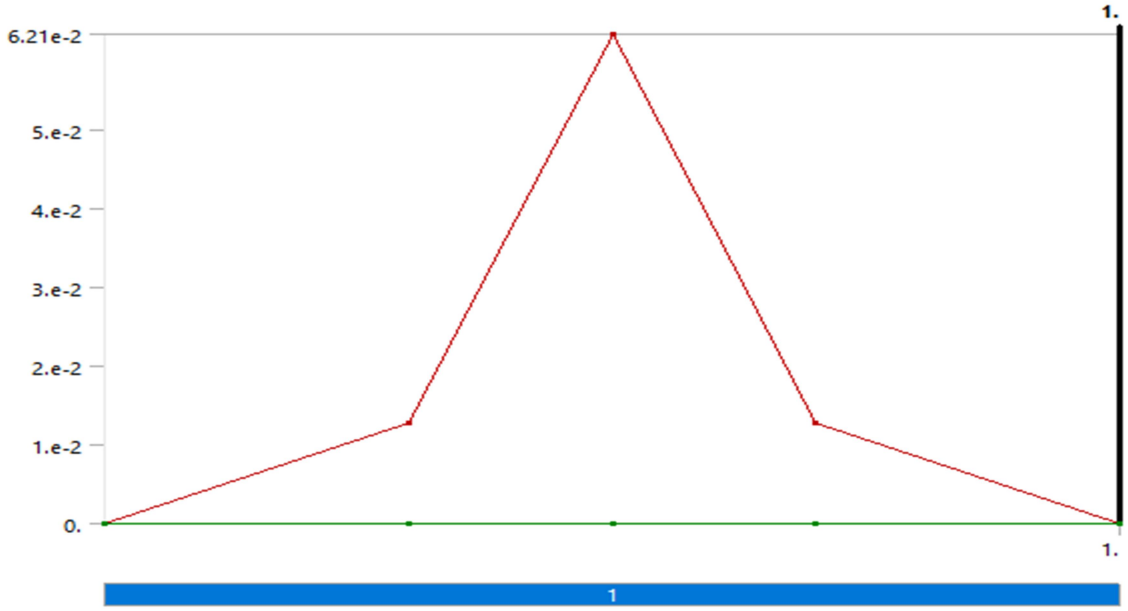

Figure 43: Input displacement for T=0.5s and a=0.5g

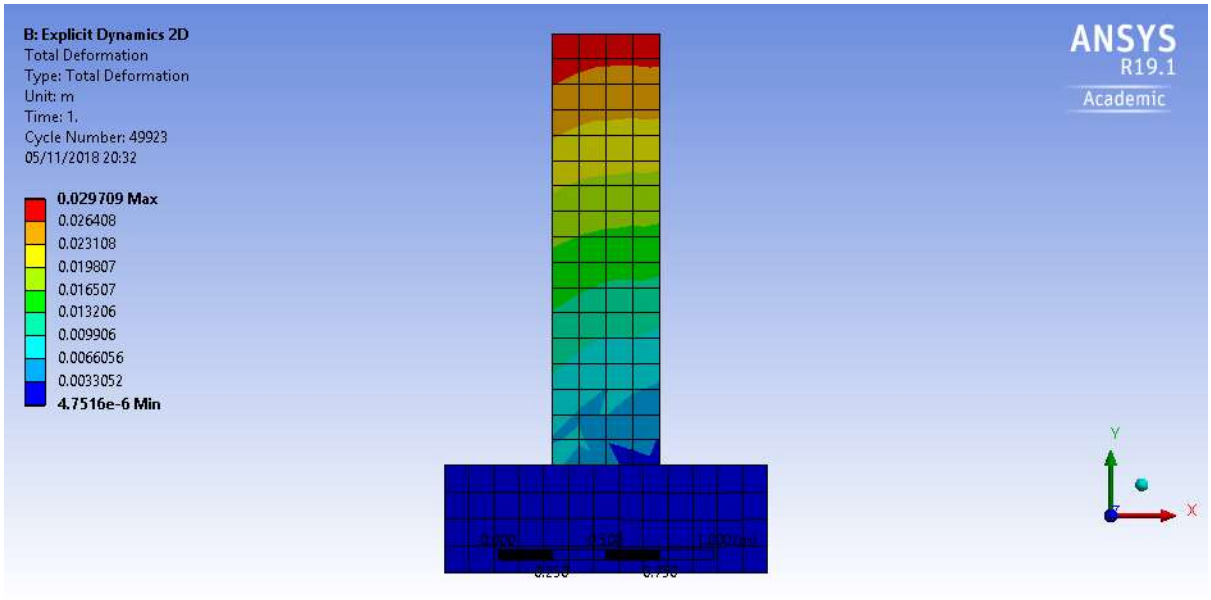

Figure 44: Total Deformation (T=0.5s , a =0.5g)

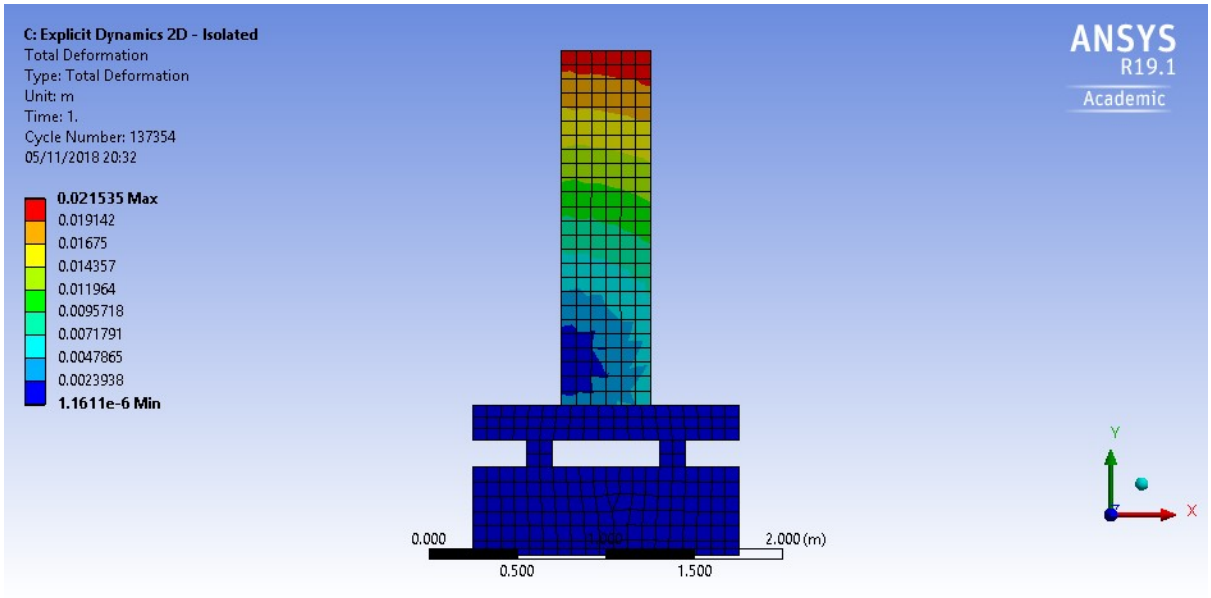

Figure 45: Total Deformation (base isolated, T=0.5s , a =0.5g)

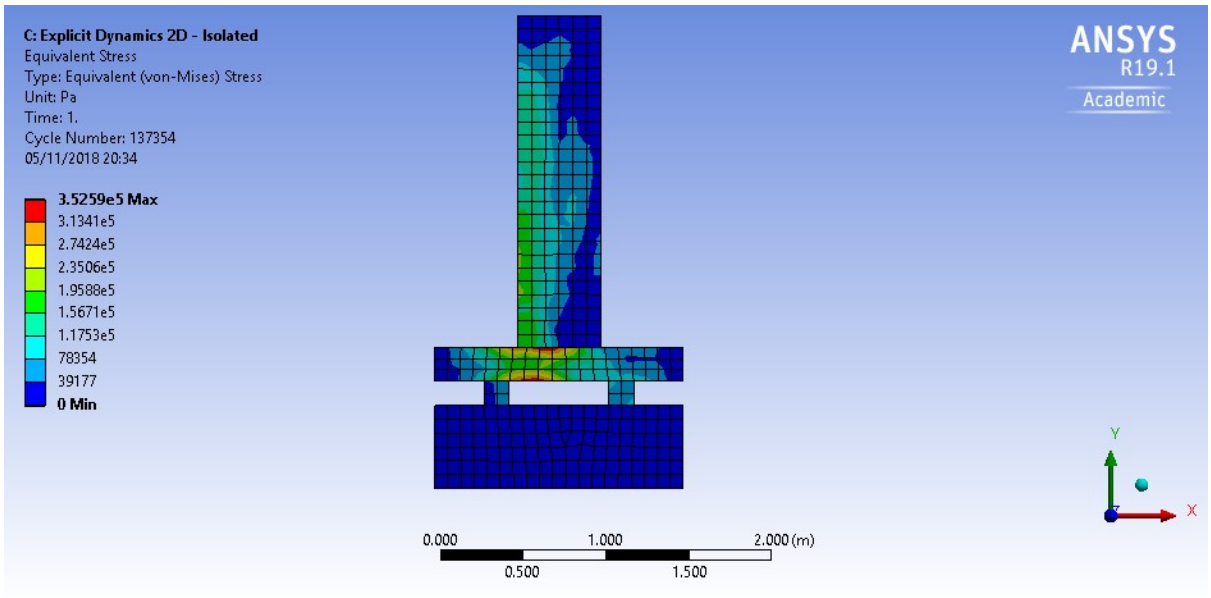

Figure 46: Von Mises stress base isolated model (T=0.5s , a =0.5g)

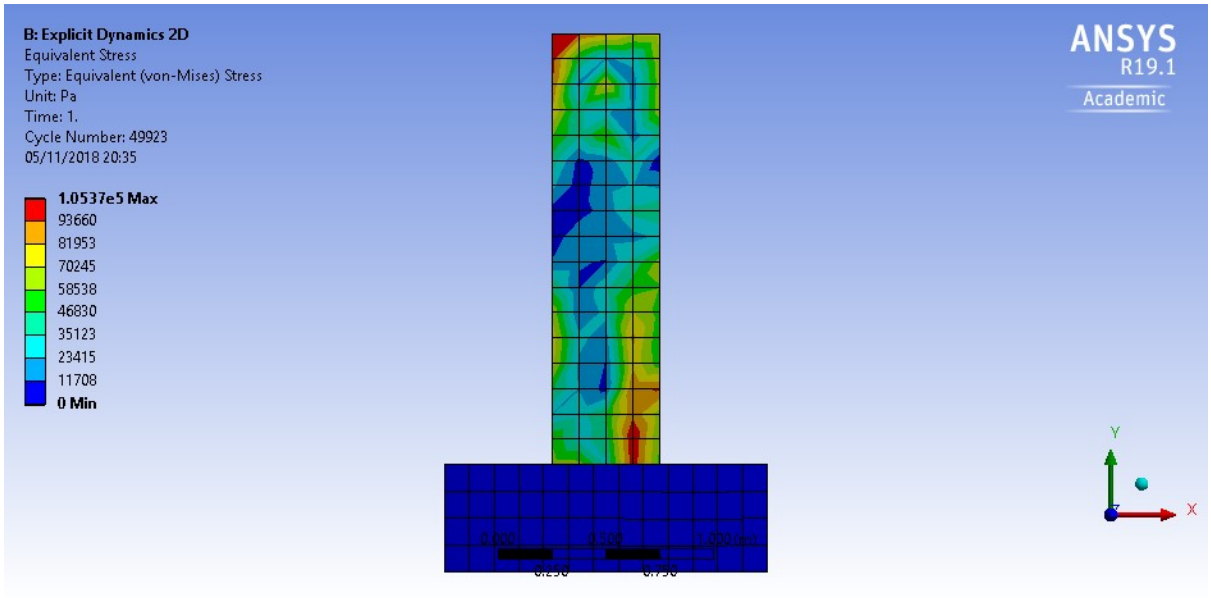

Figure 47: Von Mises stress simple column model (T=0.5s , a =0.5g)

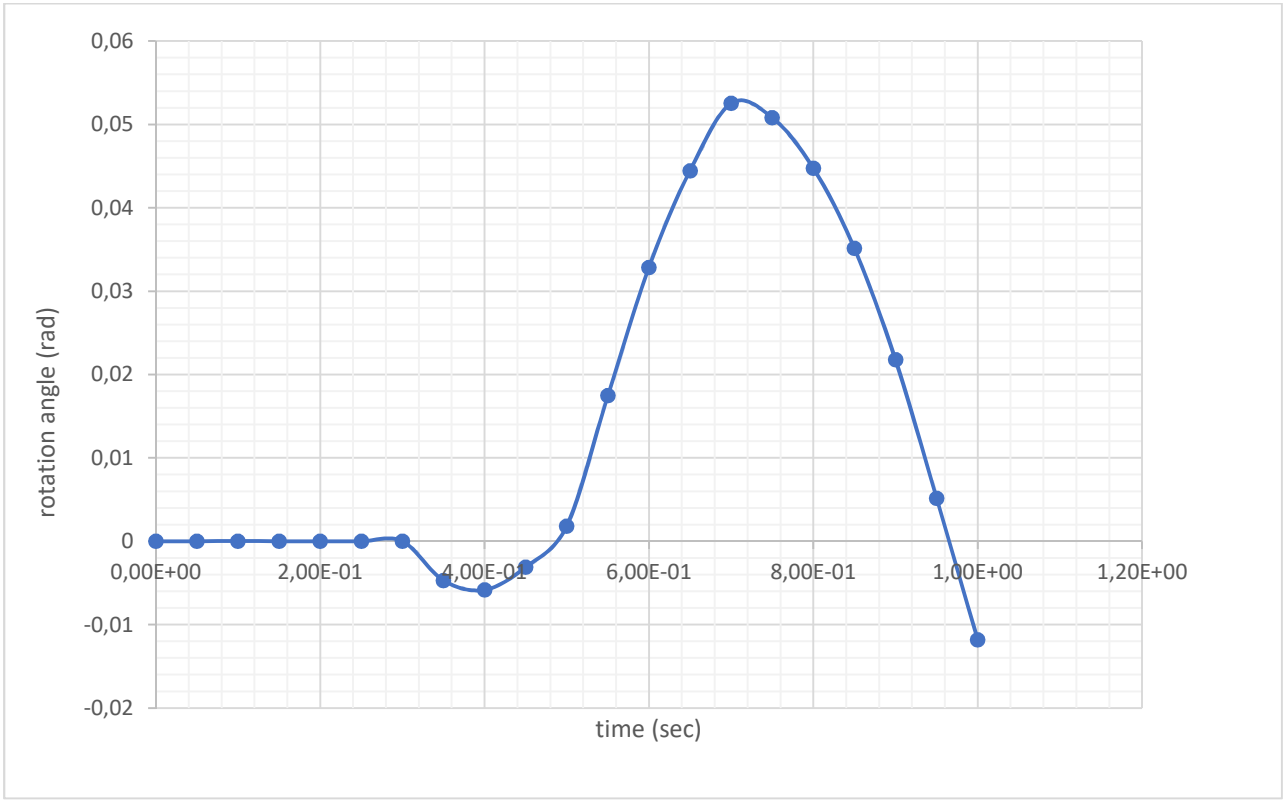

Figure 48: Rotation angle for base isolated model (T=0.5s , a =0.5g)

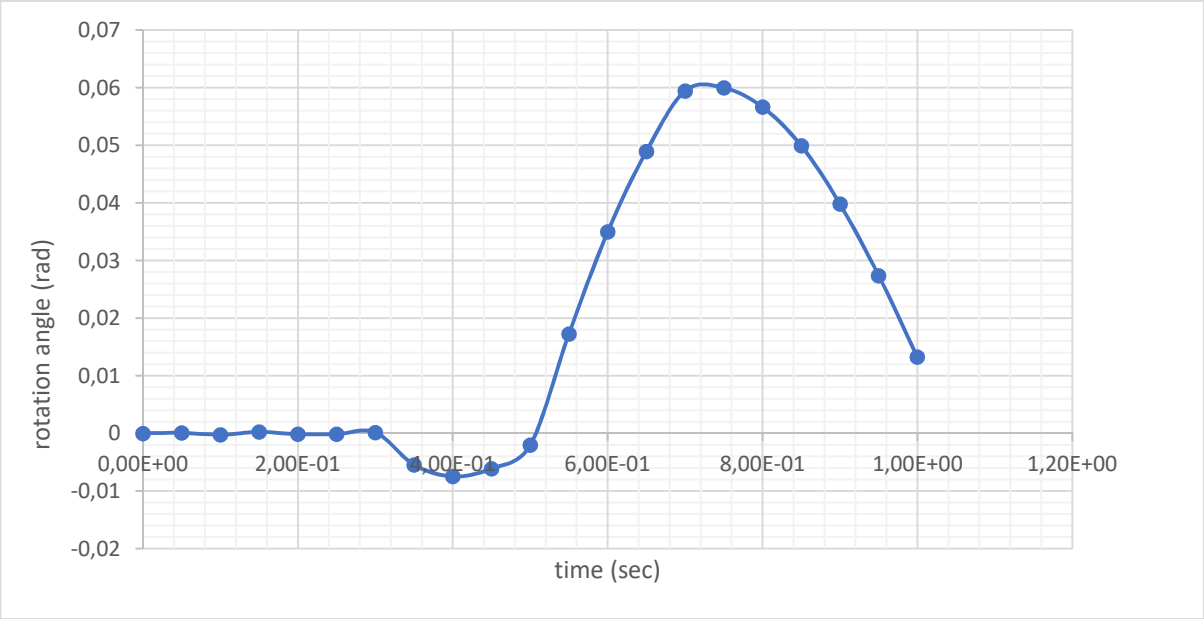

Figure 49: Rotation angle for simple column model (T=0.5s , a =0.5g)

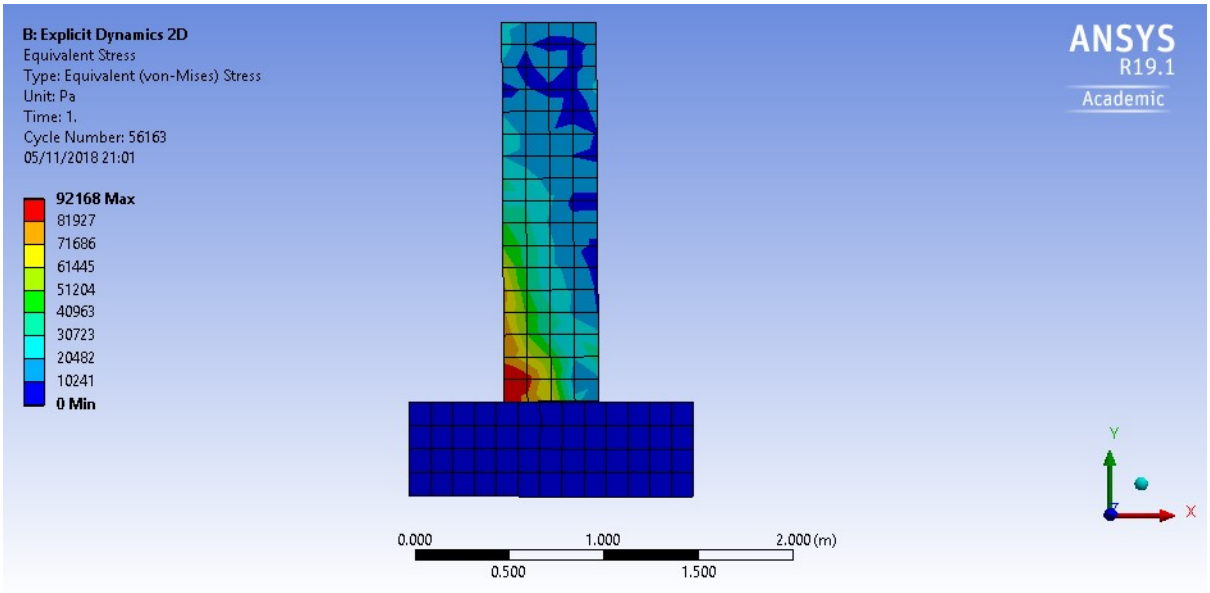

Figure 50 : Von Mises stress simple column model (T=0.5s , a =0.3g)

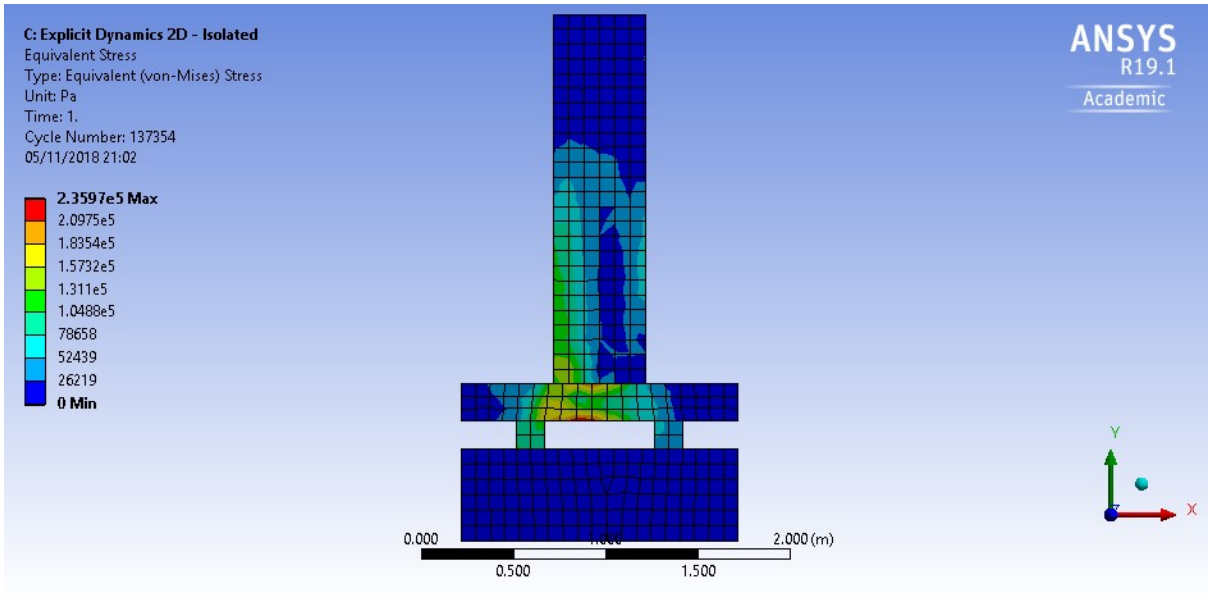

Figure 51: Von Mises stress base isolated model (T=0.5s , a =0.3g)

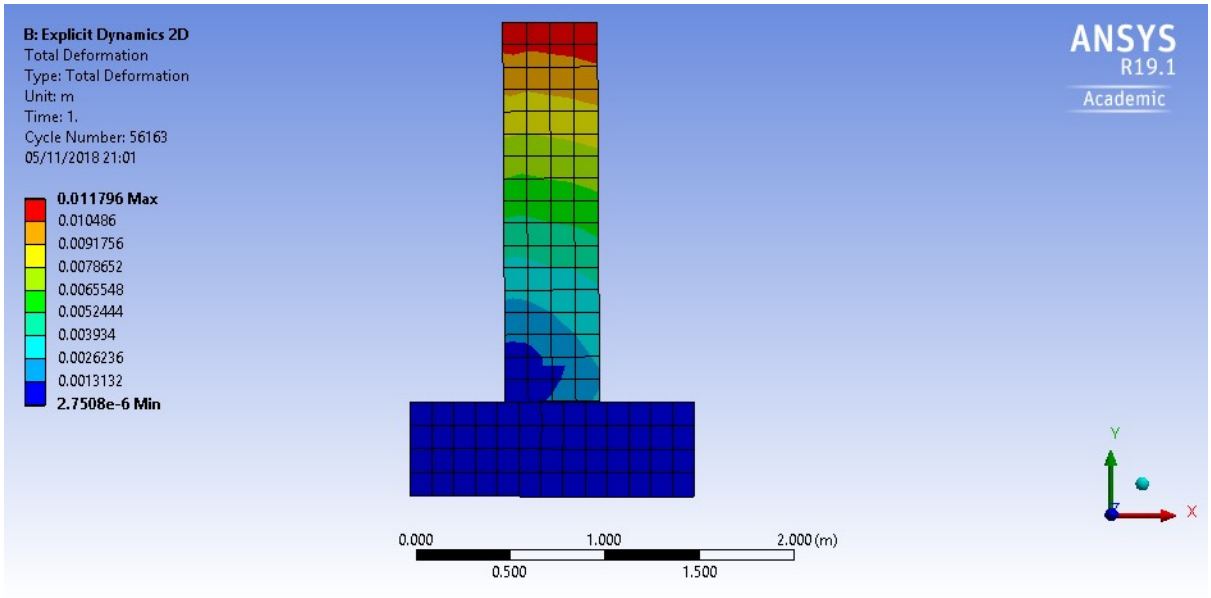

Figure 52 :Total Deformation (T=0.5s , a =0.3g)

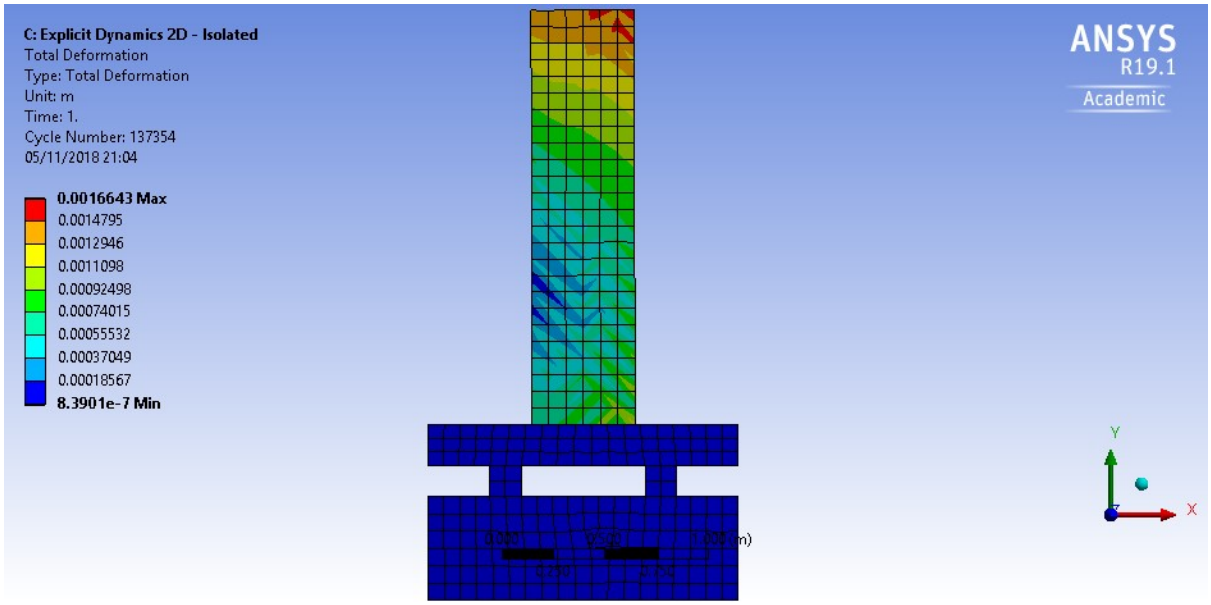

Figure 53 : Total Deformation (base isolated, T=0.5s , a =0.3g)

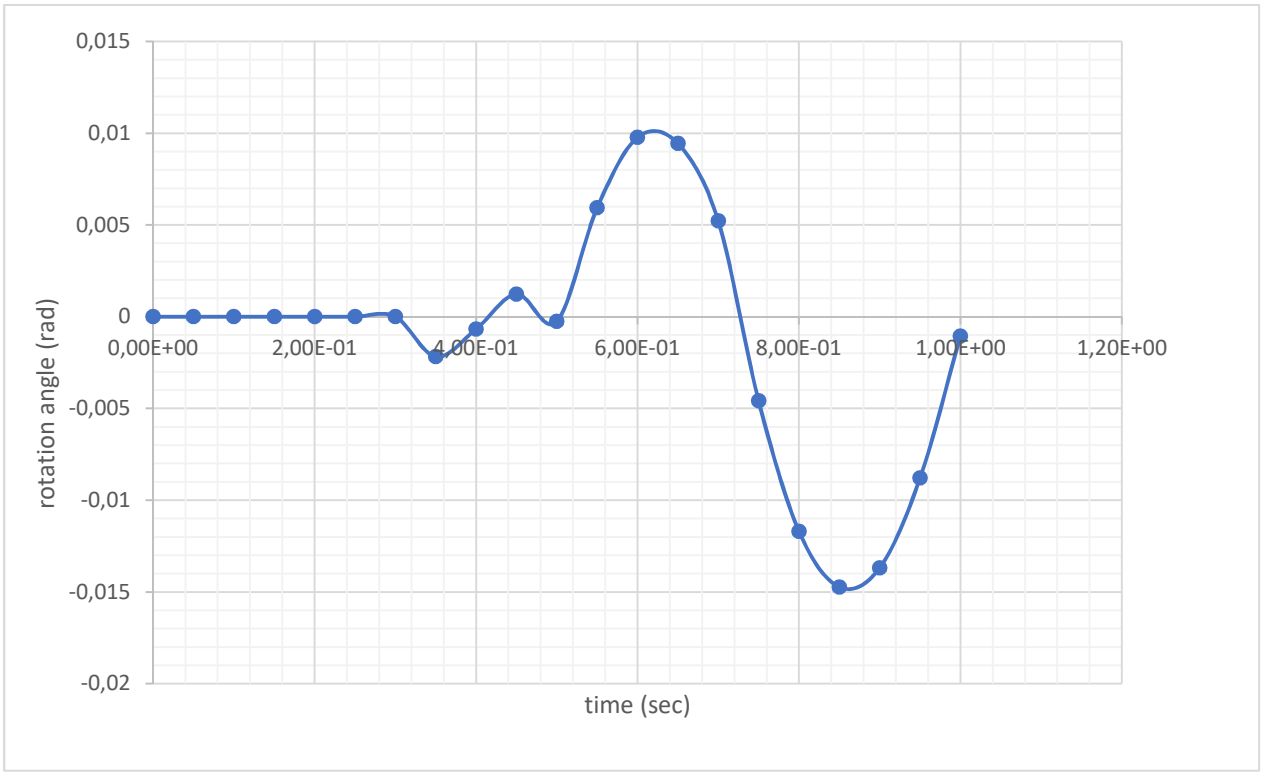

Figure 54: Rotation angle for base isolated model (T=0.5s , a =0.3g)

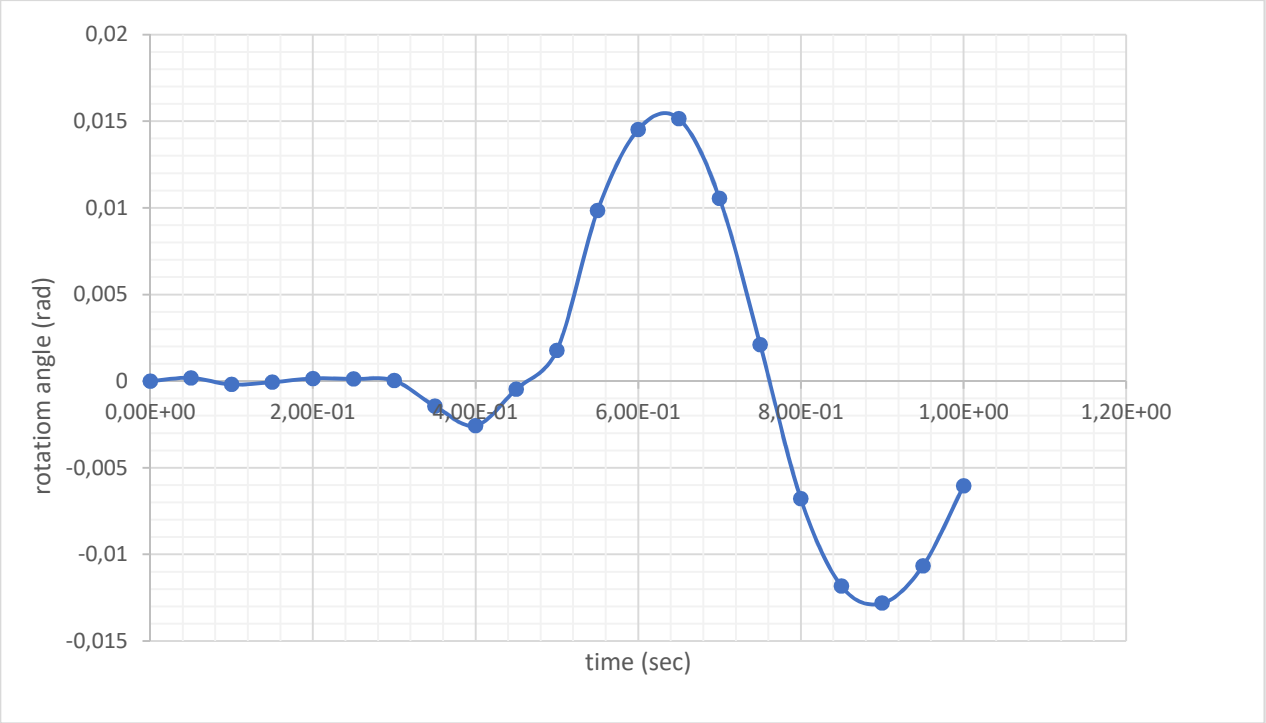

Figure 55: Rotation angle for simple column model (T=0.5s , a =0.3g)

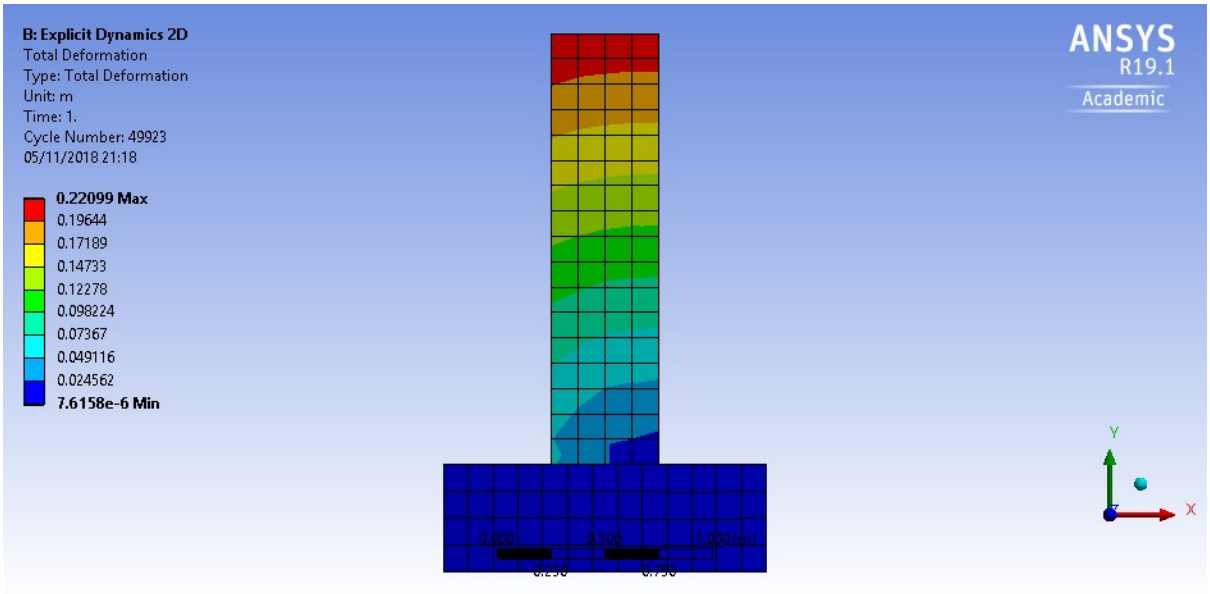

Figure 56 : Total Deformation (T=0.5s , a =0.8g)

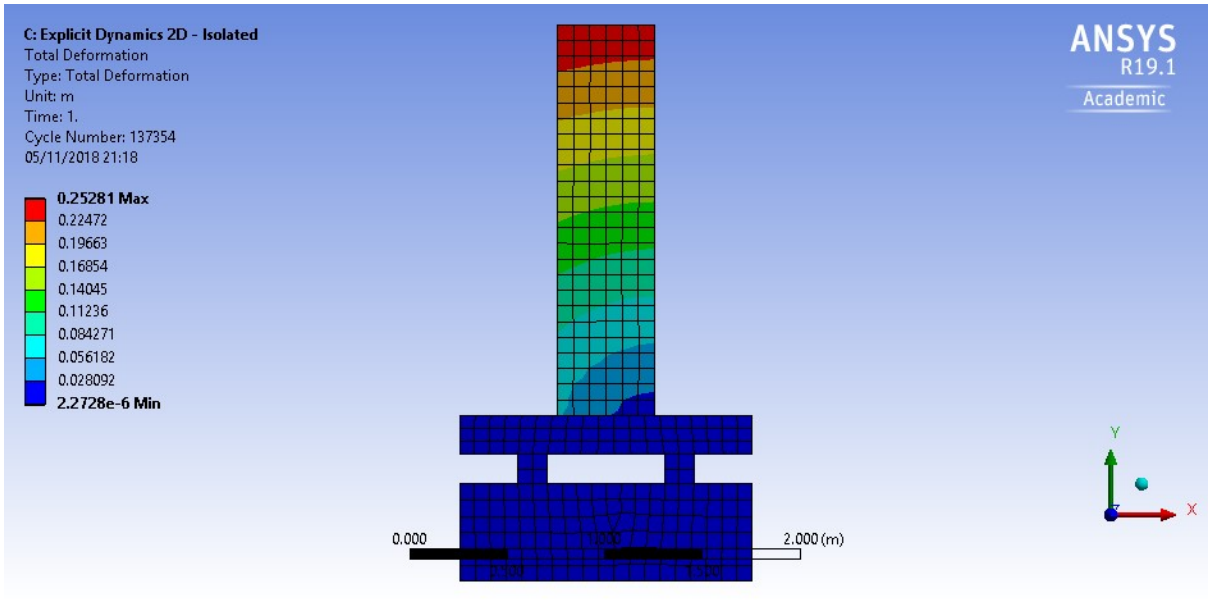

Figure 57: Total Deformation (base isolated, T=0.5s , a =0.8g)

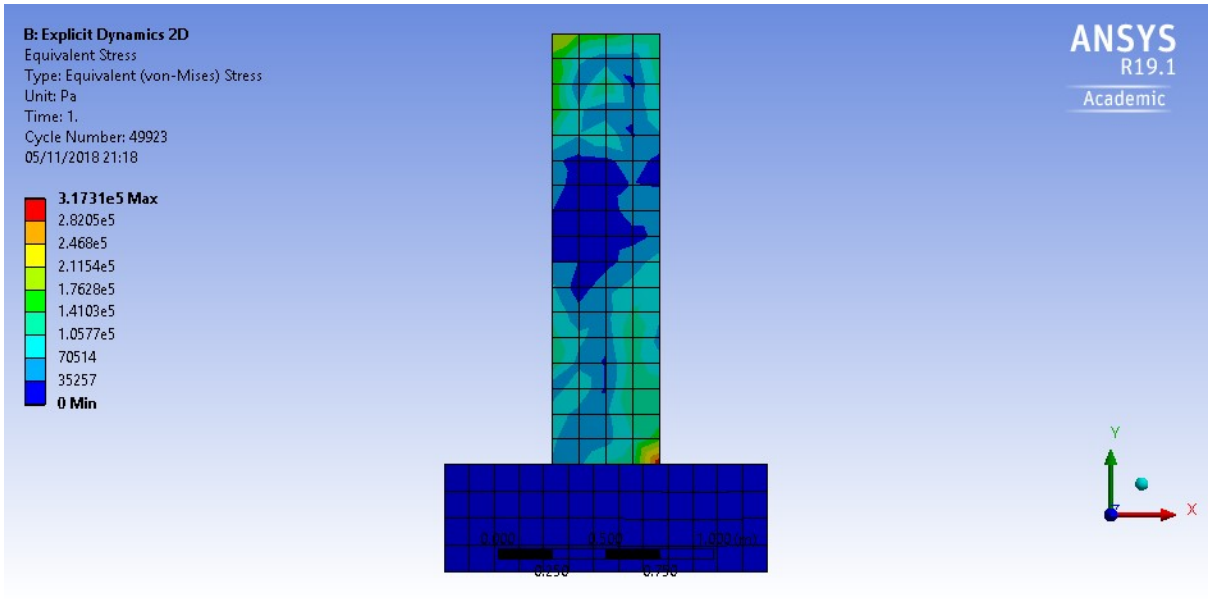

Figure 58 : Von Mises stress simple column model (T=0.5s , a =0.8g)

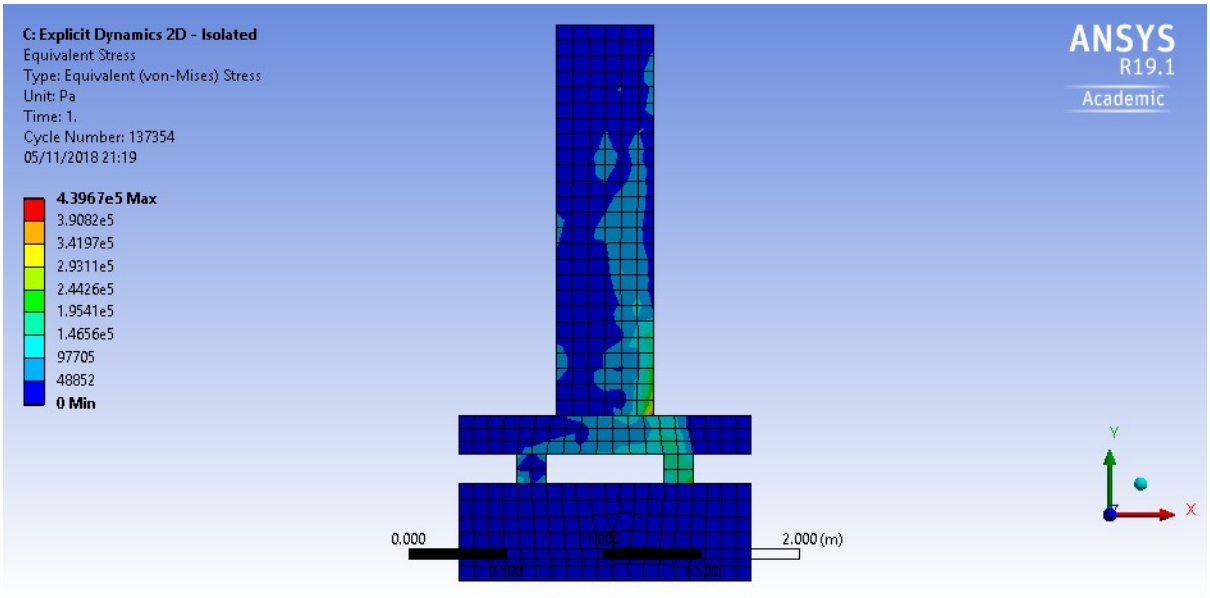

Figure 59 : Von Mises stress base isolated model (T=0.5s , a =0.8g)

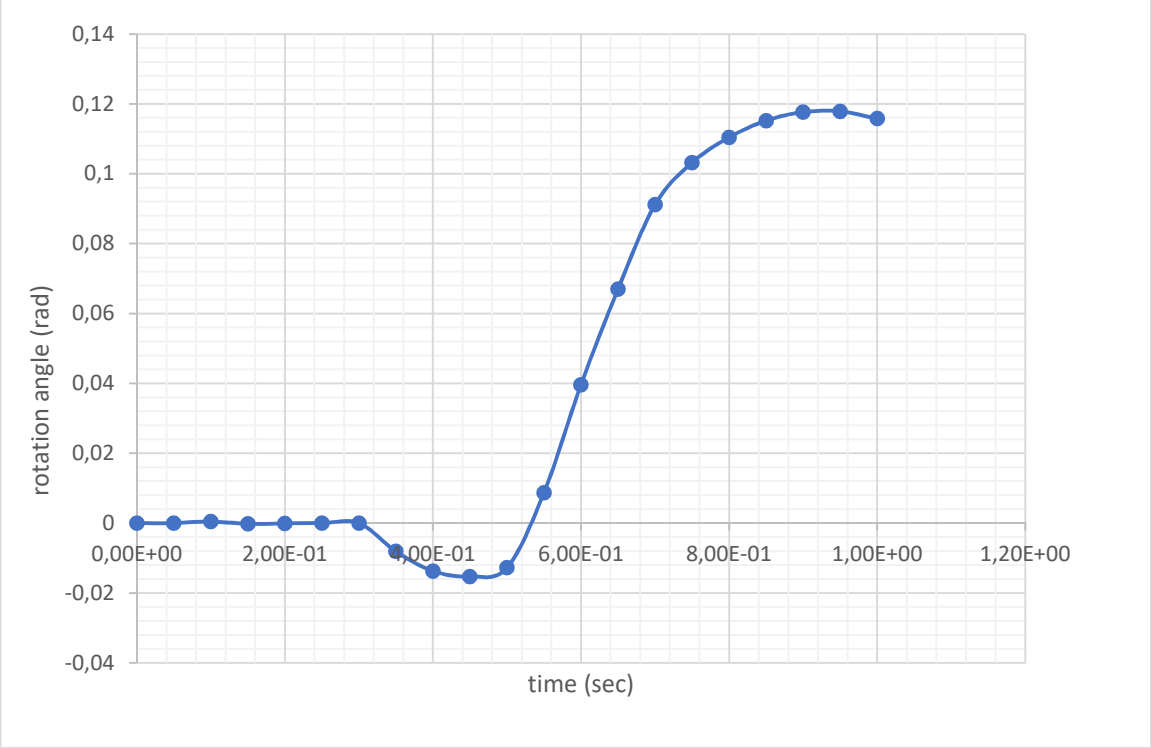

Figure 60: Rotation angle for base isolated model (T=0.5s , a =0.8g)

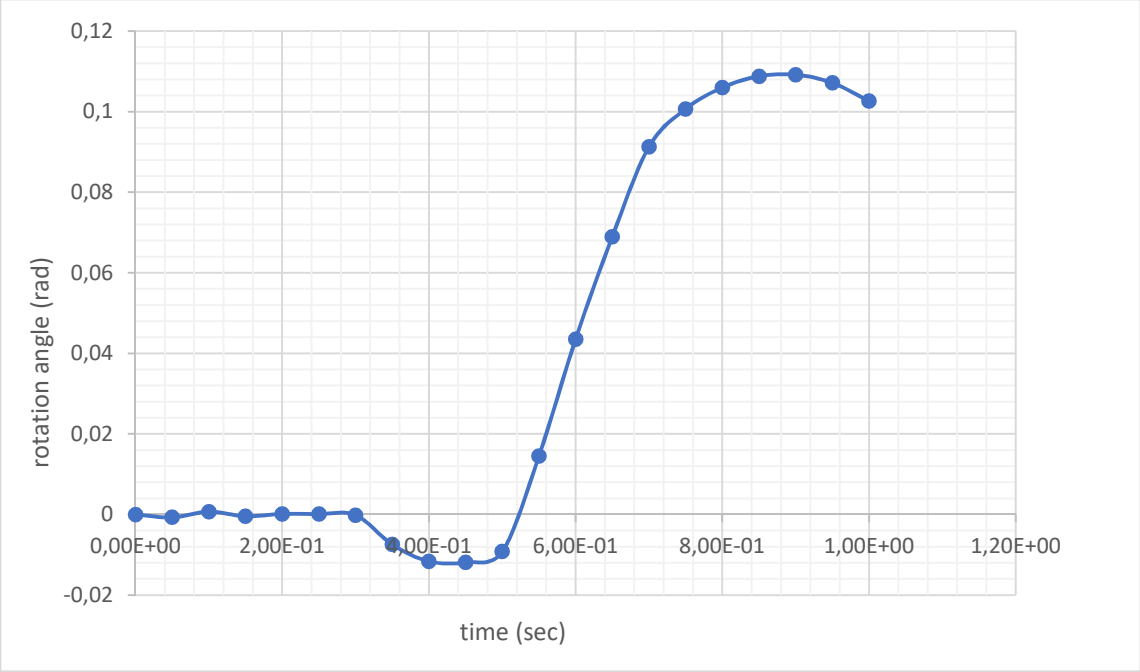

Figure 61: Rotation angle for simple column model (T=0.5s , a =0.8g)

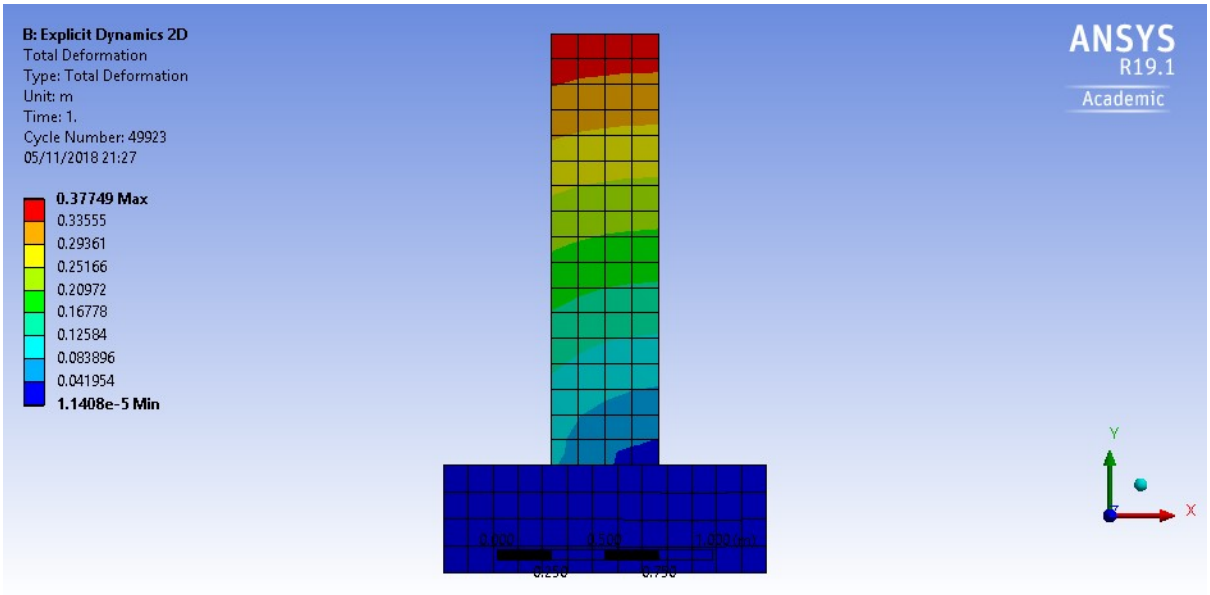

Figure 62 :Total Deformation (T=0.5s , a =1.2g)

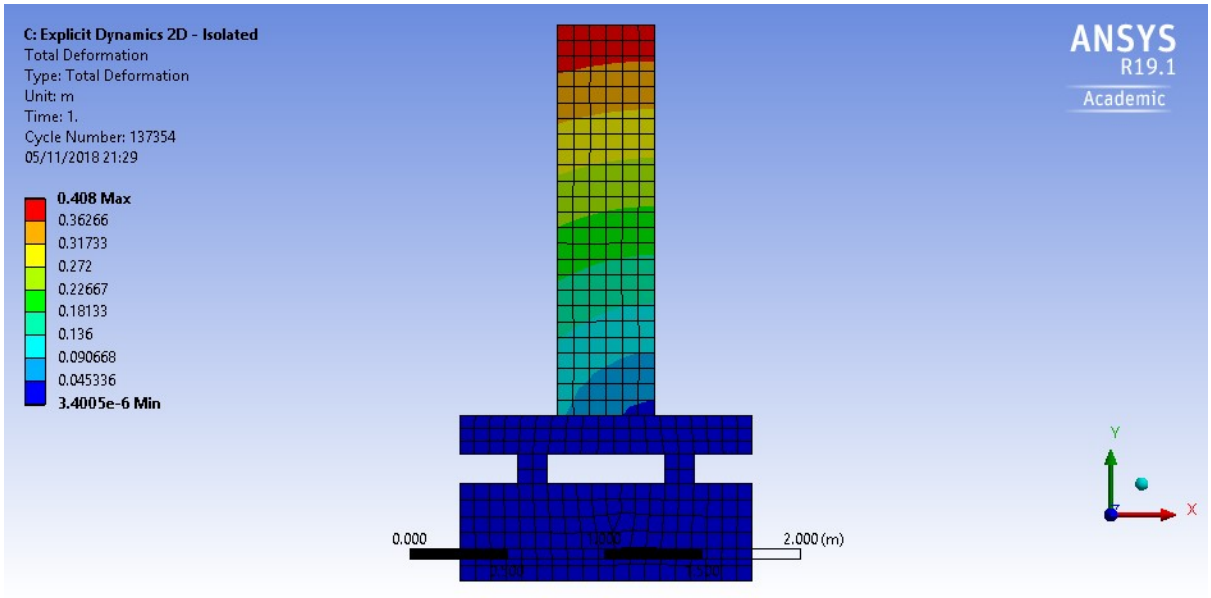

Figure 63 :Total Deformation (base isolated, T=0.5s , a =1.2g)

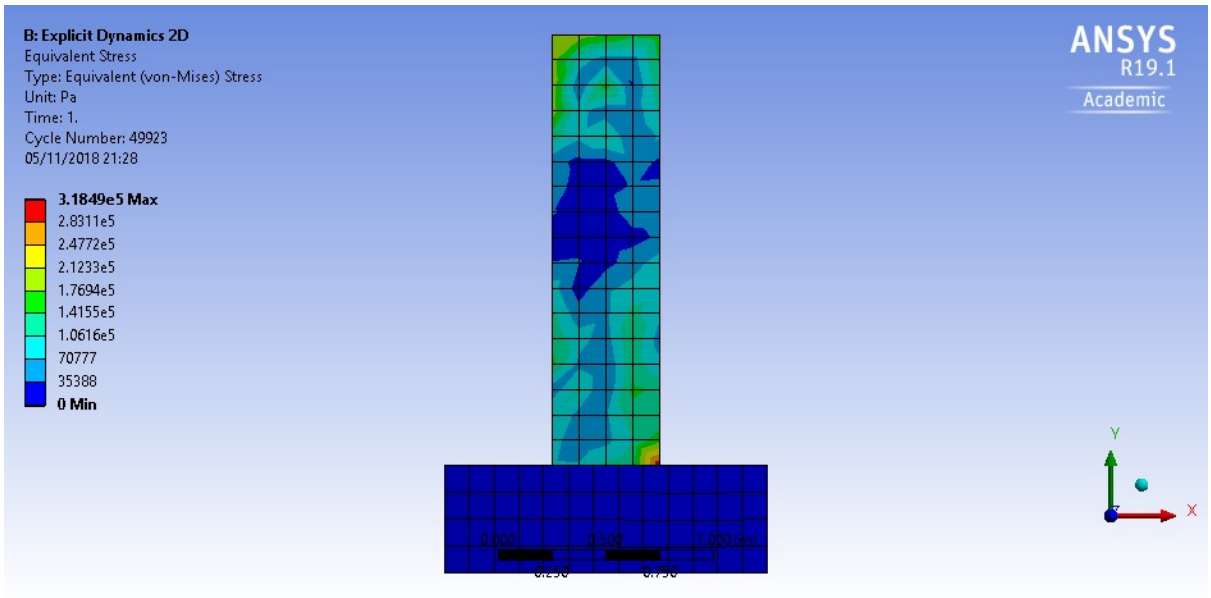

Figure 64 :Von Mises stress simple column model (T=0.5s , a =0.8g)

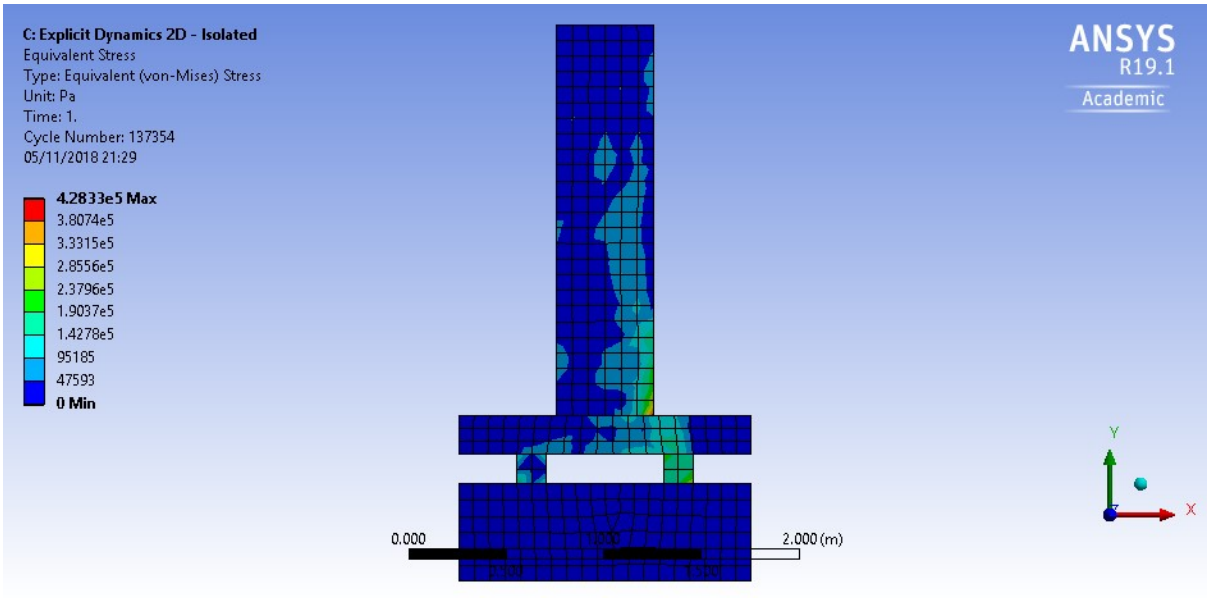

Figure 65 : Von Mises stress base isolated model (T=0.5s , a =1.2g)

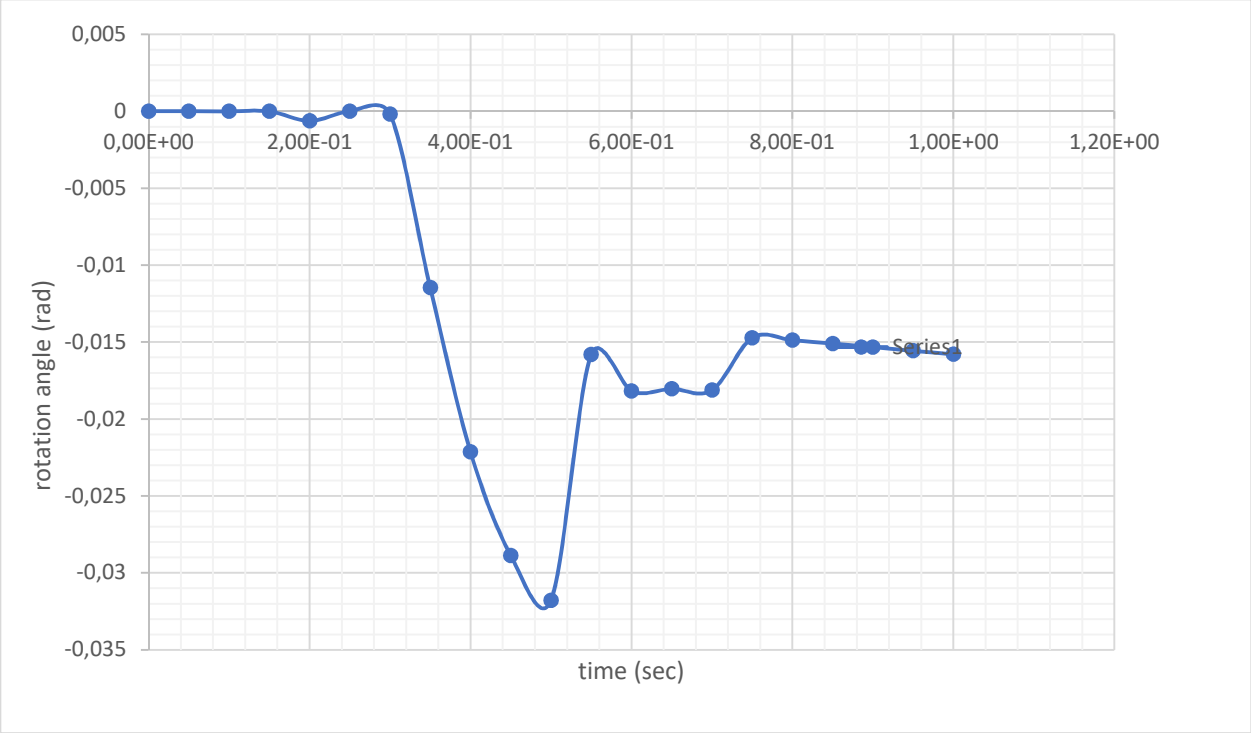

Figure 66: Rotation angle for base isolated model (T=0.5s , a =1.2g)

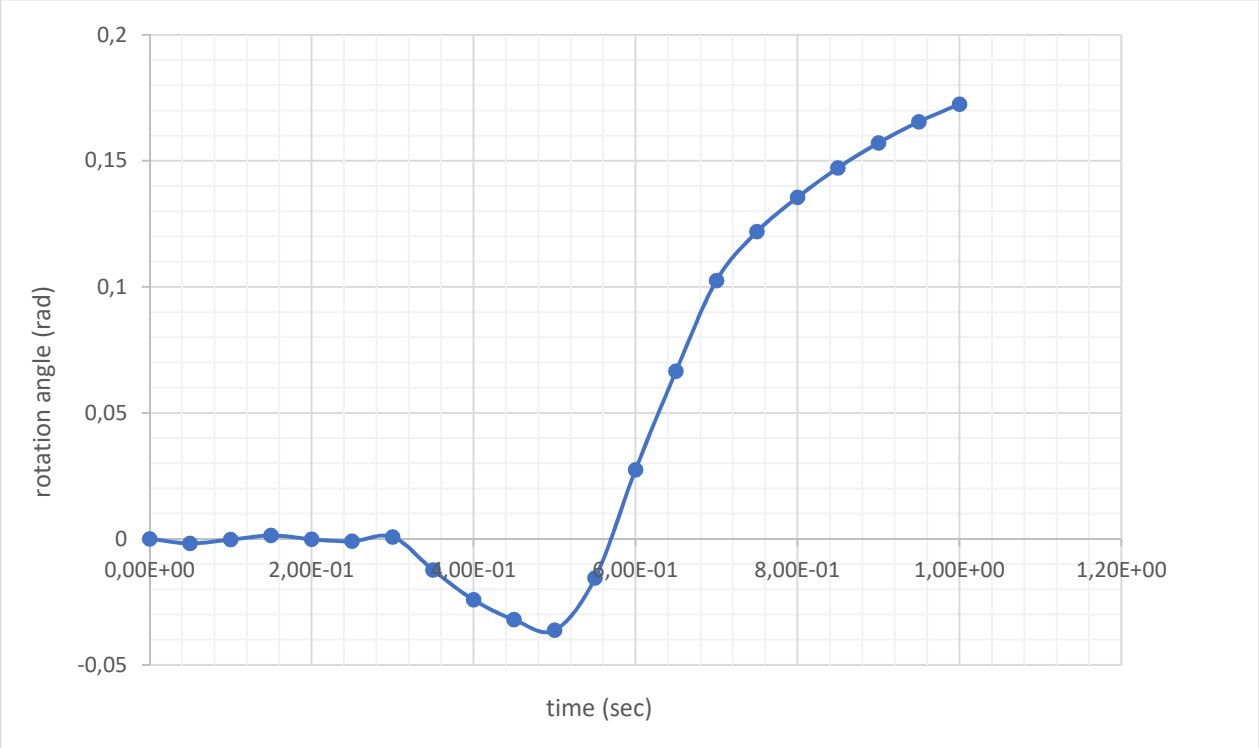

Figure 67: Rotation angle for simple column model (T=0.5s , a =1.2g)

1.3.4 Simulation for T= 0.6s and a= 0.3g, 0.5g , 0.8g and 1.2g

Time	Displacement a=0.5g	Displacement a=0.5g	Displacement a=0.3g	Displacement a=0.3g
0	0.0894611	0	0.05367666	0
0.1	0.08955088	8.97801E-05	0.053730528	5.3868E-05
0.2	0.090569698	0.001108598	0.054341819	0.000665159
0.3	0.097042827	0.007581727	0.058225696	0.004549036
0.4	0.119334683	0.029873583	0.07160081	0.01792415
0.5	0.157462511	0.068001411	0.094477507	0.040800847
0.6	0.178912946	0.089451846	0.107347768	0.053671108
0.7	0.157462511	0.068001411	0.094477507	0.040800847
0.8	0.119334683	0.029873583	0.07160081	0.01792415
0.9	0.097042827	0.007581727	0.058225696	0.004549036
1	0.090569698	0.001108598	0.054341819	0.000665159
1.1	0.08955088	8.97801E-05	0.053730528	5.3868E-05
1.2	0.0894611	0	0.05367666	0

Table 5: Displacement input data for T=0.6 sec

Time	Displacement a=0.8g	Displacement a=0.8g	Displacement a=1.2g	Displacement a=1.2g
0	0.14313776	0	0.21470664	0
0.1	0.143281408	0.000143648	0.214922112	0.000215472
0.2	0.144911517	0.001773757	0.217367276	0.002660636
0.3	0.155268523	0.012130763	0.232902784	0.018196144
0.4	0.190935493	0.047797733	0.28640324	0.0716966
0.5	0.251940018	0.108802258	0.377910026	0.163203386
0.6	0.286260714	0.143122954	0.429391071	0.214684431
0.7	0.251940018	0.108802258	0.377910026	0.163203386
0.8	0.190935493	0.047797733	0.28640324	0.0716966
0.9	0.155268523	0.012130763	0.232902784	0.018196144
1	0.144911517	0.001773757	0.217367276	0.002660636
1.1	0.143281408	0.000143648	0.214922112	0.000215472
1.2	0.14313776	0	0.21470664	0

Table 6 : Displacement input data for T=0.6 sec (continue)

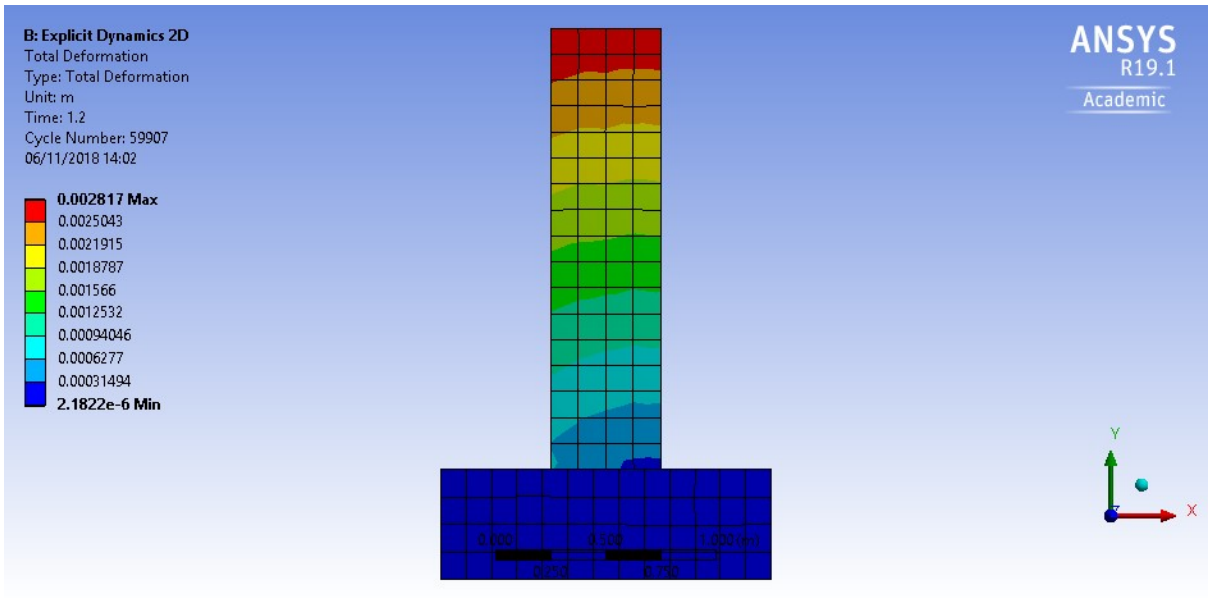

Figure 68: Total Deformation (T=0.6s , a =0.3g)

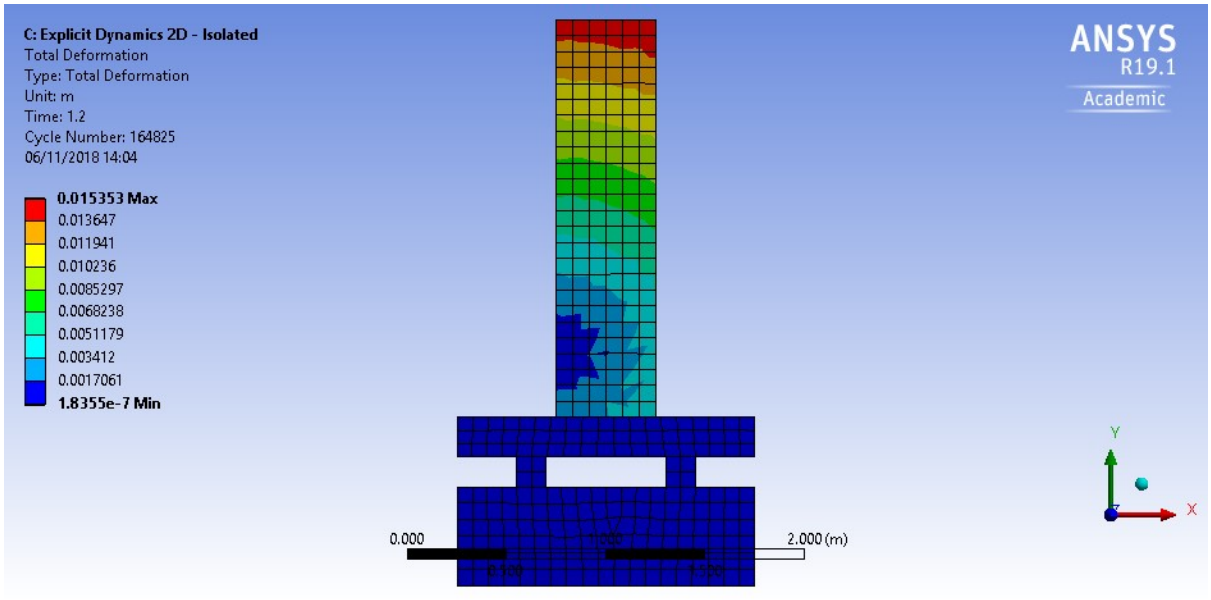

Figure 69 : Total Deformation (base isolated, T=0.6s , a =0.3g)

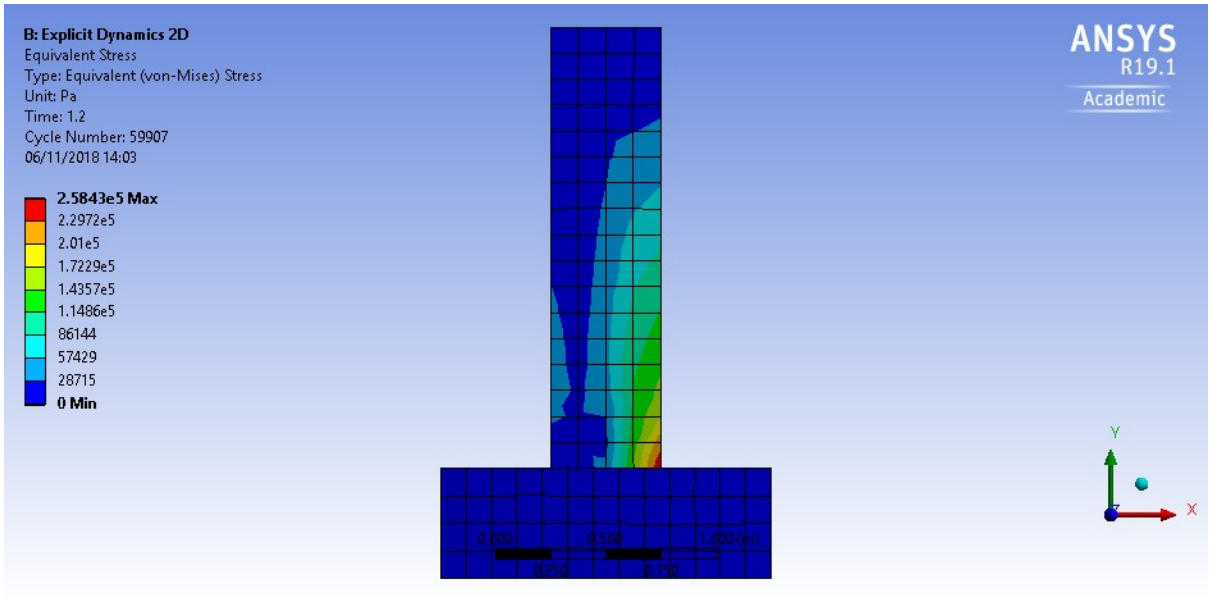

Figure 70: Von Mises stress simple column model (T=0.6s , a =0.3g)

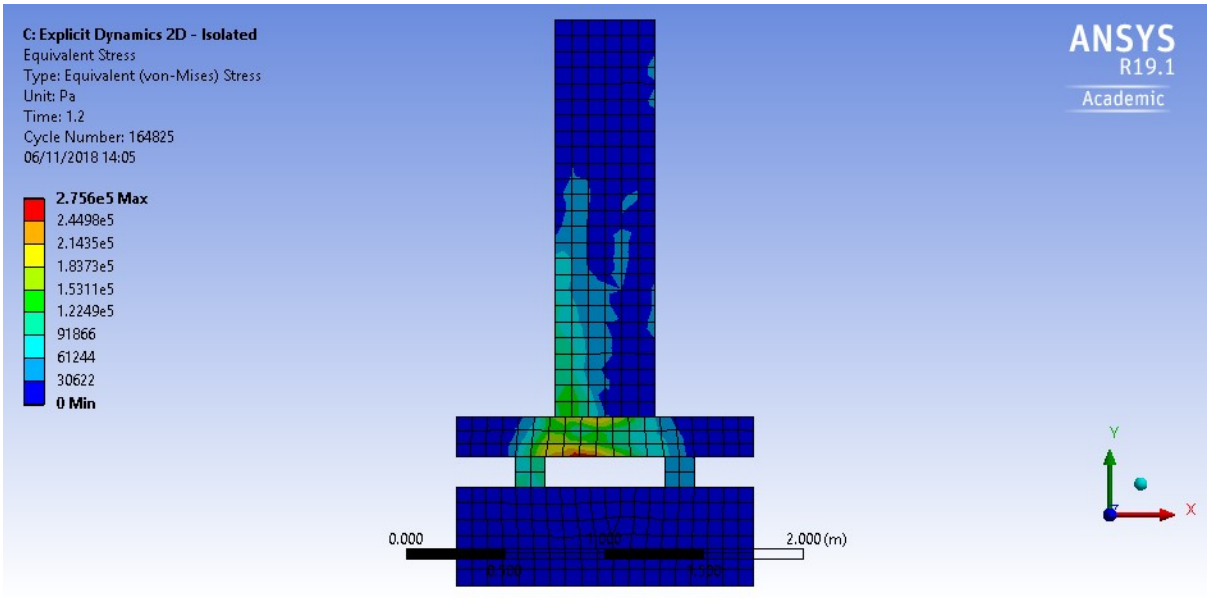

Figure 71 : Von Mises stress base isolated model (T=0.6s , a =0.3g)

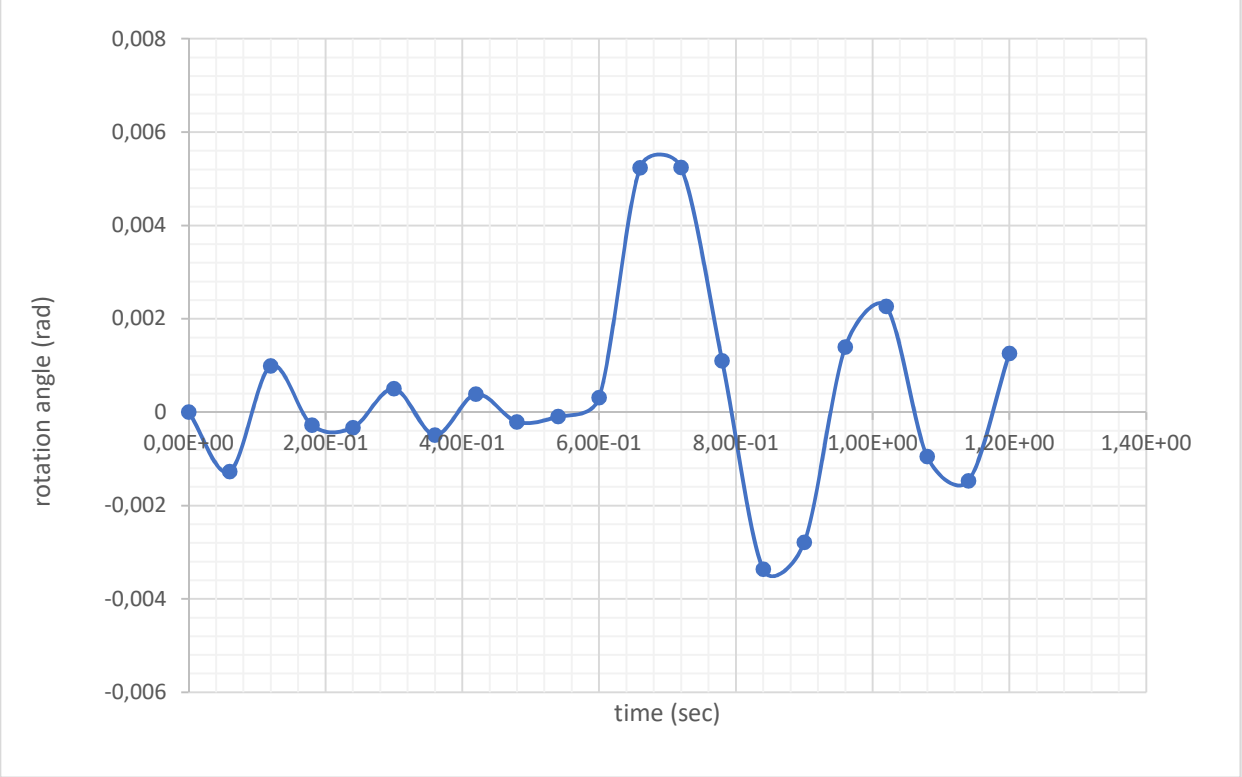

Figure 72 : Rotation angle for simple column model (T=0.6s , a =0.3g)

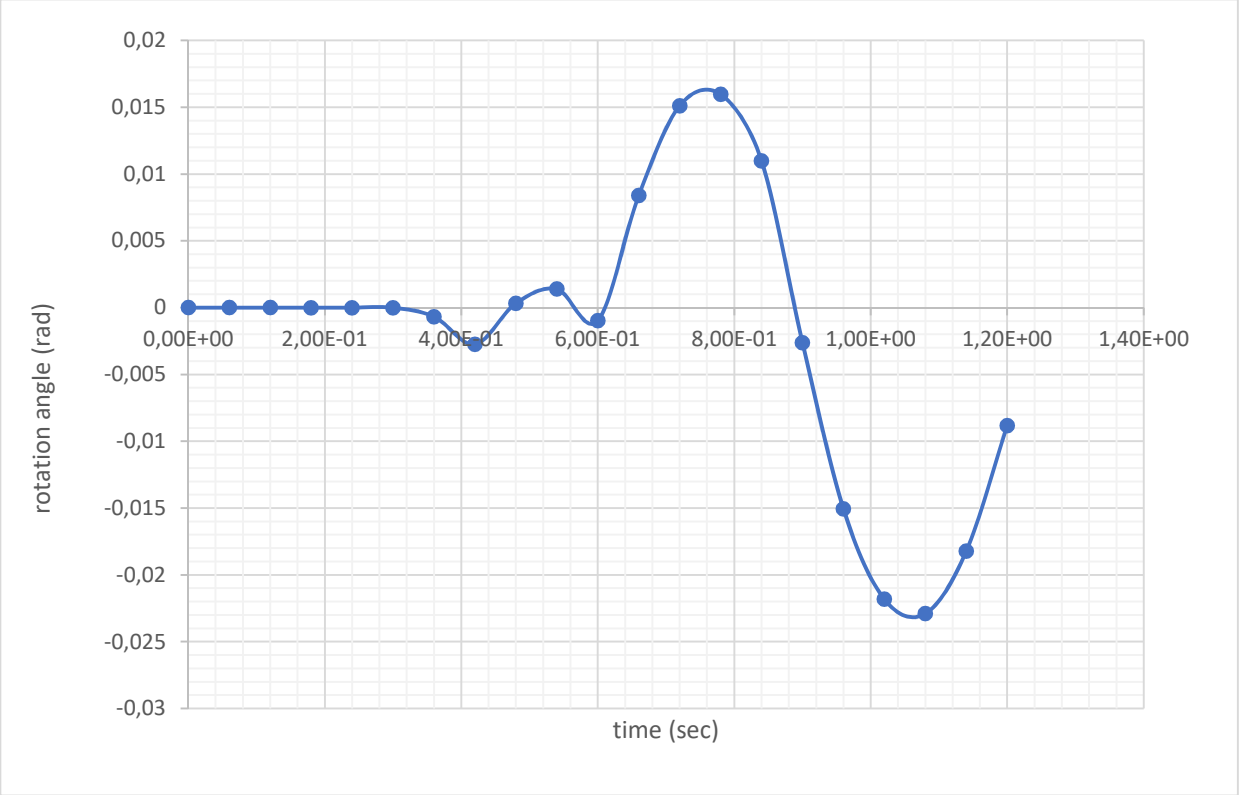

Figure 73 : Rotation angle for base isolated model (T=0.6s , a =0.3g)

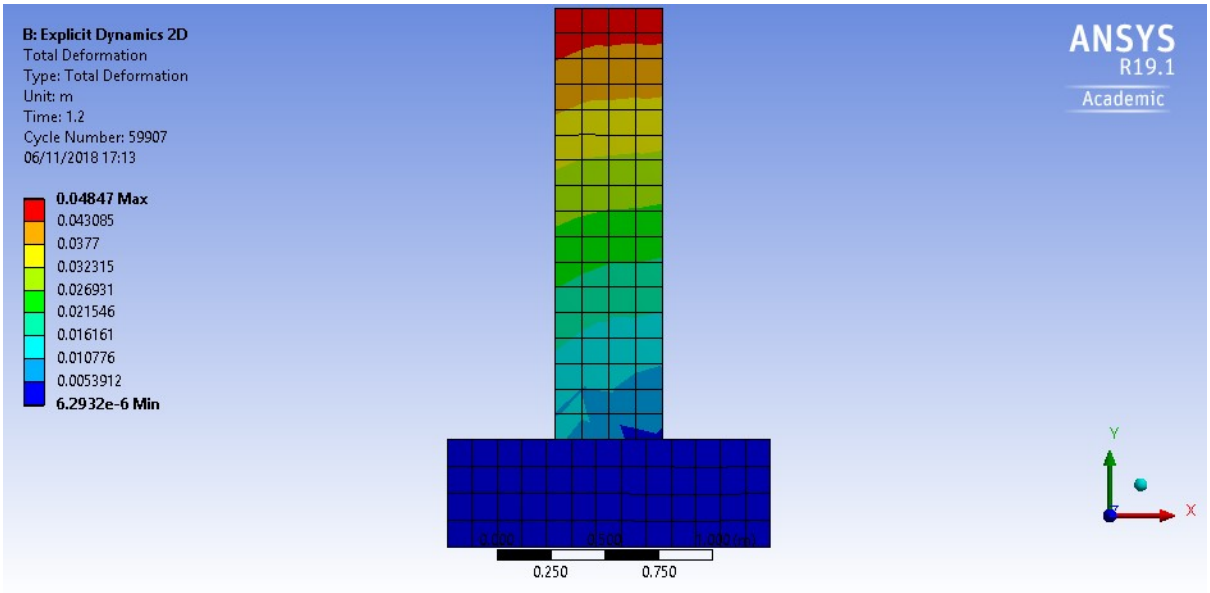

Figure 74 : Total Deformation (simple column, T=0.6s , a =0.5g)

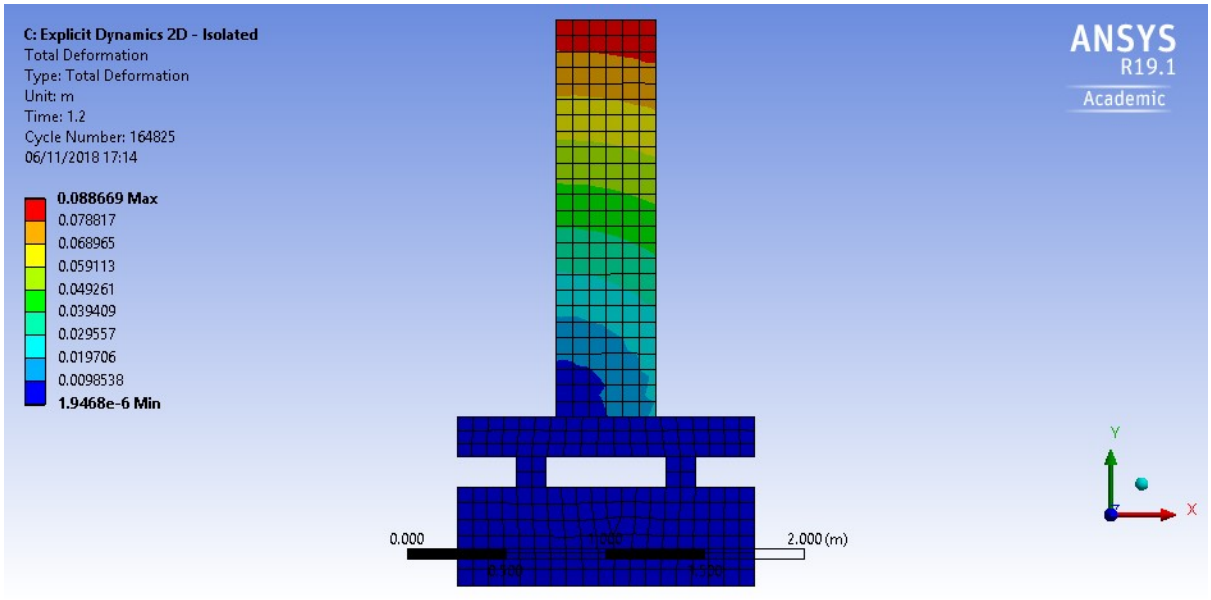

Figure 75 : Total Deformation (base isolated, T=0.6s , a =0.5g)

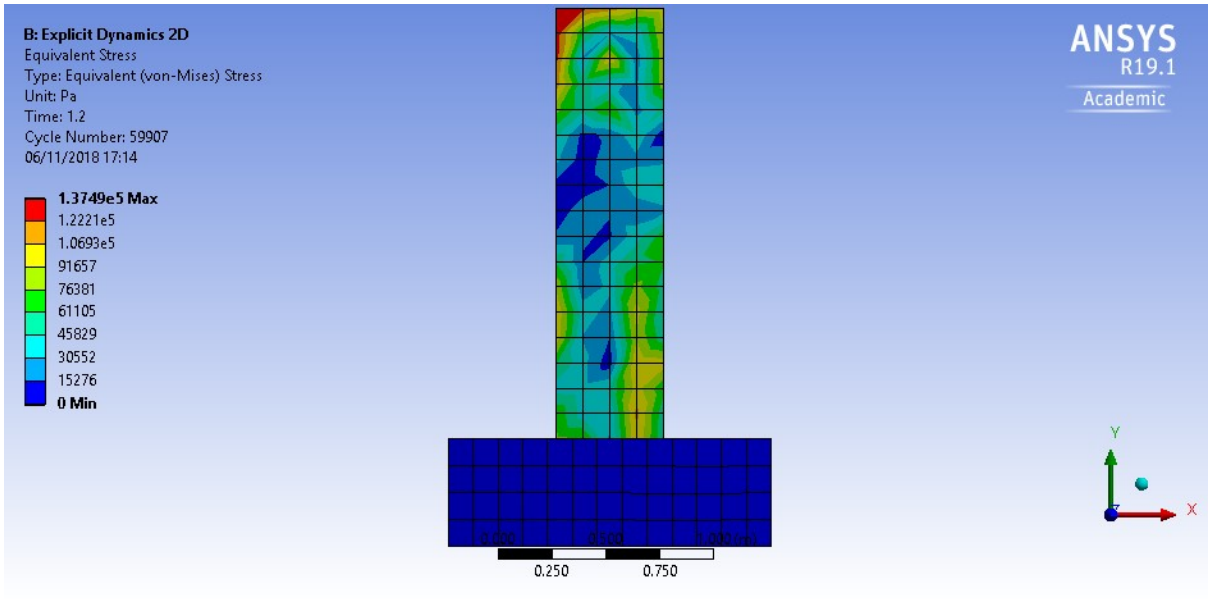

Figure 76 : Von Mises stress simple column model (T=0.6s , a =0.5g)

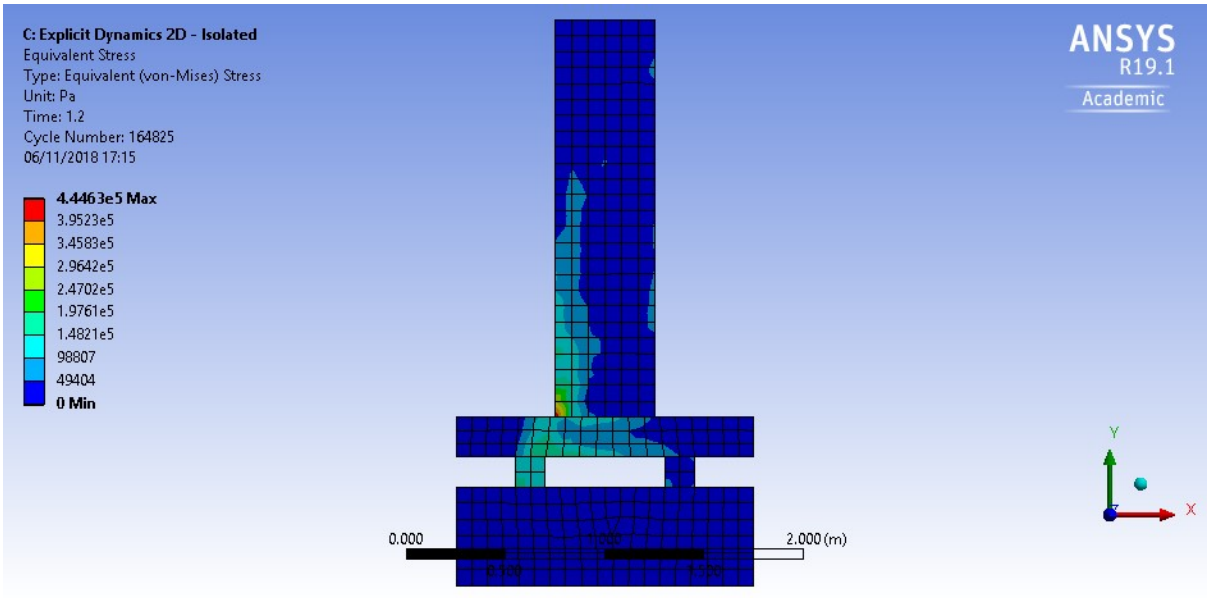

Figure 77 : Von Mises stress base isolated model (T=0.6s , a =0.5g)

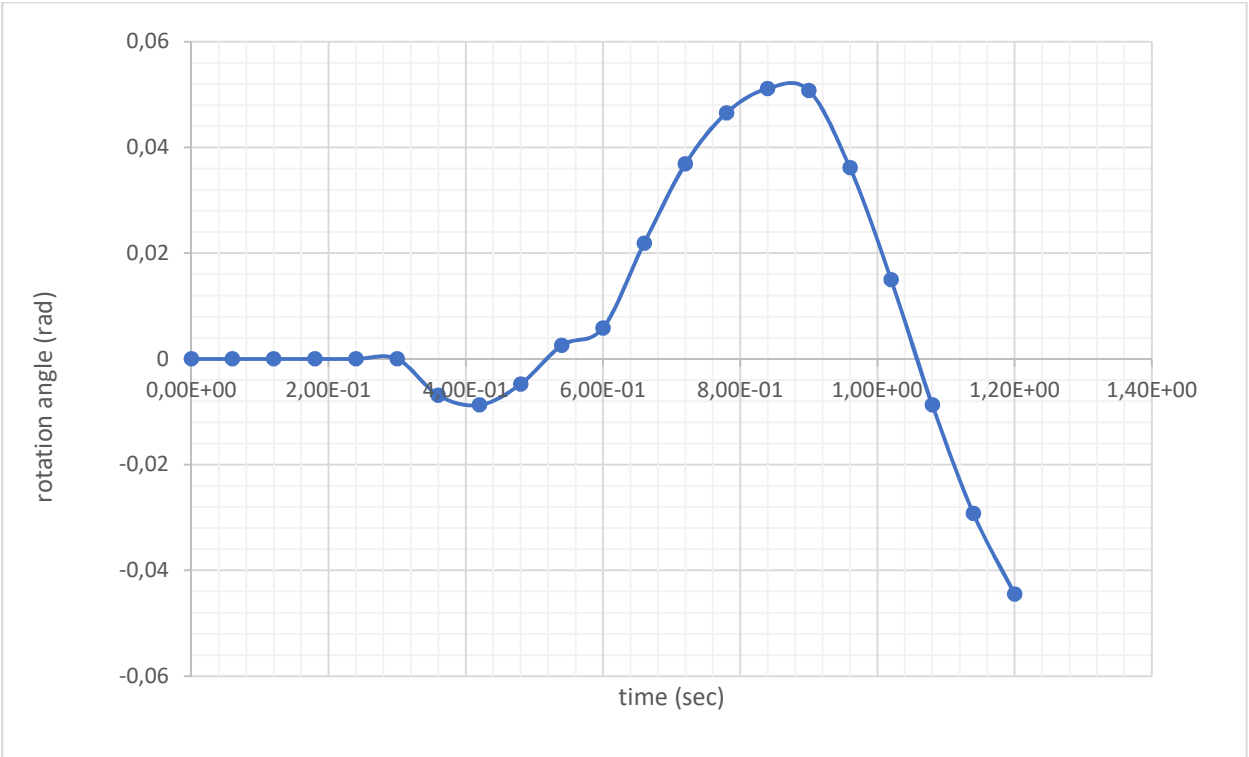

Figure 78 : Rotation angle for base isolated model (T=0.6s , a =0.5g)

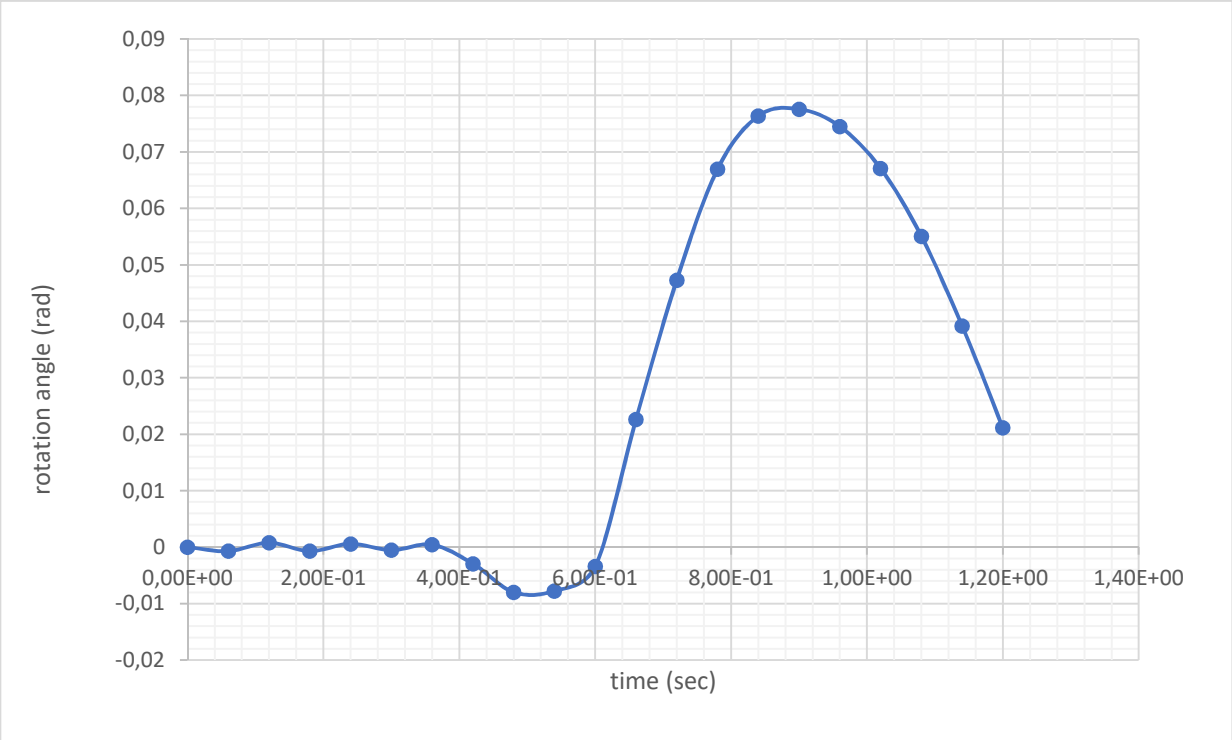

Figure 79: Rotation angle for simple column model (T=0.6s , a =0.5g)

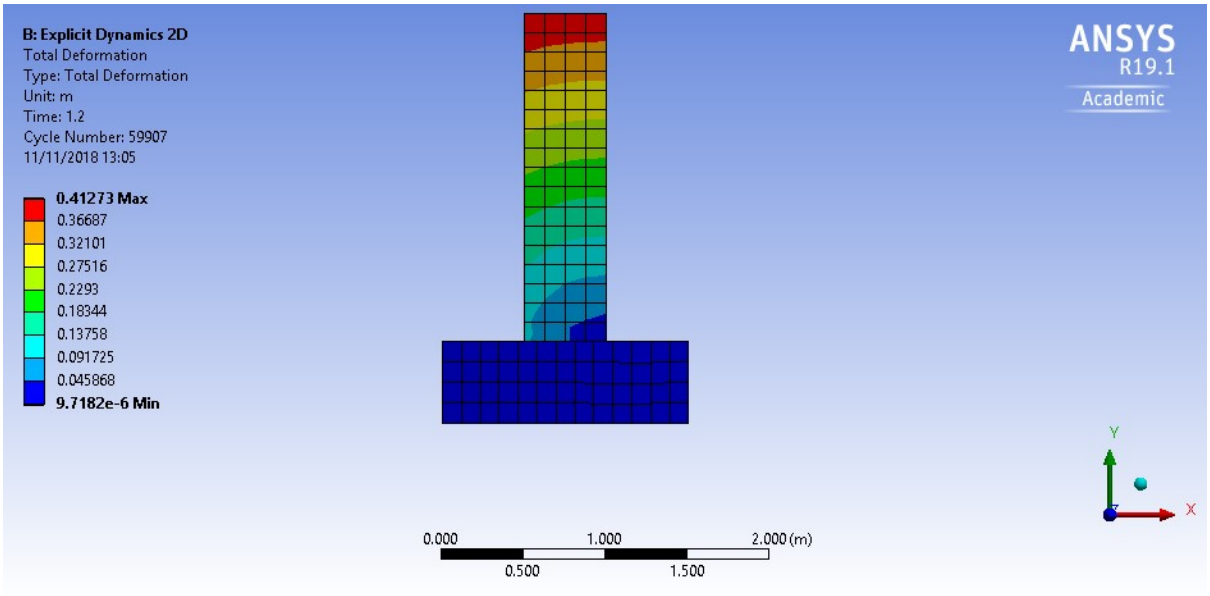

Figure 80 : Total Deformation (simple column, T=0.6s , a =0.8g)

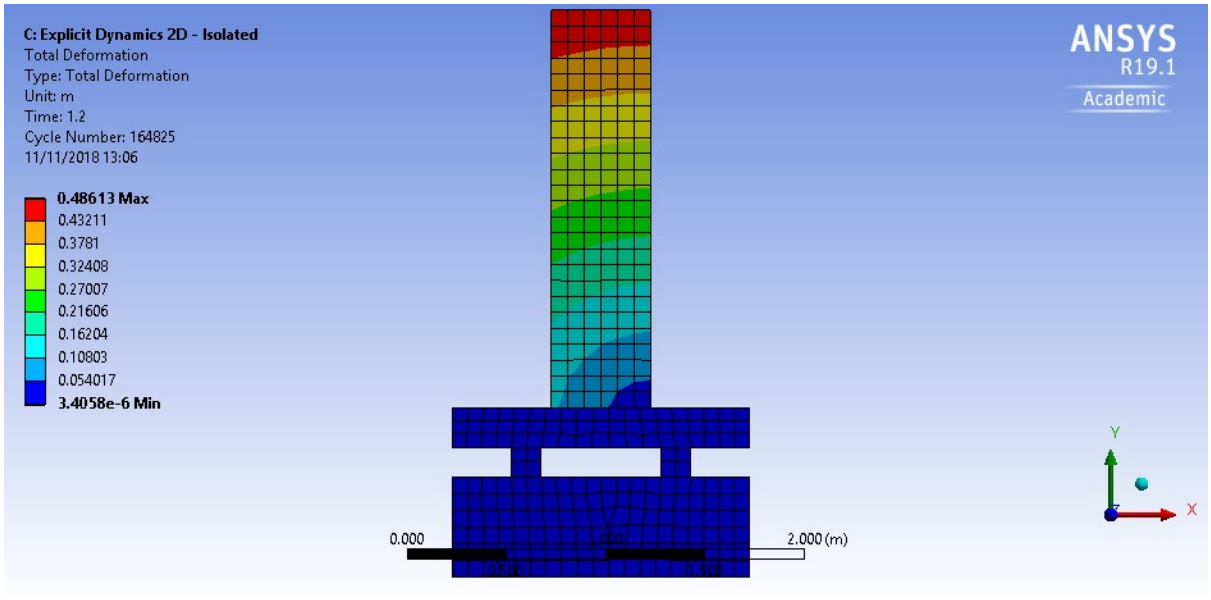

Figure 81 : Total Deformation (base isolated, T=0.6s , a =0.8g)

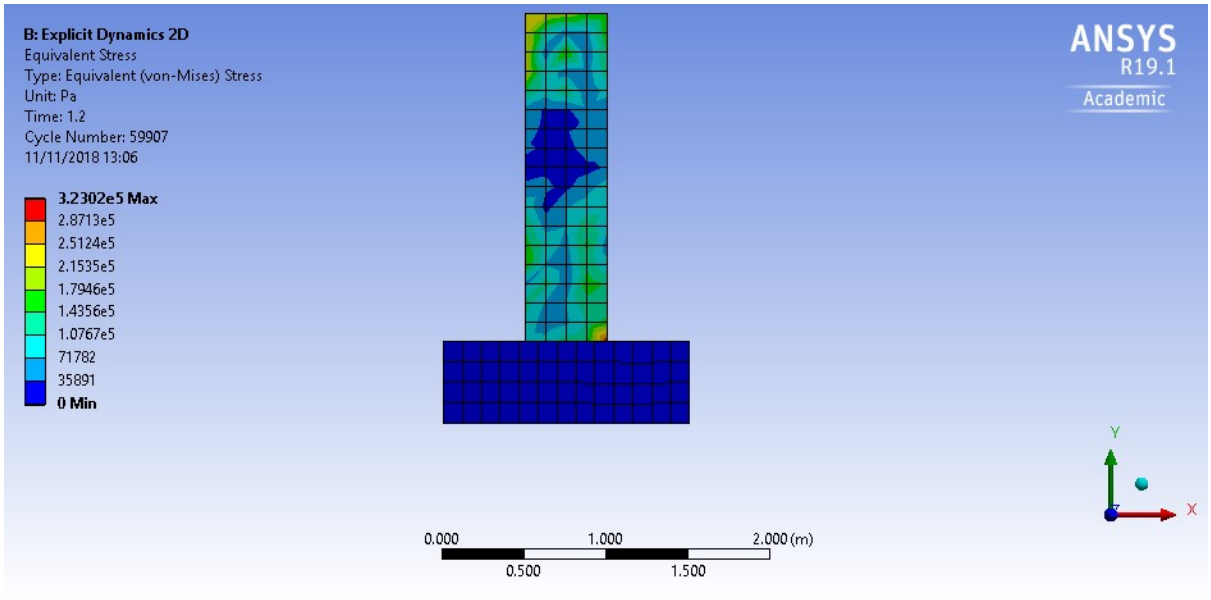

Figure 82 : Von Mises stress for simple column model (T=0.6s , a =0.8g)

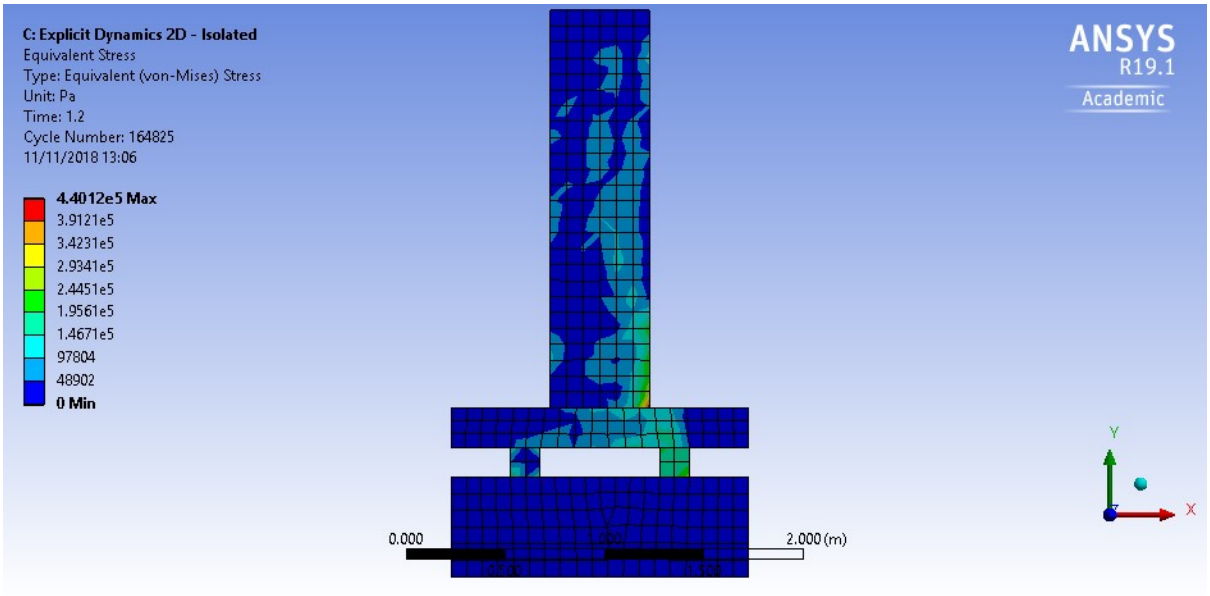

Figure 83 : Von Mises stress (base isolated model, T=0.6s, a =0.8g)

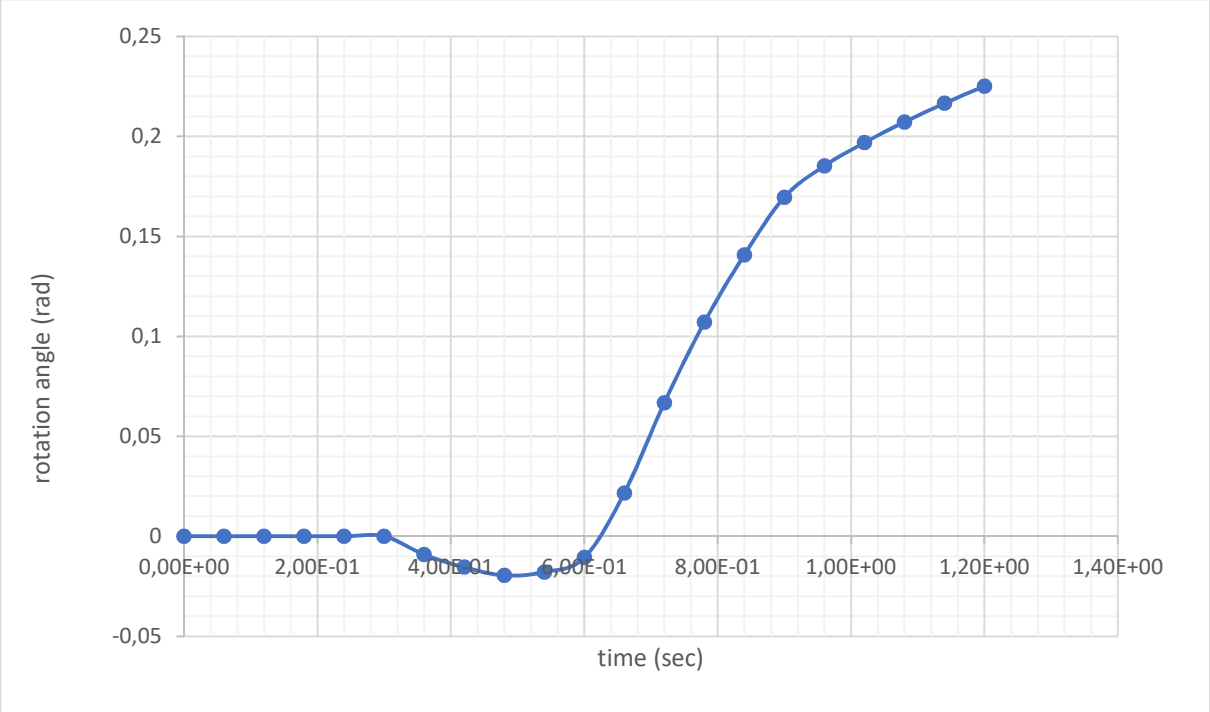

Figure 84: Rotation angle for base isolated model (T=0.6s , a =0.8g)

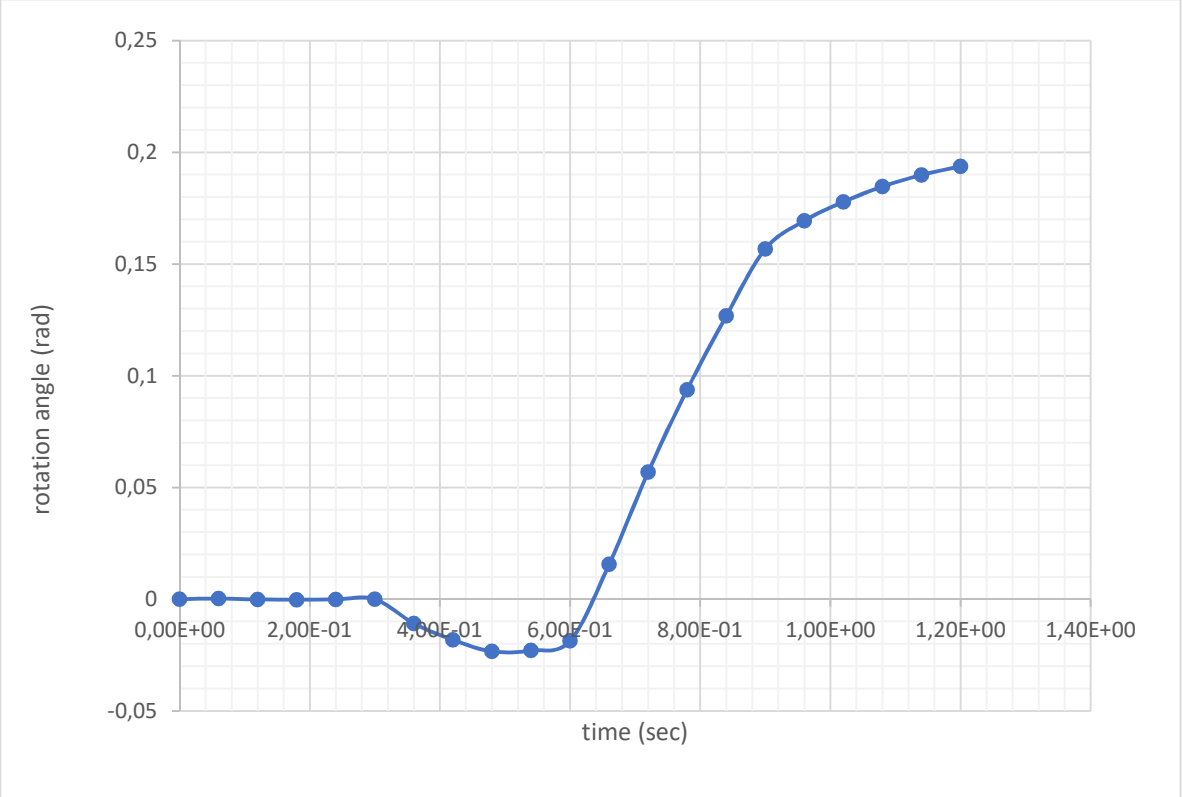

Figure 85: Rotation angle for simple column model (T=0.6s , a =0.8g)

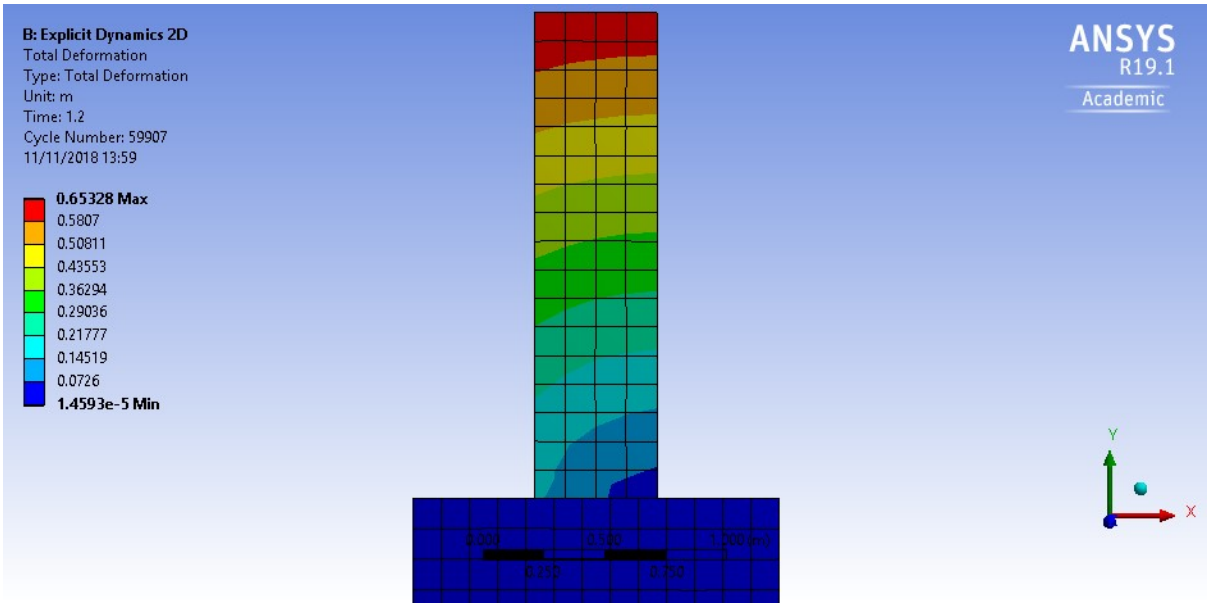

Figure 86 : Total Deformation (simple column, T=0.6s , a =1.2g)

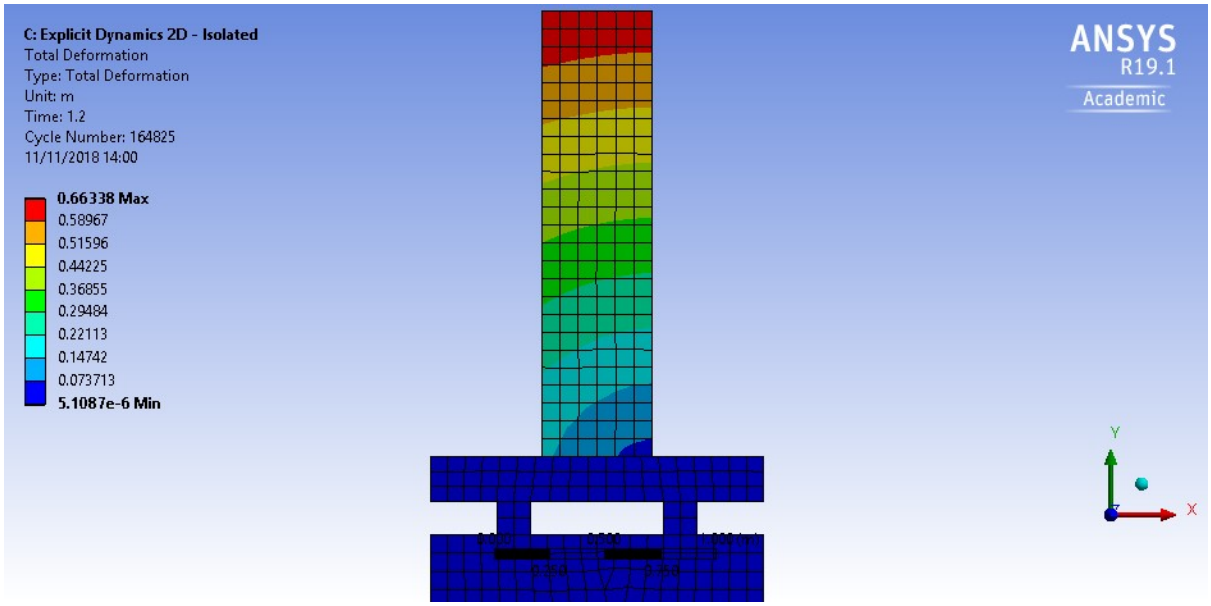

Figure 87 : Total Deformation (base-isoplated, T=0.6s , a =1.2 g)

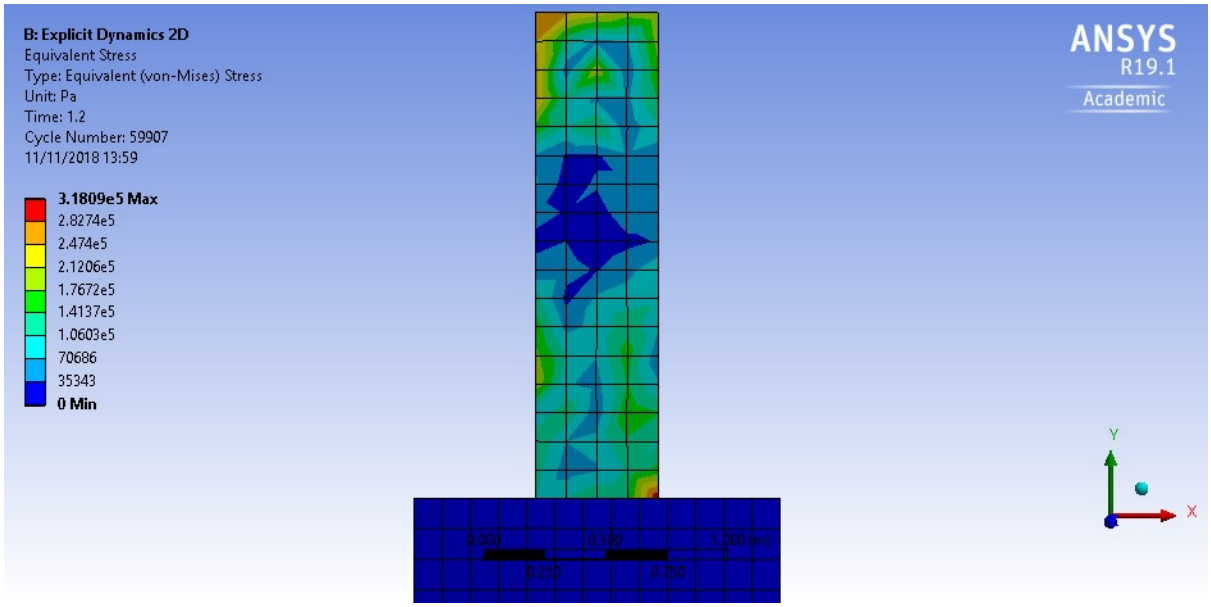

Figure 88 : Von Mises stress (simple column model, T=0.6s, a =1.2g)

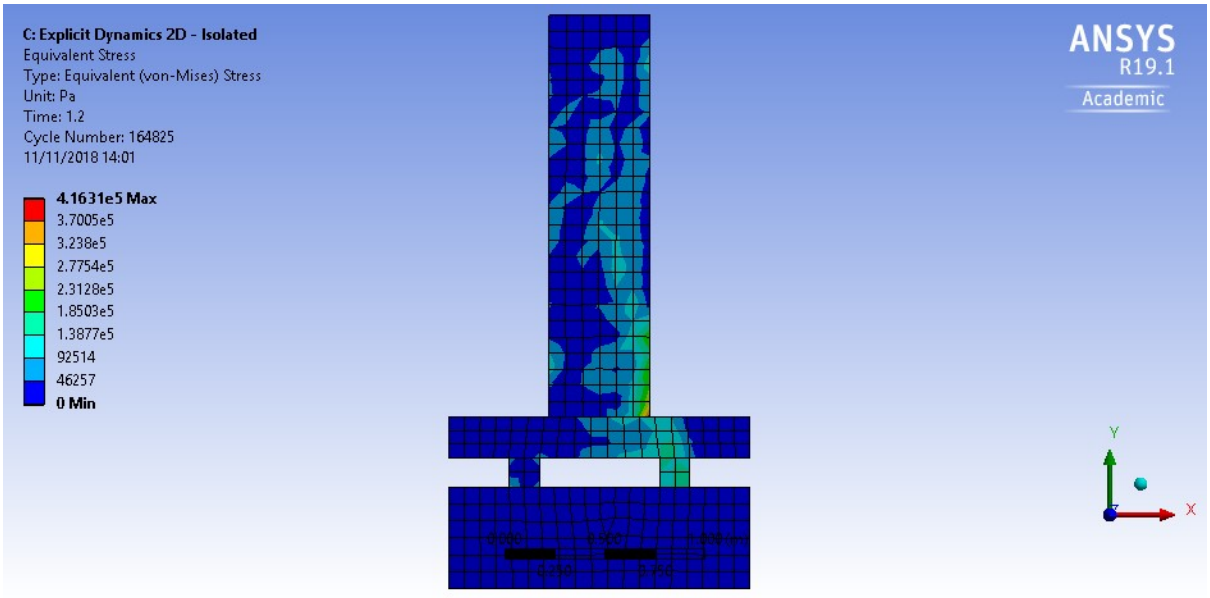

Figure 89 : Von Mises stress (base isolated model, T=0.6s, a =1.2g)

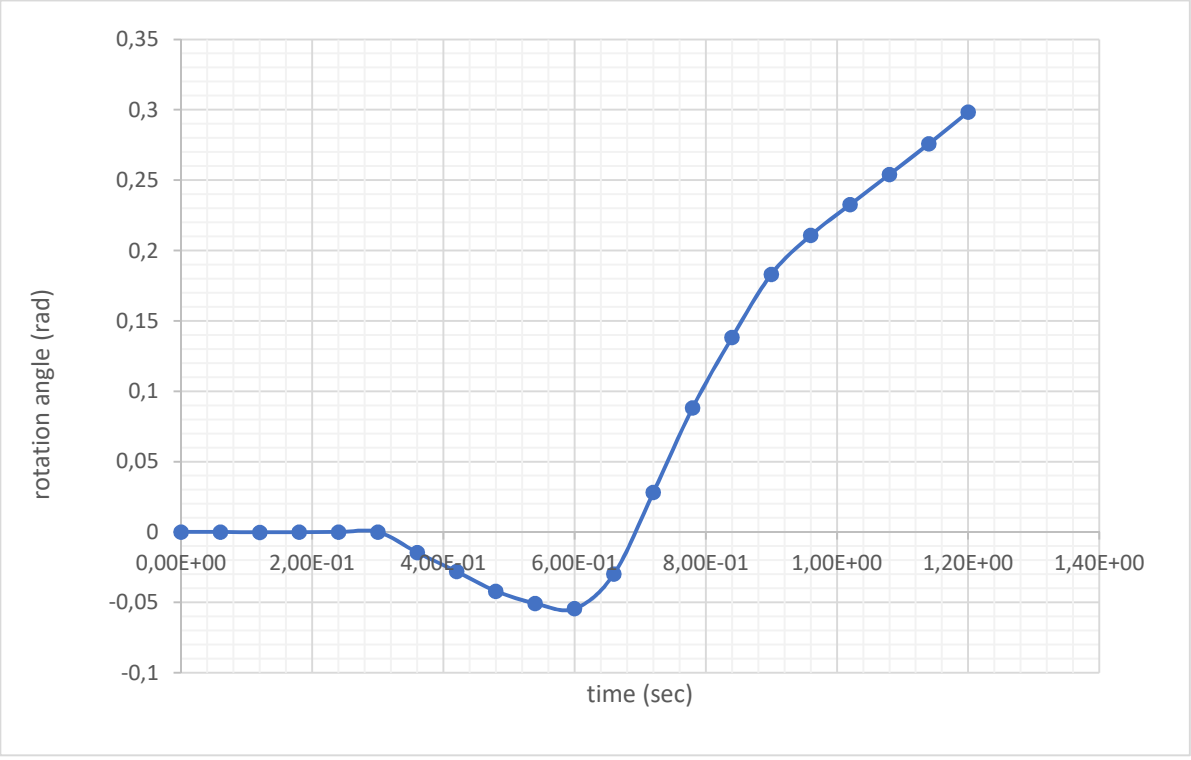

Figure 90 : Rotation angle for base isolated model (T=0.6s , a =1.2g)

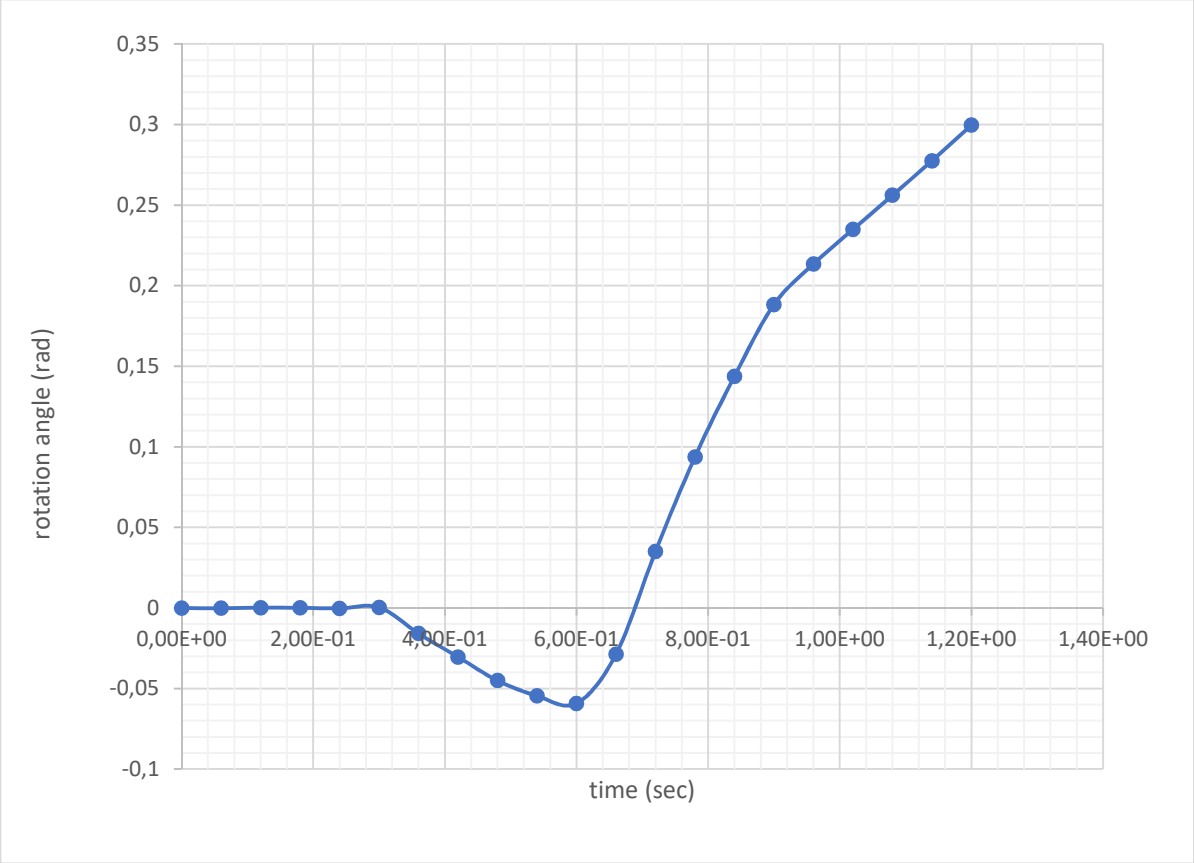

Figure 91 : Rotation angle for simple column model (T=0.6s , a =1.2g)

1.3.5 Simulation for T= 1.2 s and a= 0.15g 0.3g, 0.5g , 0.8g and 1.2g

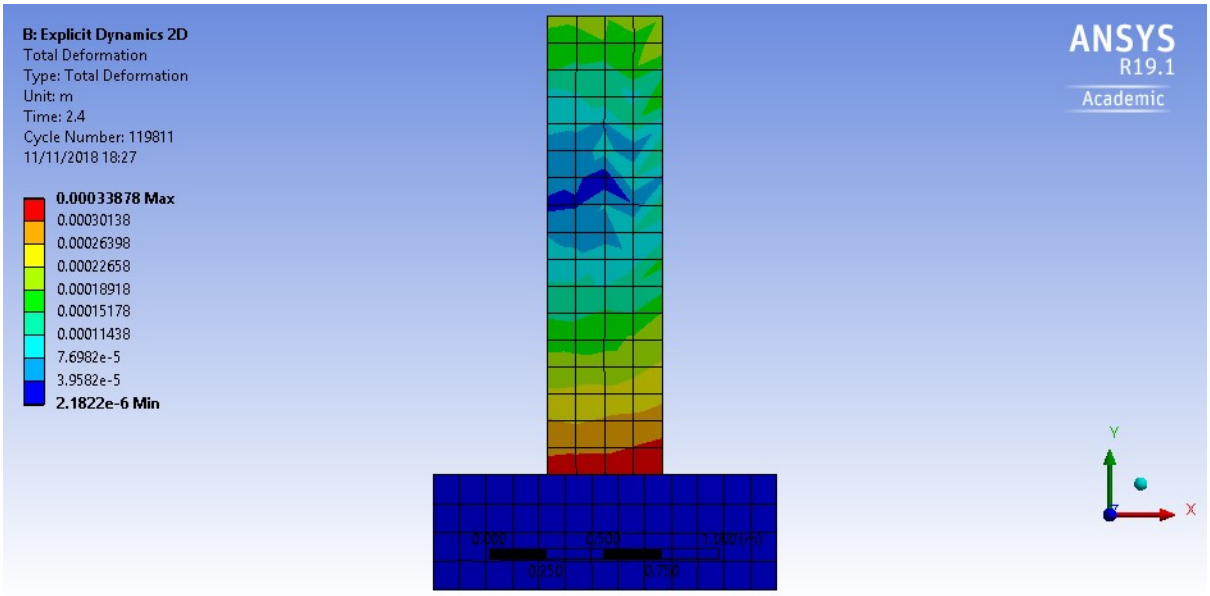

Figure 92: Total Deformation (simple column T=1.2s , a =0.15 g)

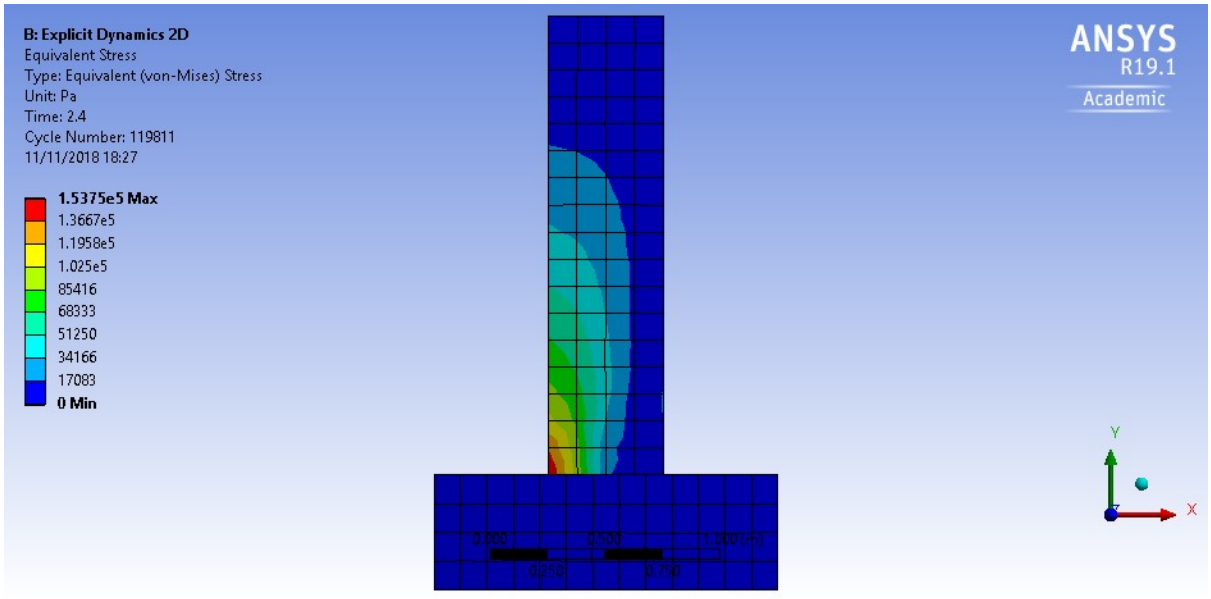

Figure 93 : Stress distribution (simple column, T=1.2s , a =0.15 g)

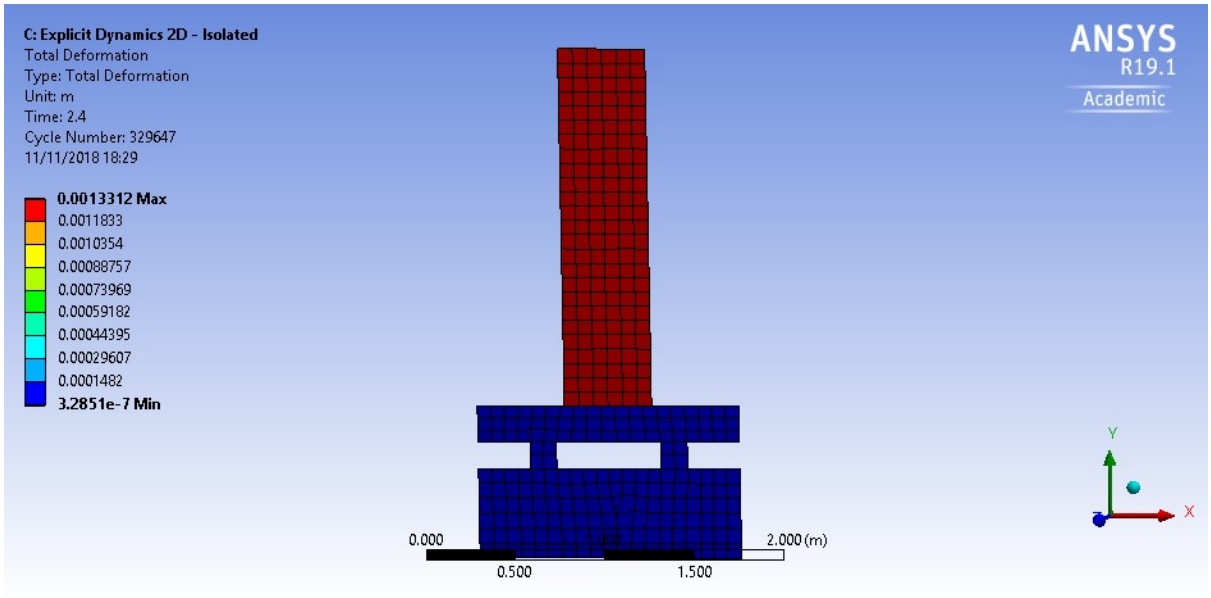

Figure 94 : Total Deformation (base-isoplated, T=1.2s , a =0.15 g)

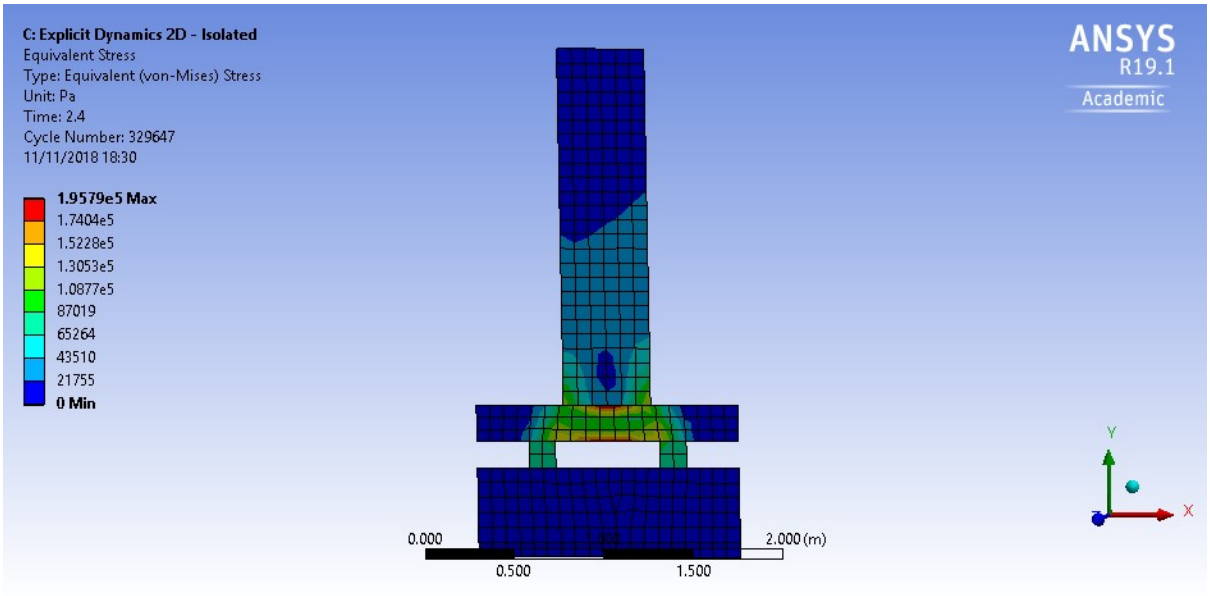

Figure 95 : Stress distribution (base-isolated T=1.2s , a =0.15 g)

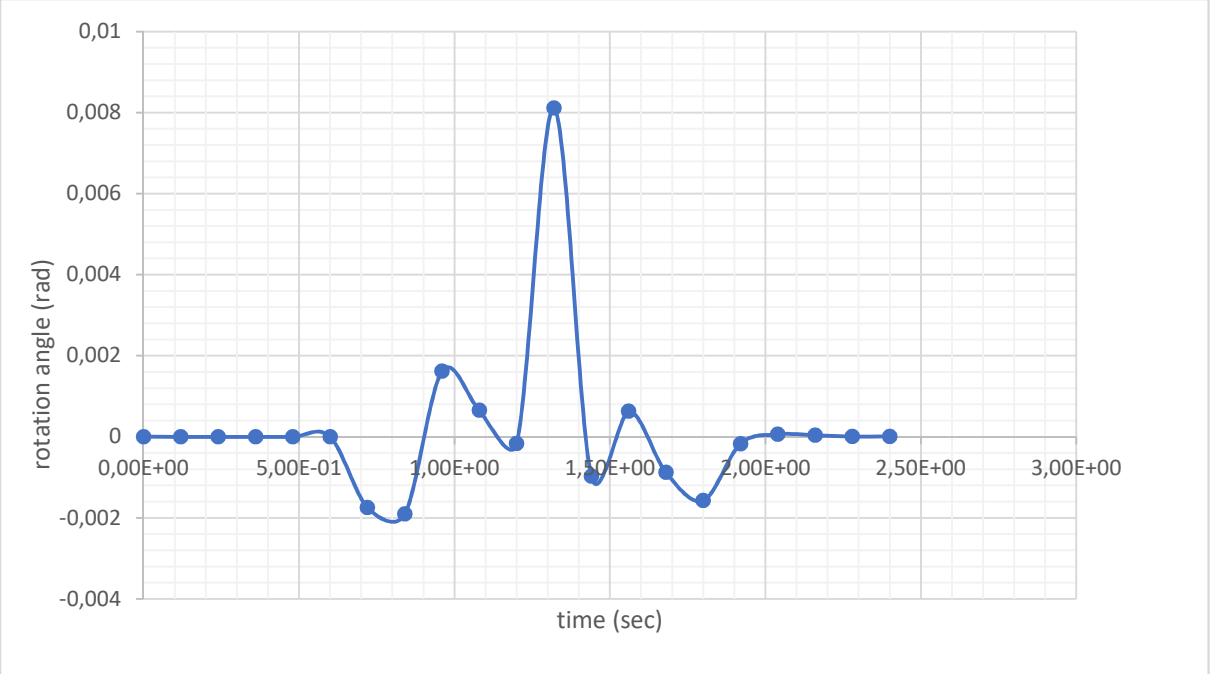

Figure 96: Rotation angle for base isolated model (T=1.2s , a =0.15g)

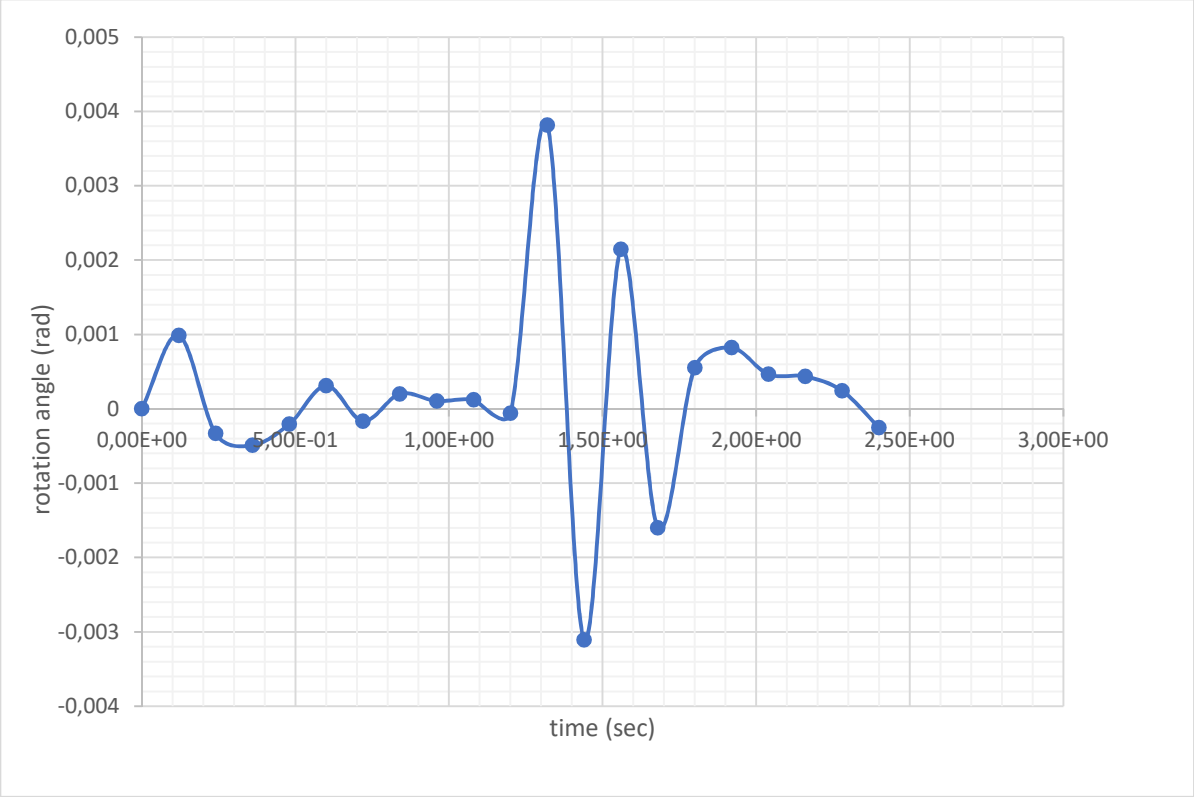

Figure 97 : Rotation angle for simple column model (T=1.2s , a =0.15g)

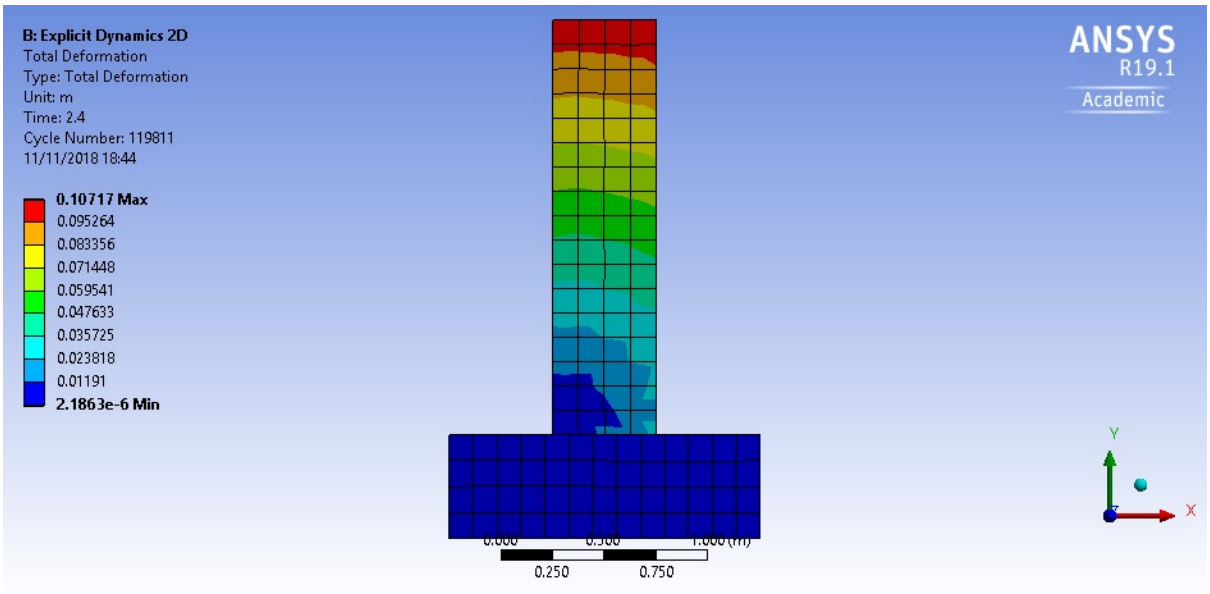

Figure 98: Total deformation (simple column T=1.2s , a =0.3 g)

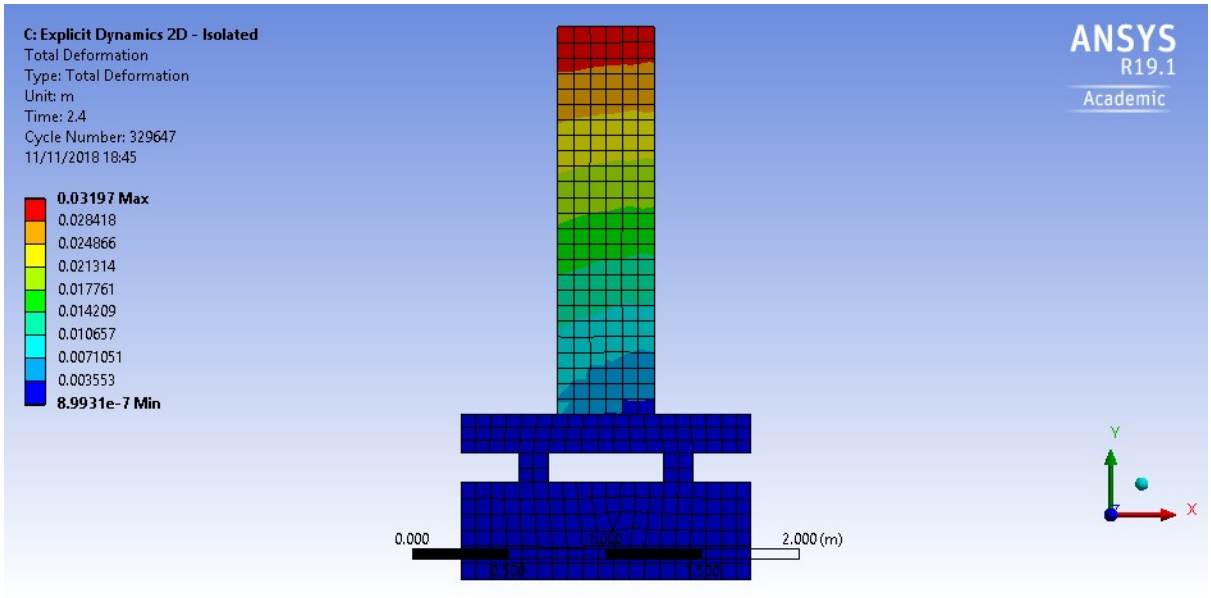

Figure 99 : Total deformation (base-isolated T=1.2s , a =0.3 g)

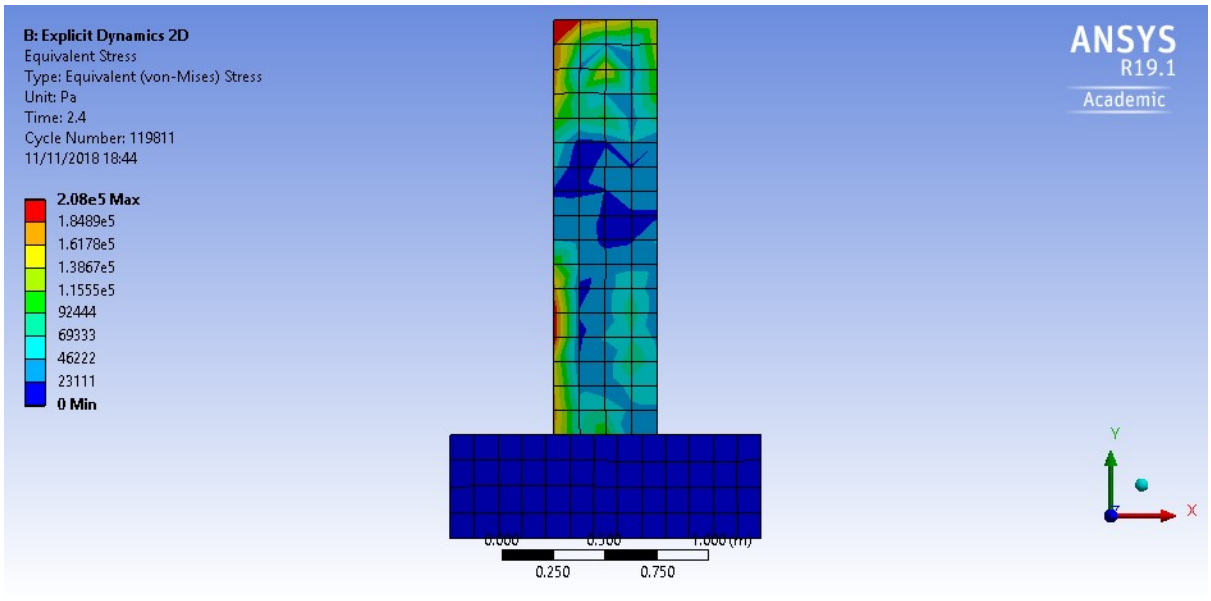

Figure 100 : Stress distribution (simple column T=1.2s , a =0.3 g)

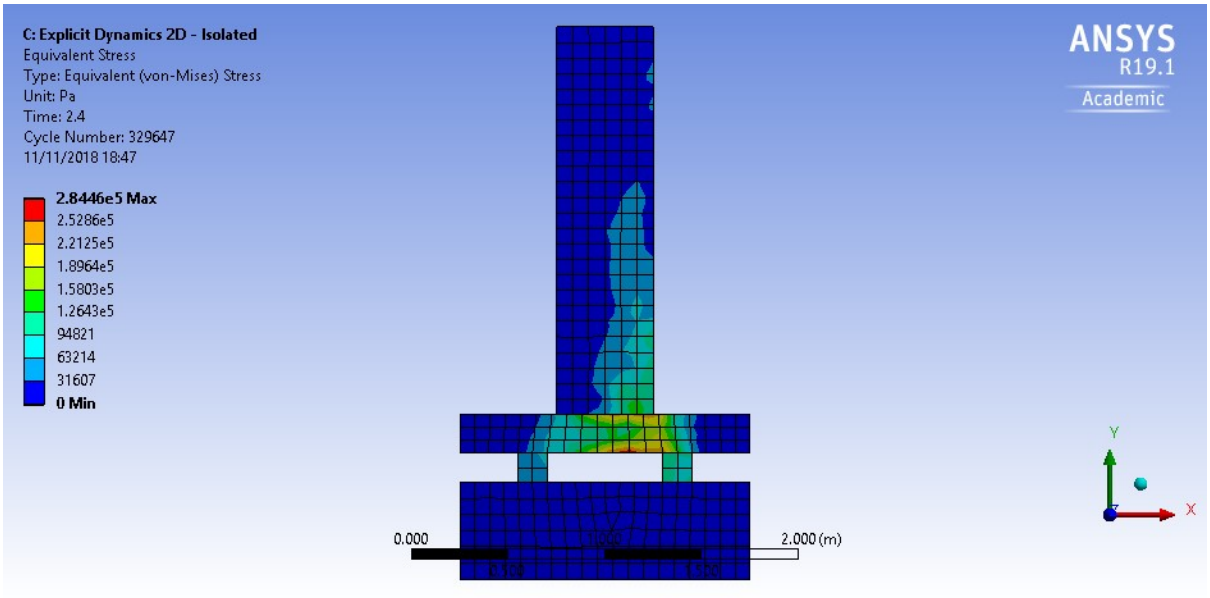

Figure 101 : Stress distribution (base-isolated T=1.2s , a =0.3 g)

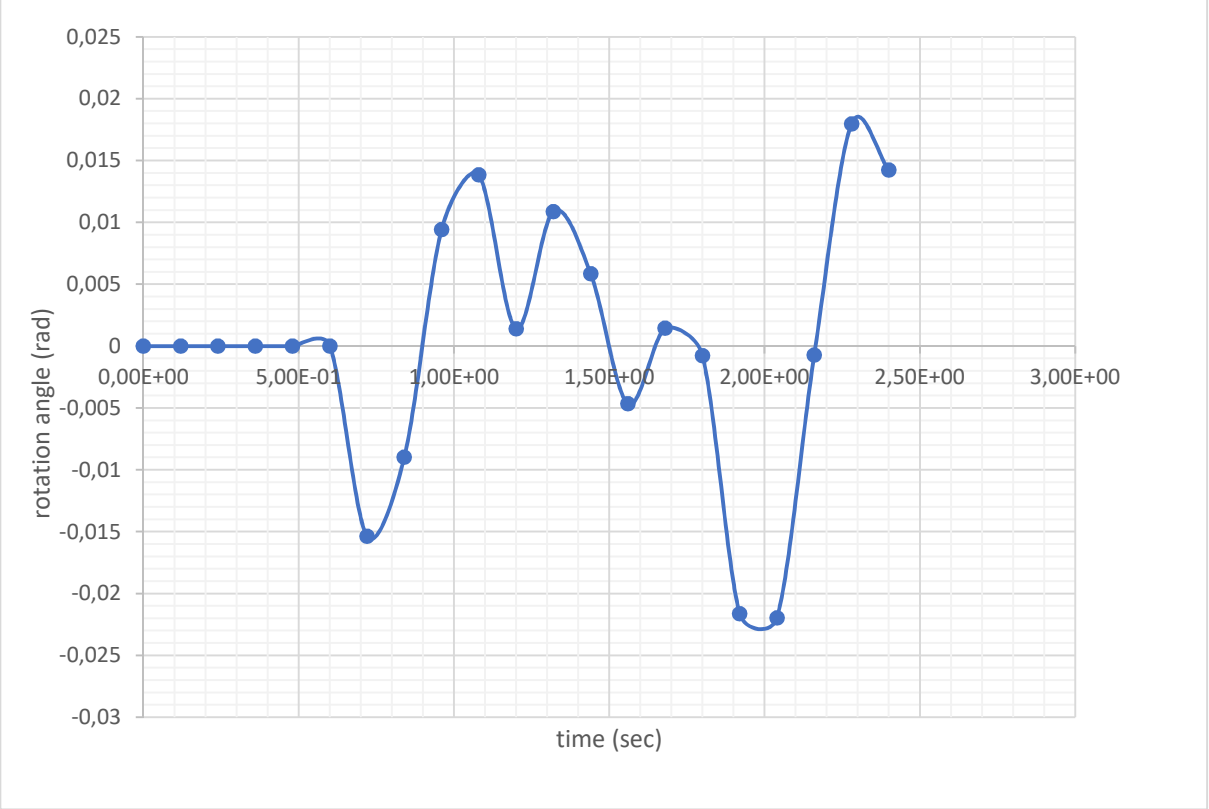

Figure 102 : Rotation angle for simple base-isolated (T=1.2s , a =0.3g)

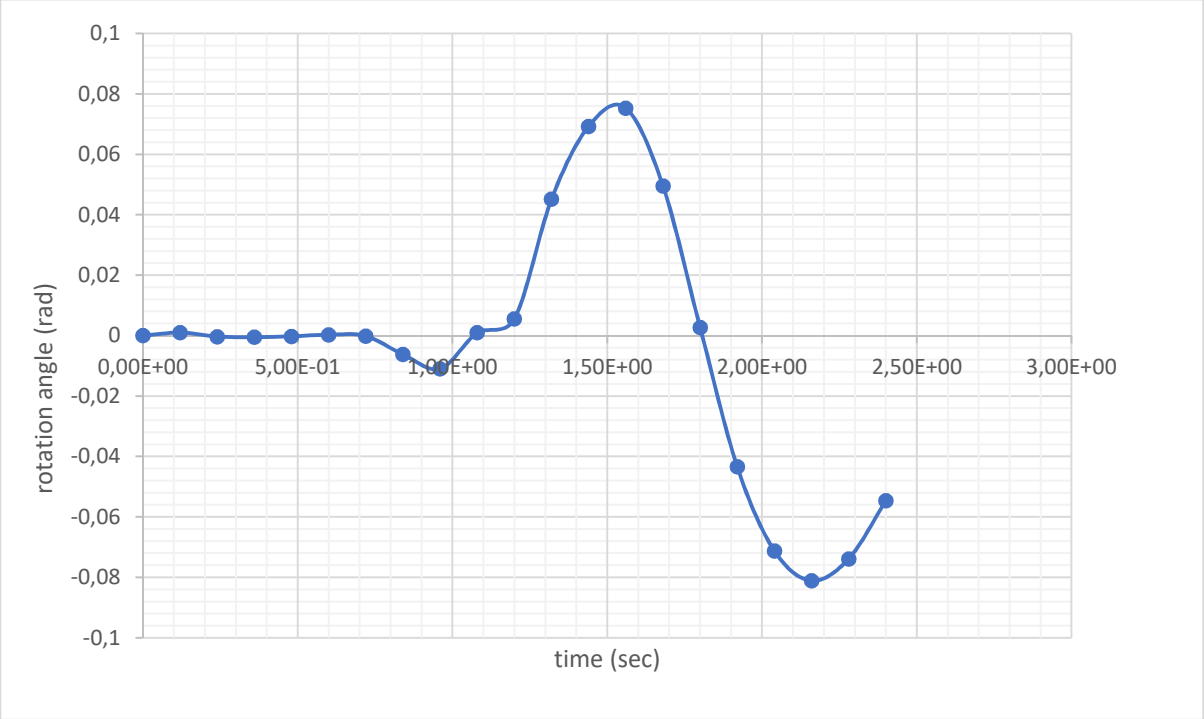

Figure 103: Rotation angle for simple column model (T=1.2s , a =0.3g)

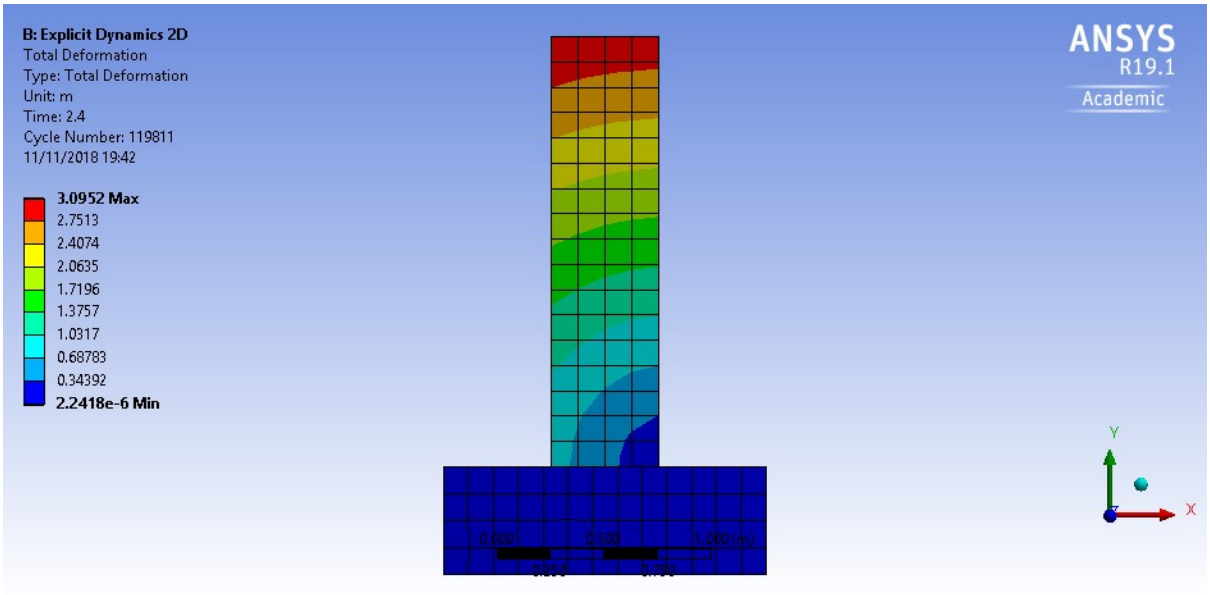

Figure 104: Total deformation (simple column T=1.2s , a =0.5 g)

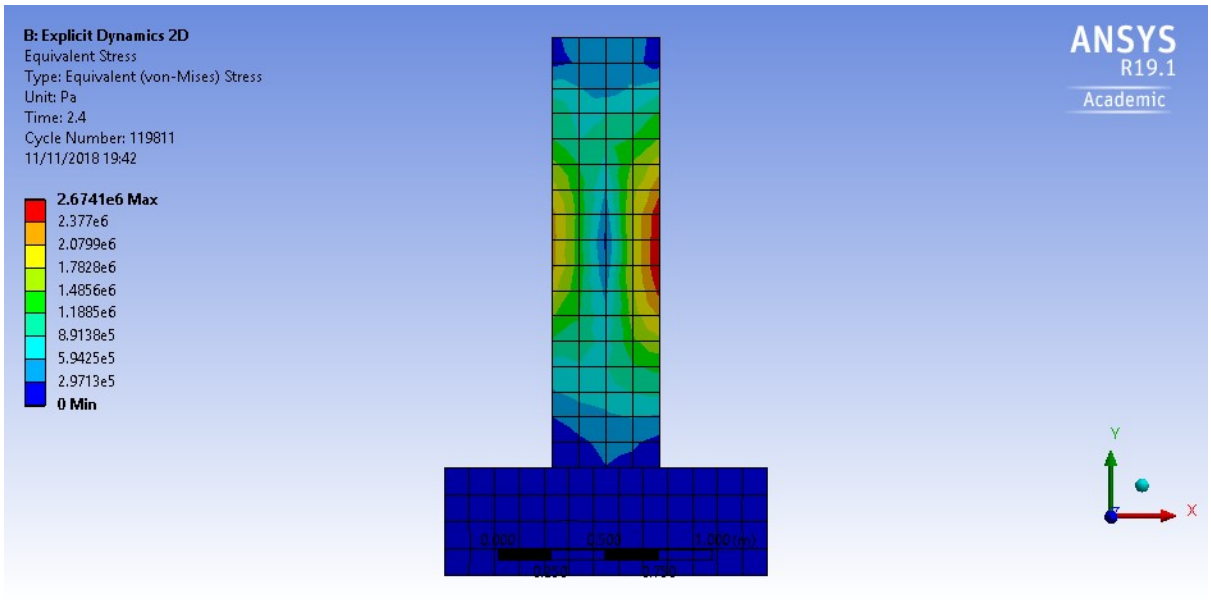

Figure 105: Stress distribution (simple column T=1.2s , a =0.5 g)

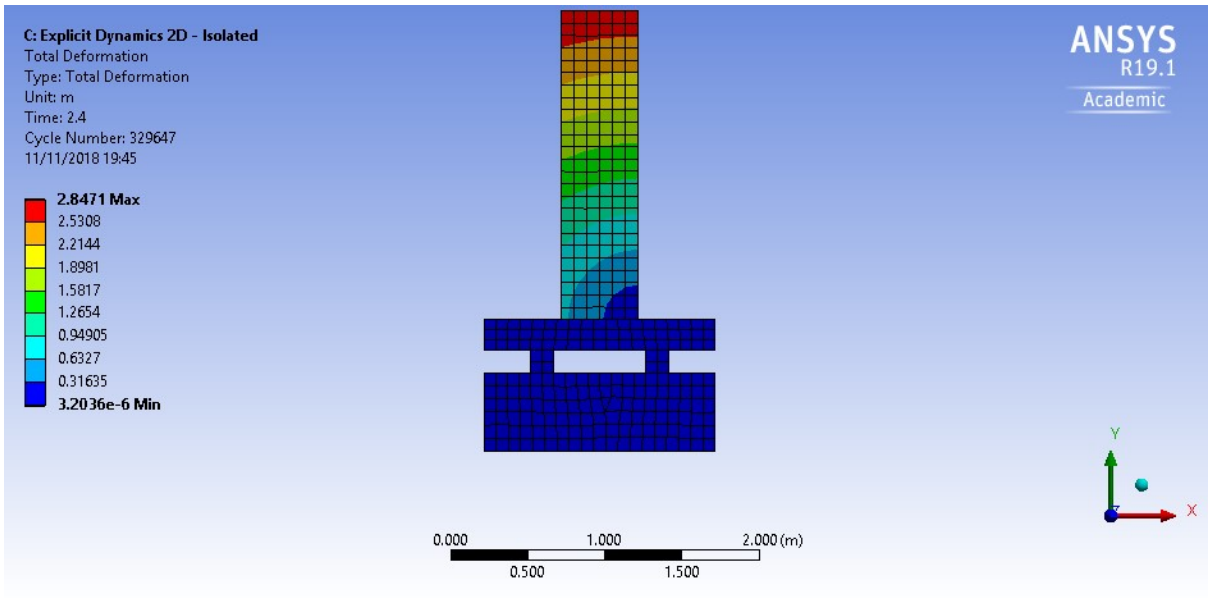

Figure 106: Total deformation (base-isolated T=1.2s , a =0.5 g)

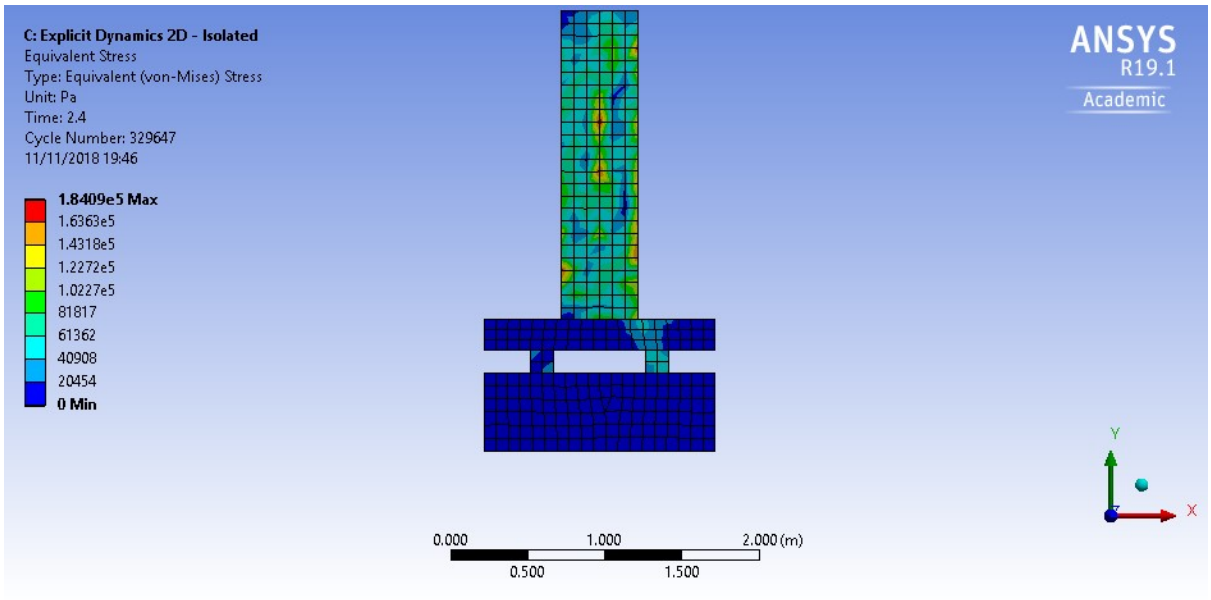

Figure 107: Stress distribution (base-isolated T=1.2s , a =0.5 g)

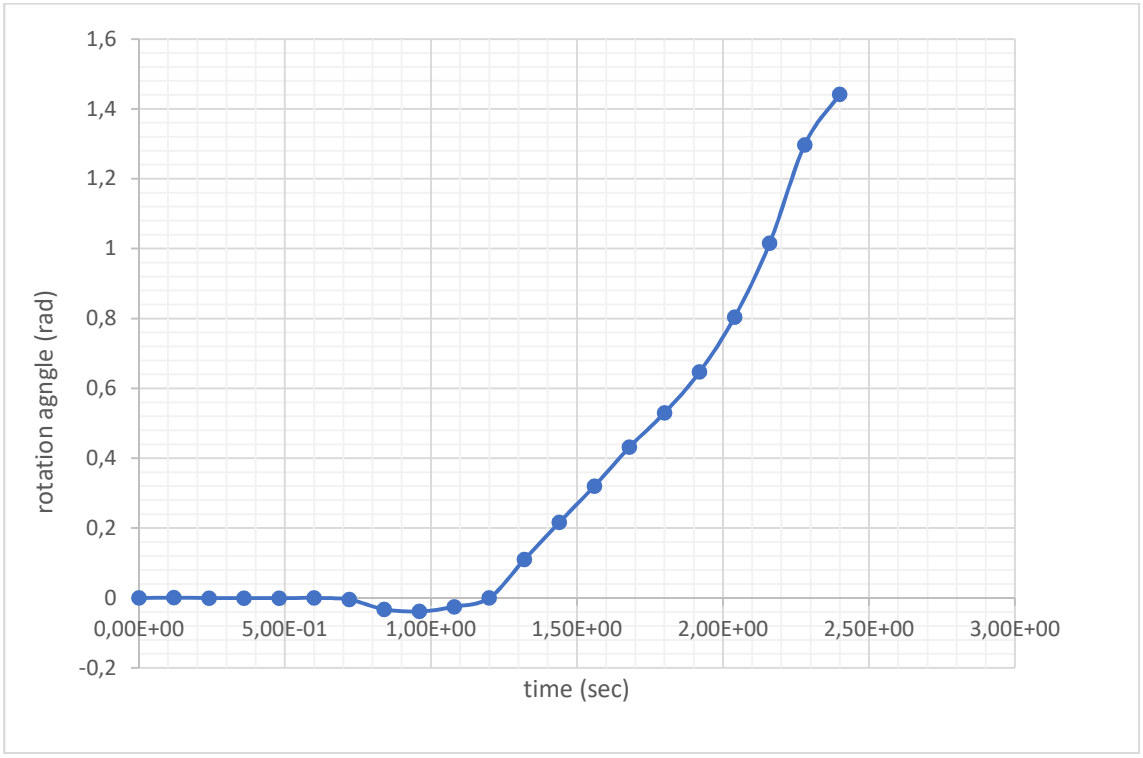

Figure 108: Rotation angle for simple column model (T=1.2s , a =0.5g)

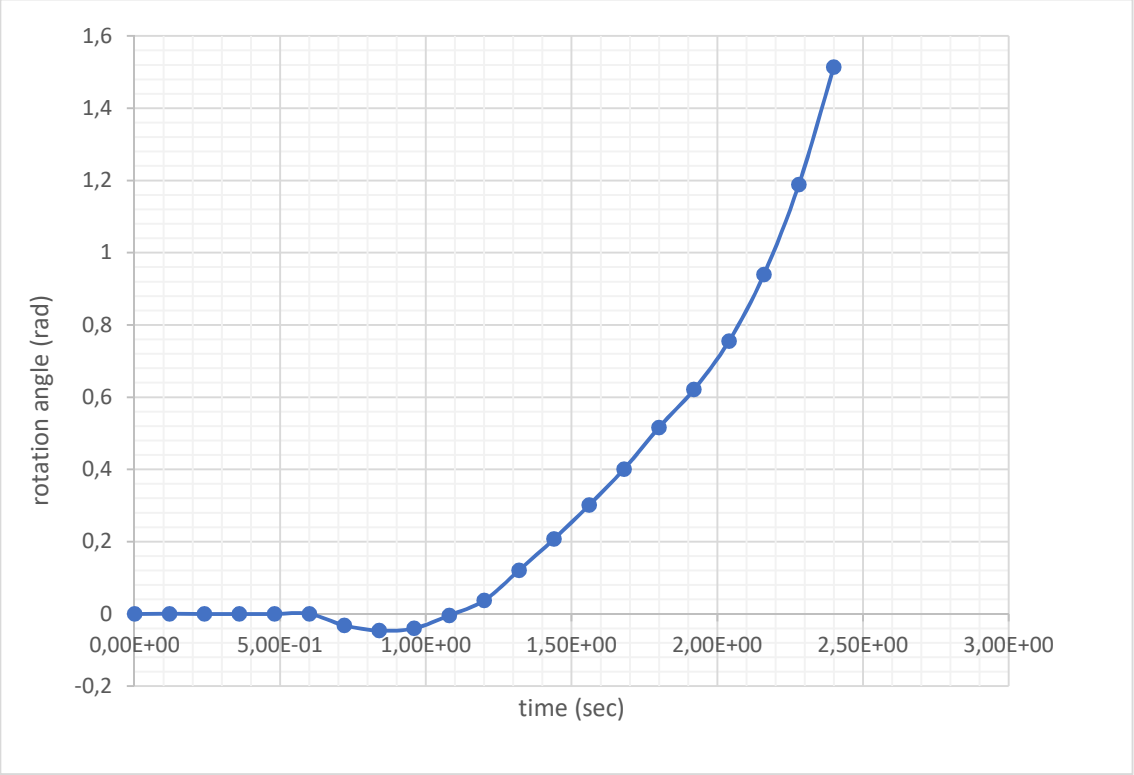

Figure 109: Rotation angle for base-isolated model (T=1.2s , a =0.5g)

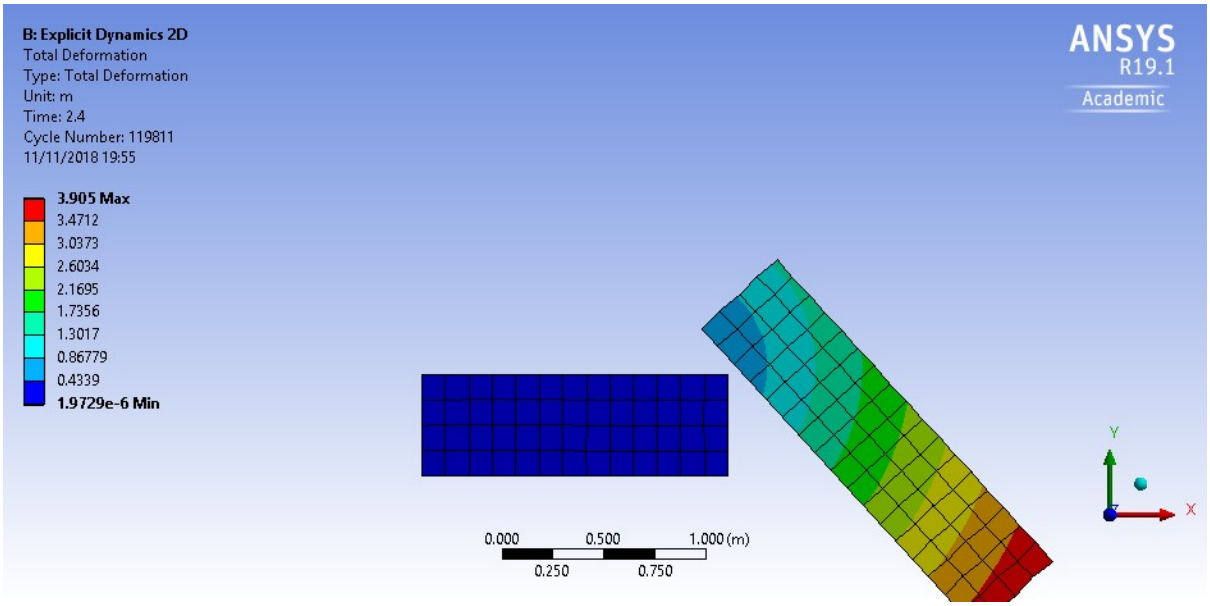

Figure 110: Total deformation (simple column T=1.2s , a =0.8 g)

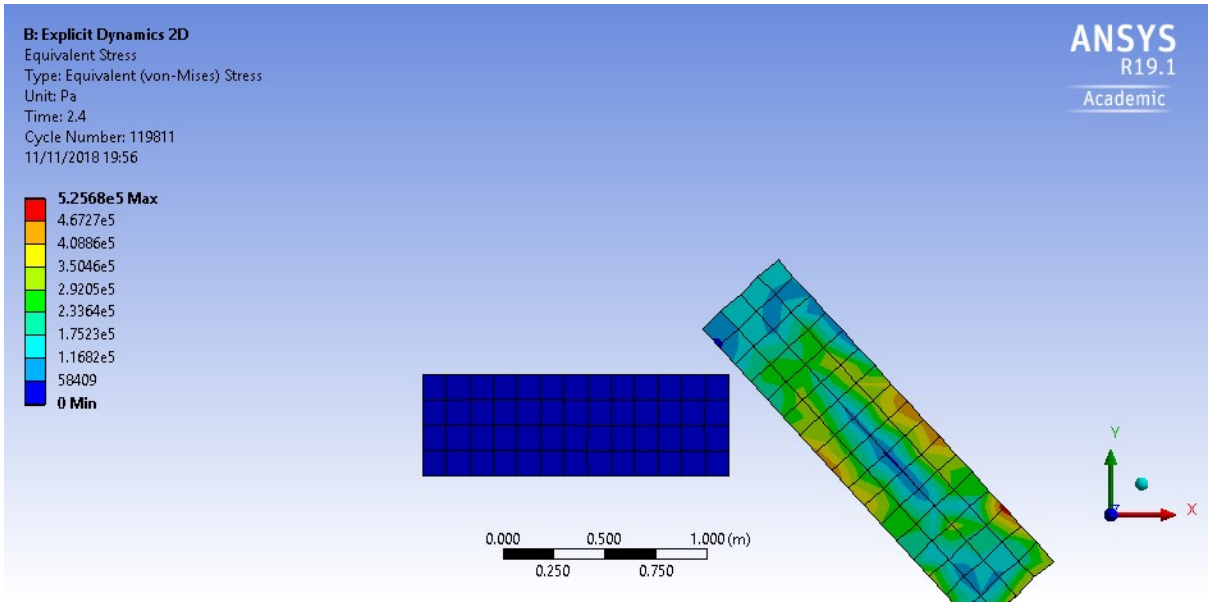

Figure 111: Stress distribution (simple column T=1.2s , a =0.8 g)

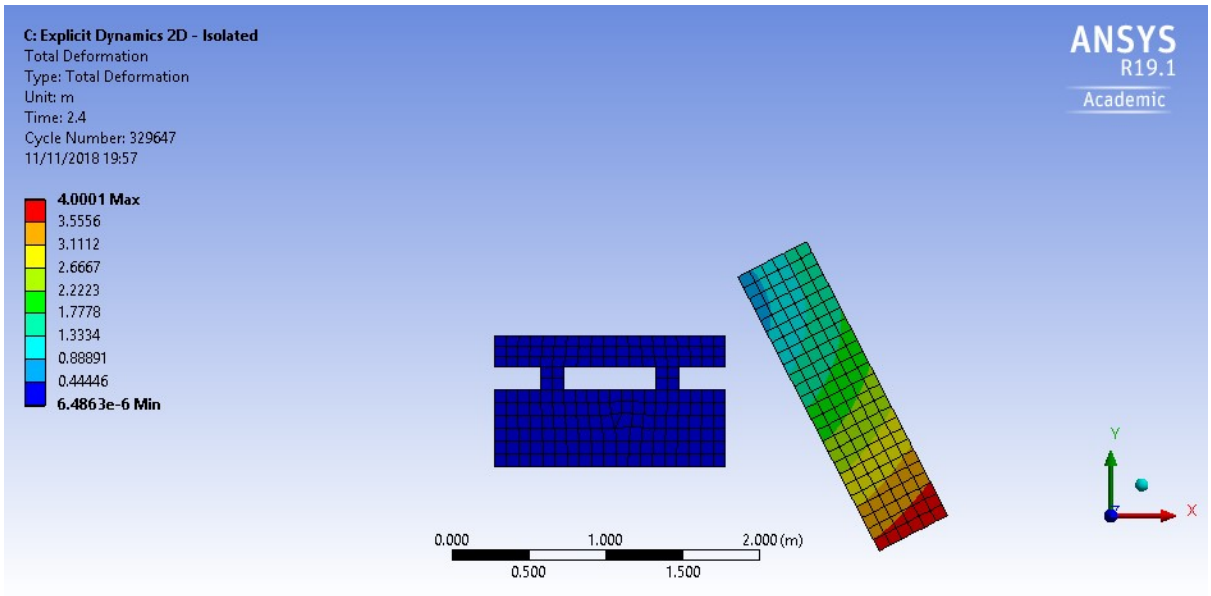

Figure 112 :Deformation (base-isolated T=1.2s , a =0.8 g)

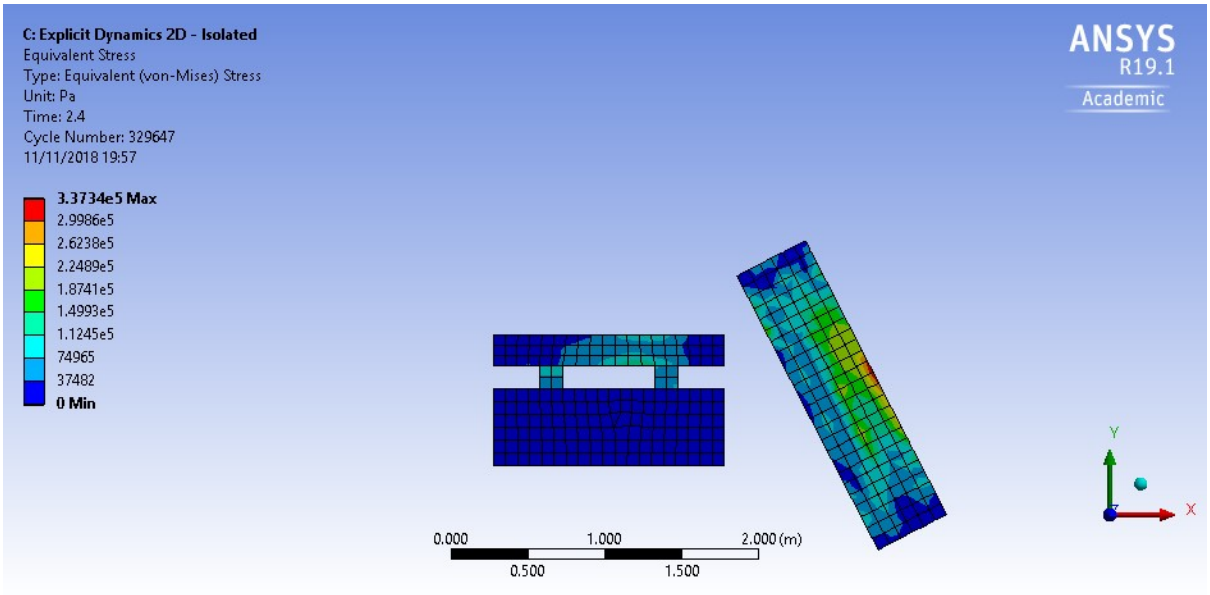

Figure 113 : Stress distribution (base-isolated T=1.2s , a =0.8g)

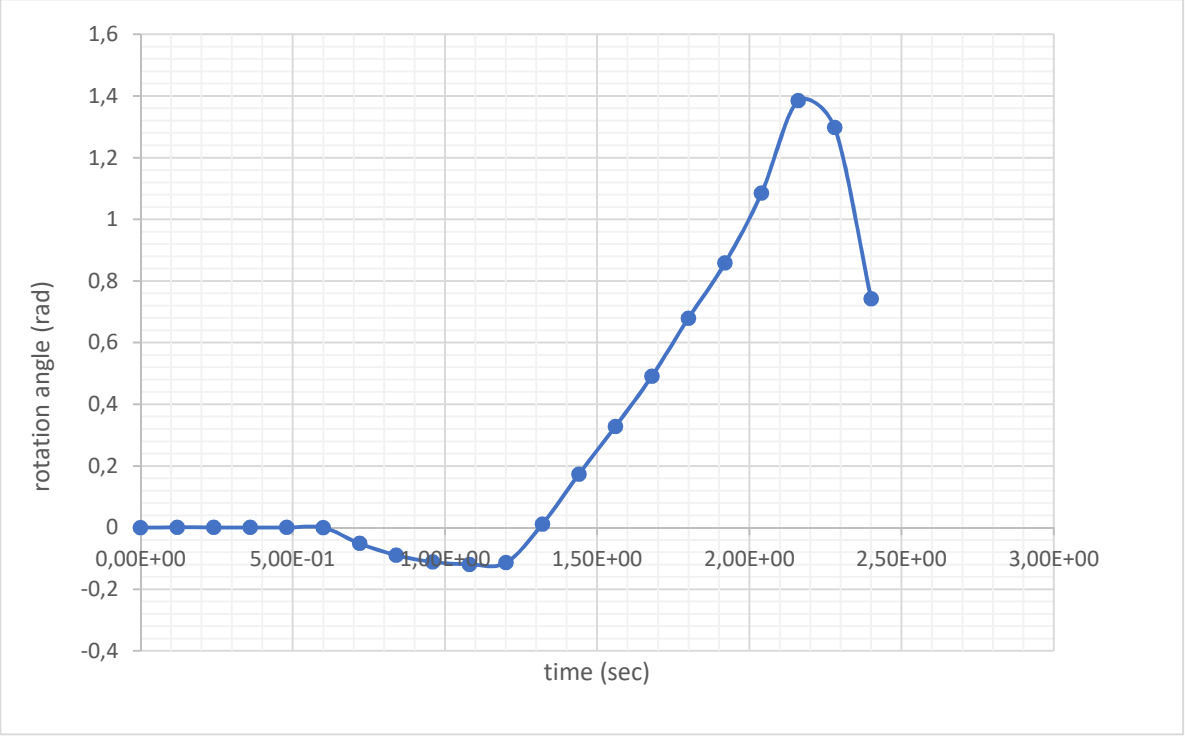

Figure 114 : Rotation angle for simple column model (T=1.2s , a =0.8g)

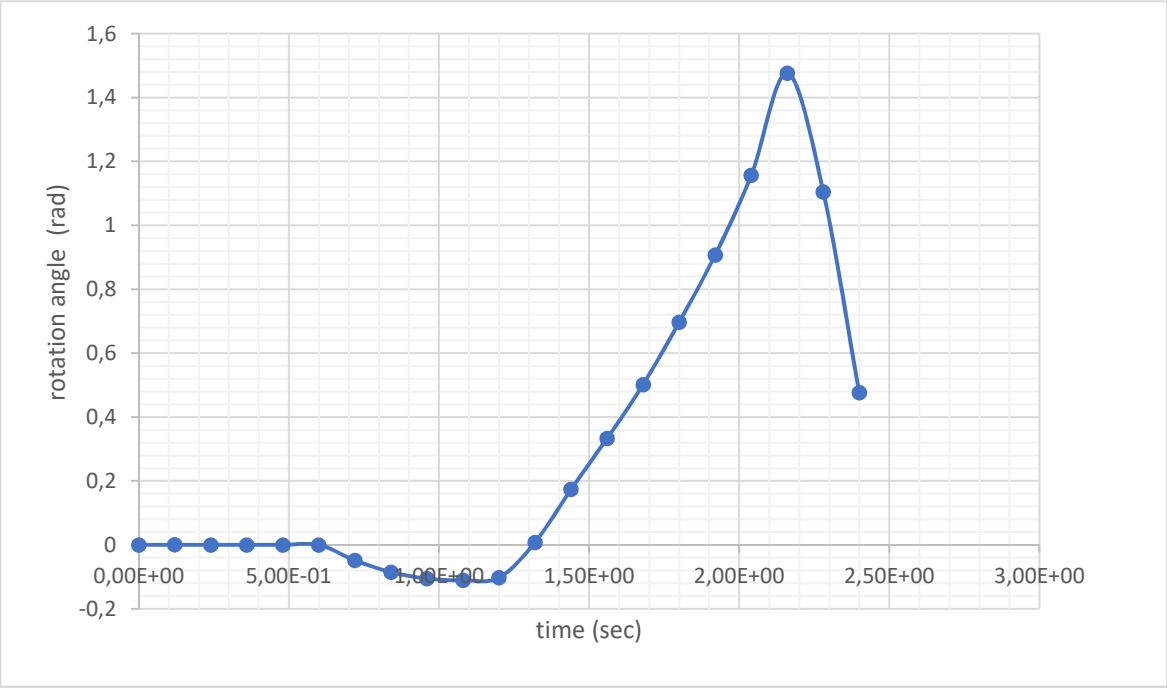

Figure 115 : Rotation angle for base-isolated model (T=1.2s , a =0.8g)

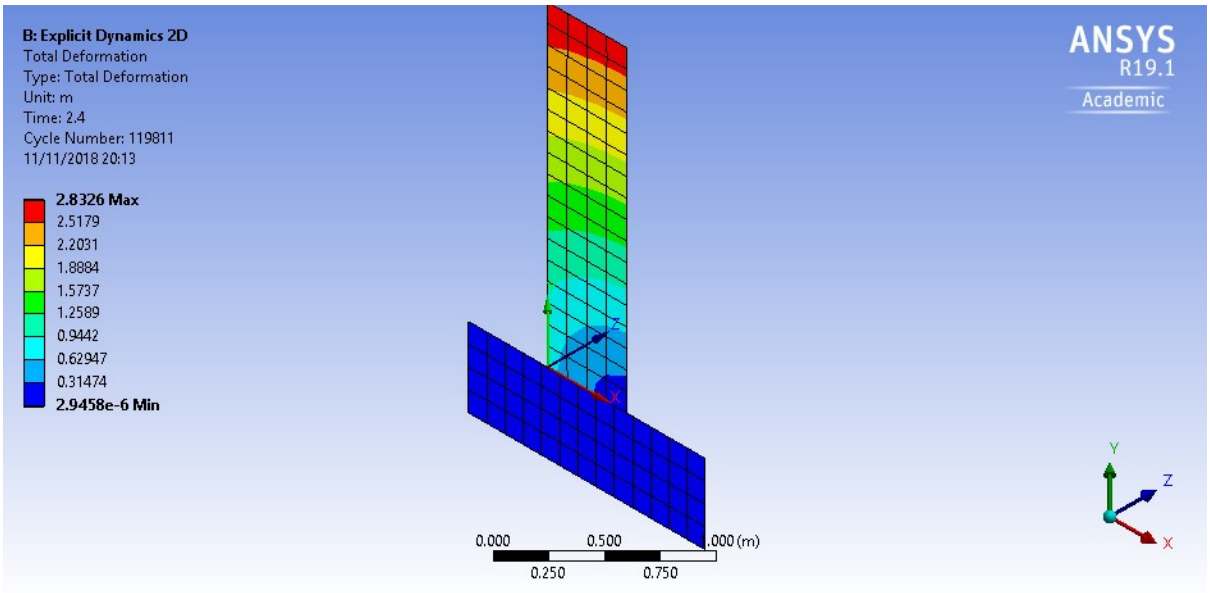

Figure 116 :Deformation (simple column T=1.2s , a =1.2 g)

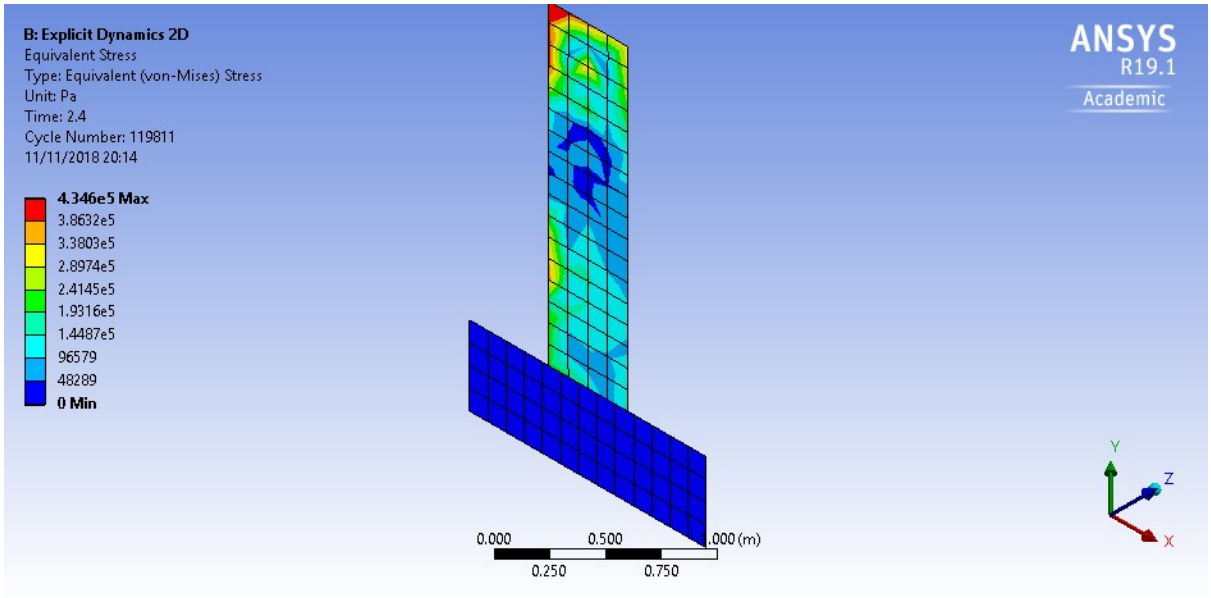

Figure 117 : Stress distribution (simple column)T=1.2s , a =1.2 g)

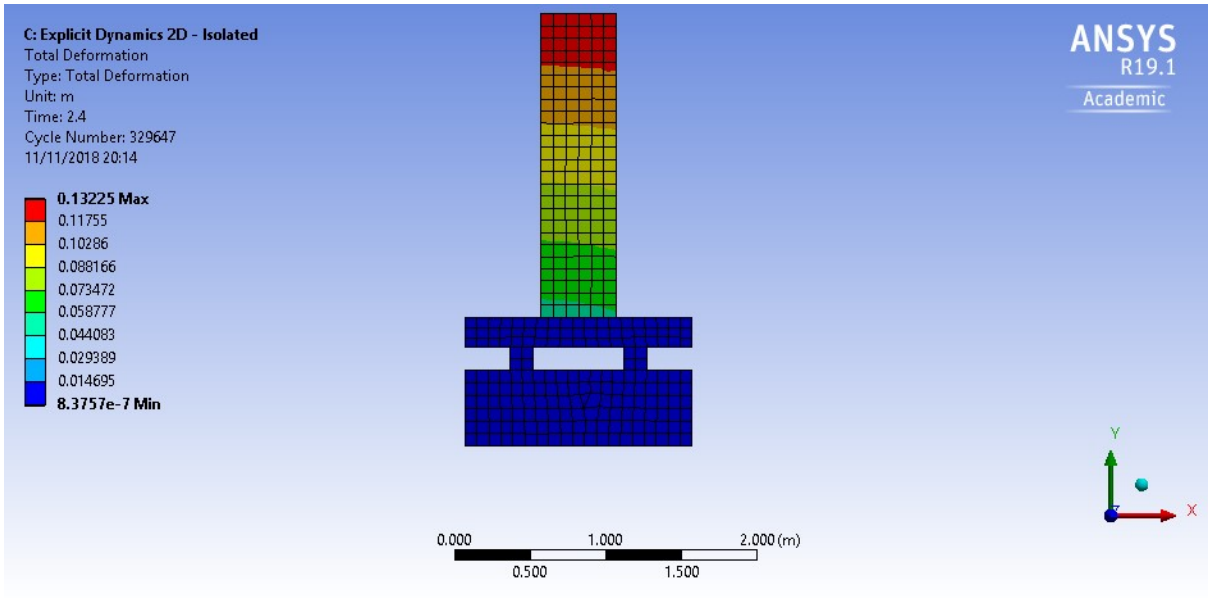

Figure 118: Deformation (base-isolated T=1.2s , a =1.2 g)

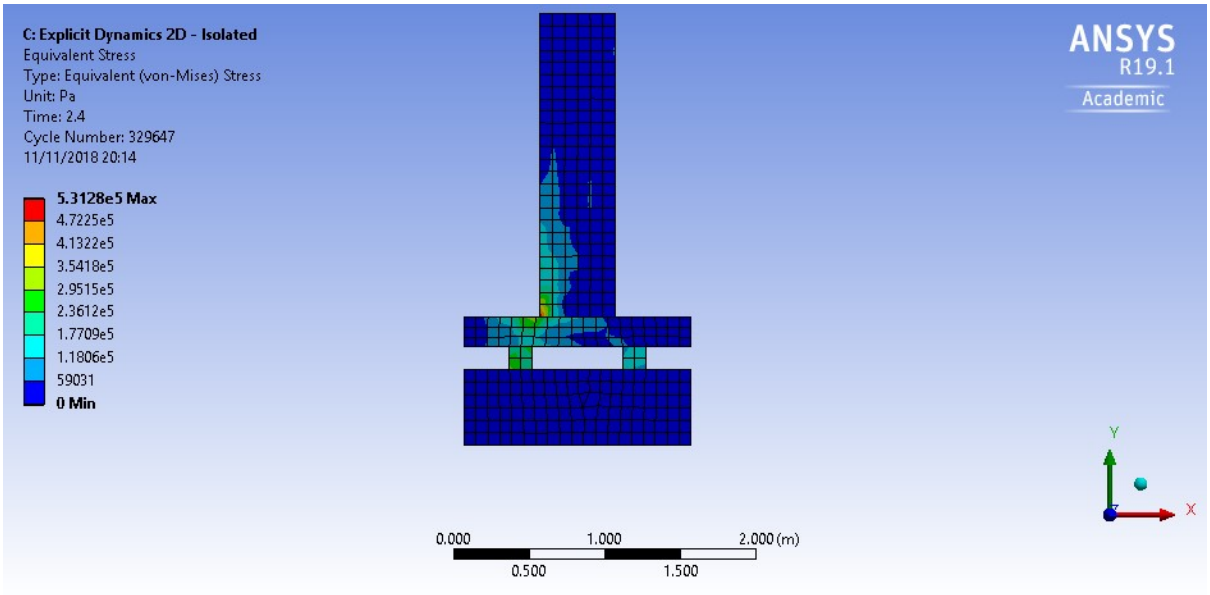

Figure 119 : Stress distribution (base-isolated T=1.2s , a =1.2 g)

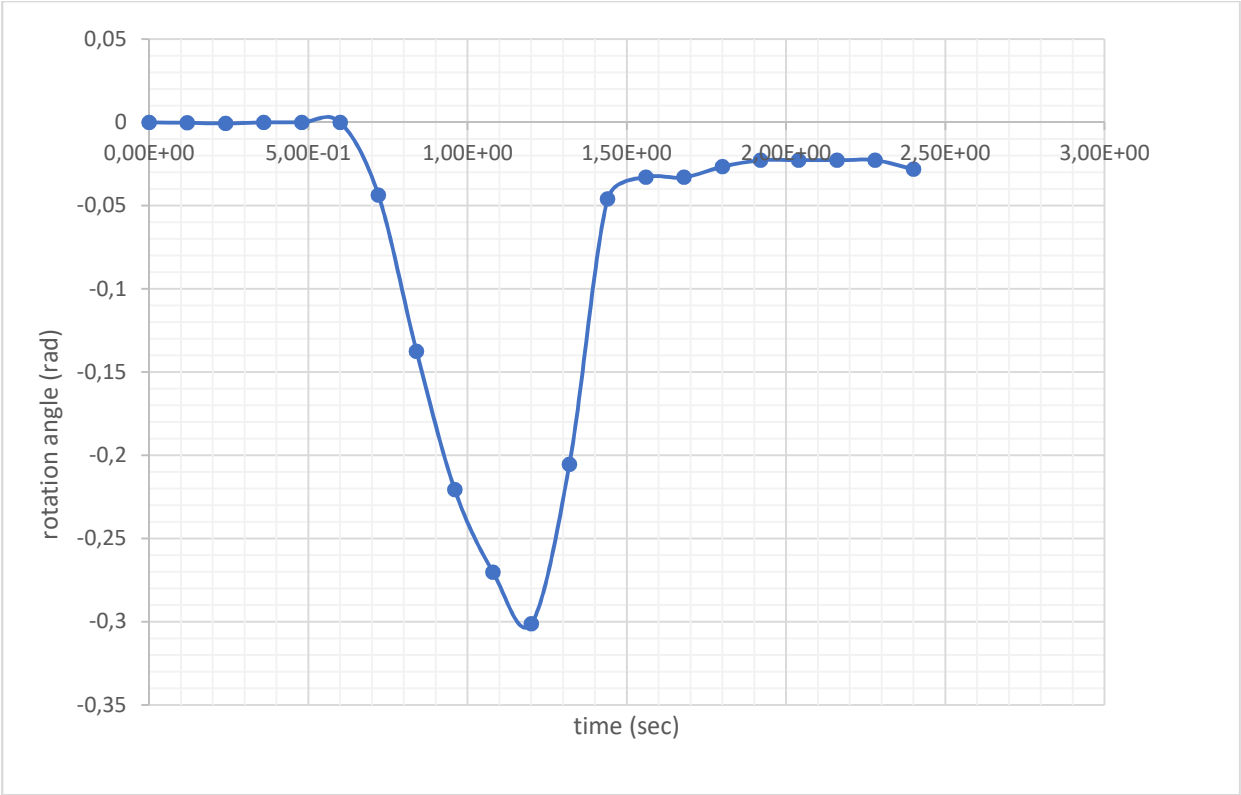

Figure 120: : Rotation angle for simple column model (T=1.2s , a =1.2g)

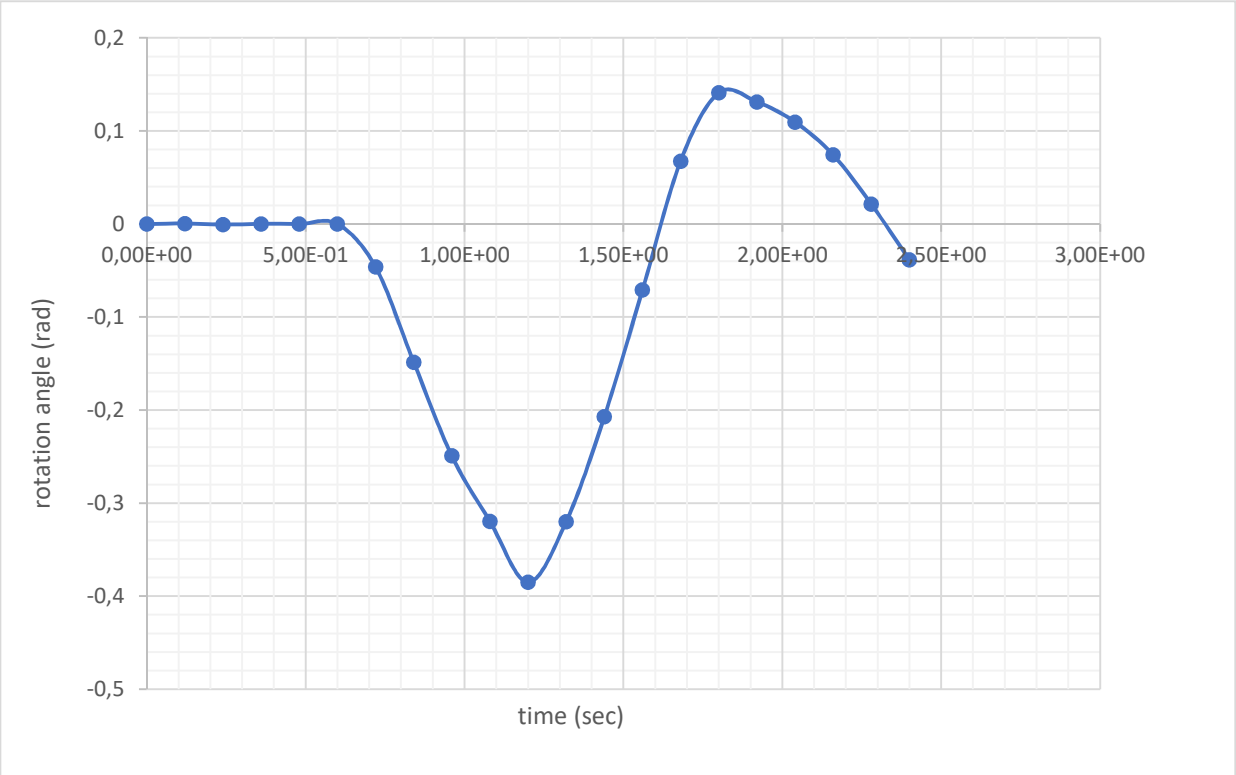

Figure 121: : Rotation angle for base-isolated model (T=1.2s , a =1.2g)

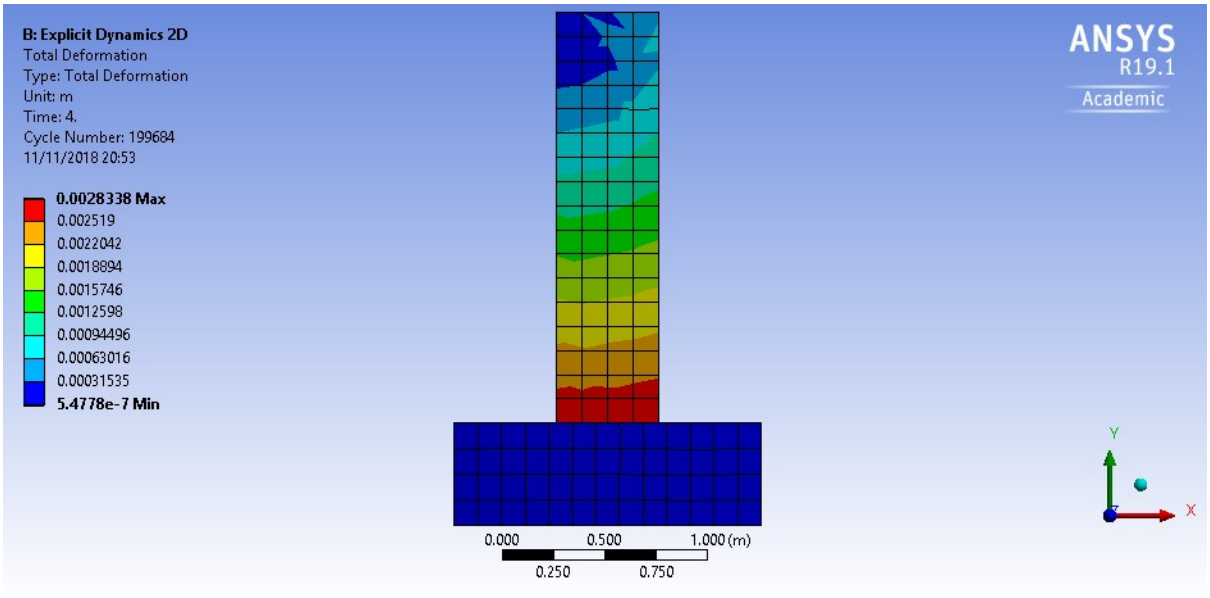

Figure 122: Deformation (simple column T=2s , a =0.15 g)

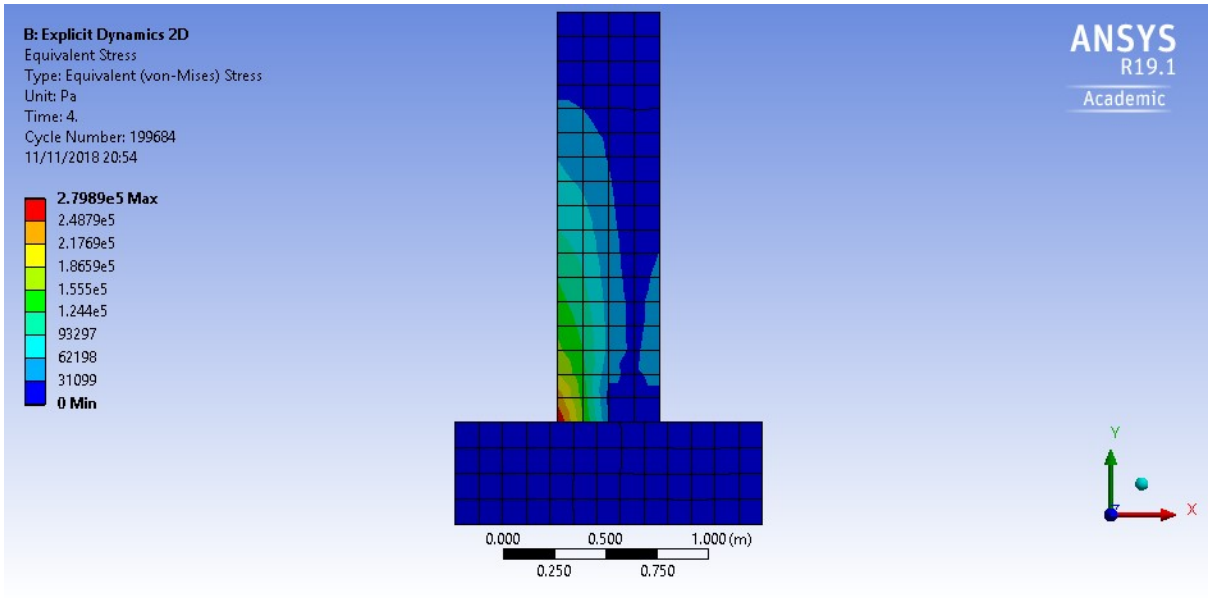

Figure 123: Stress distribution (simple column T=2s , a =0.15 g)

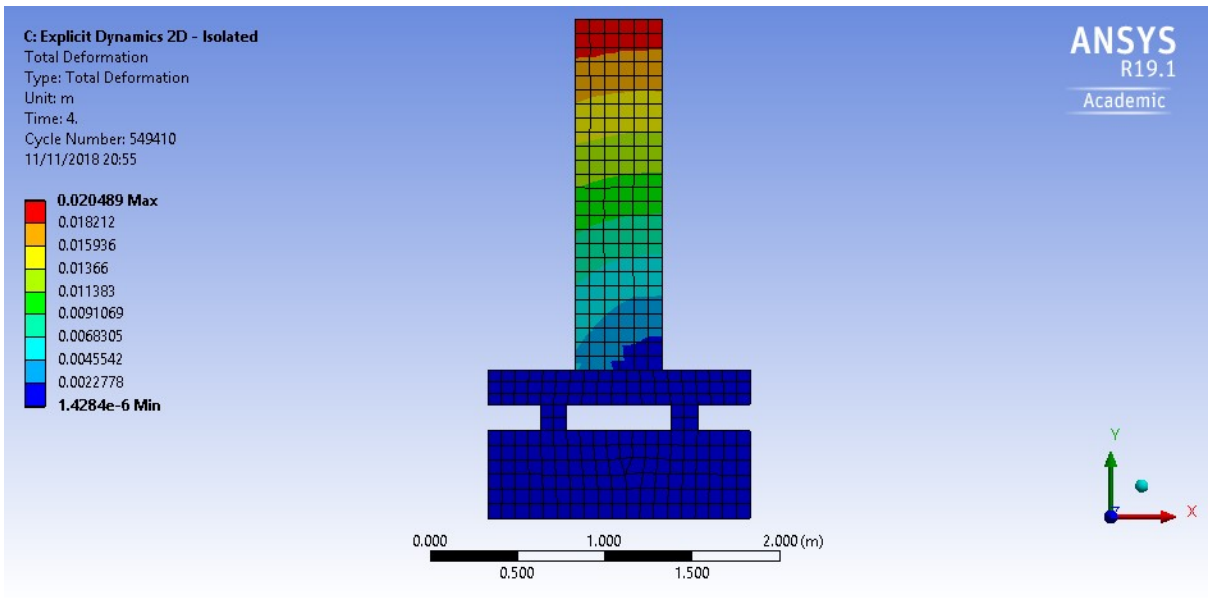

Figure 124: Deformation (base isolated T=2s , a =0.15 g)

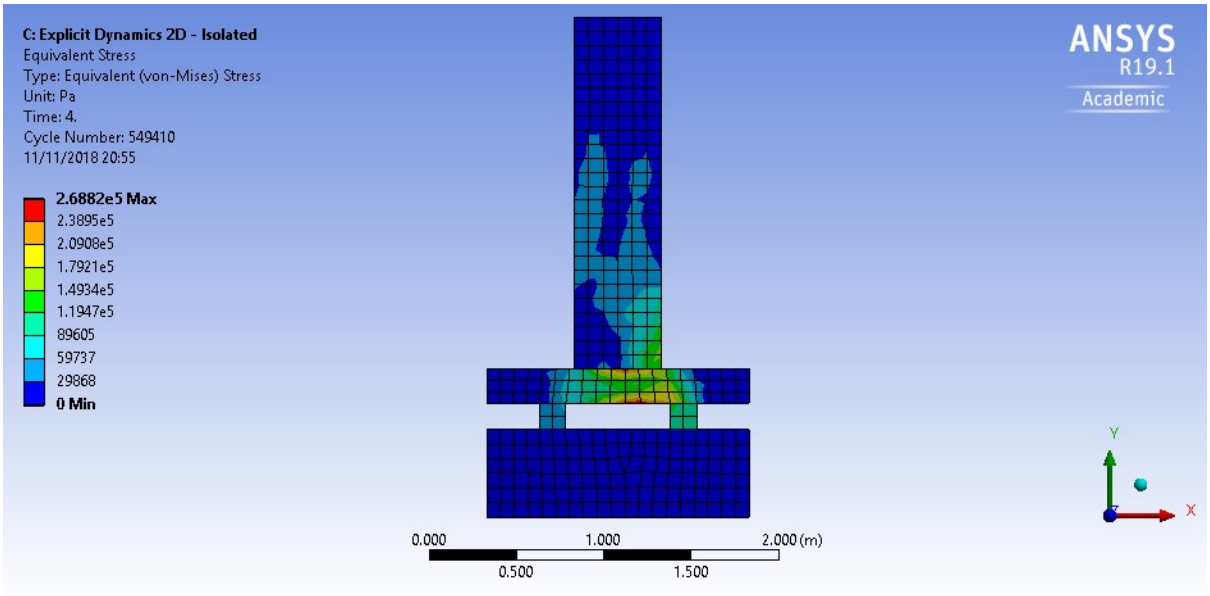

Figure 125: Stress distribution (base isolated T=2s , a =0.15 g)

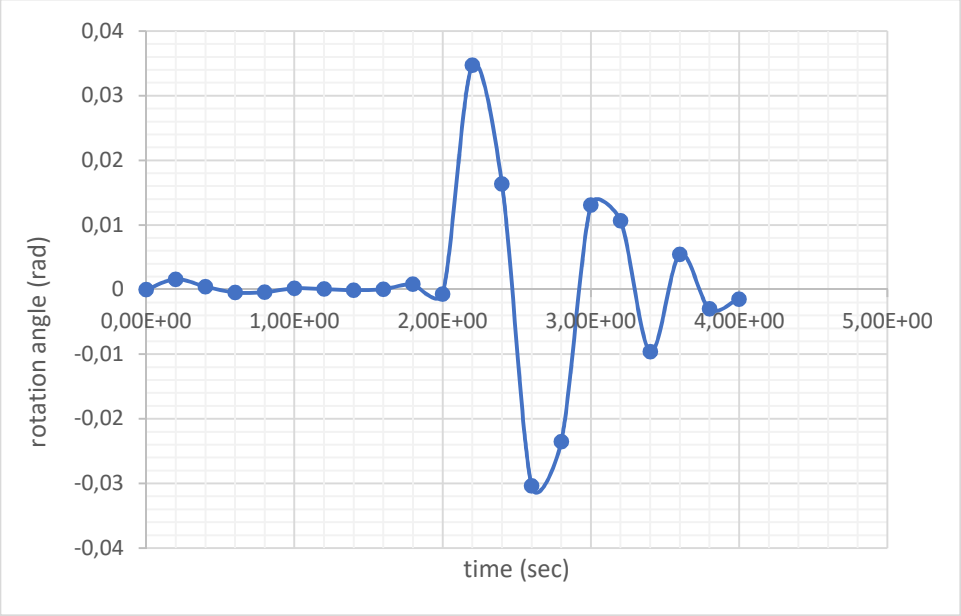

Figure 126 :Rotation angle for simple column model (T=2s , a =0.15g)

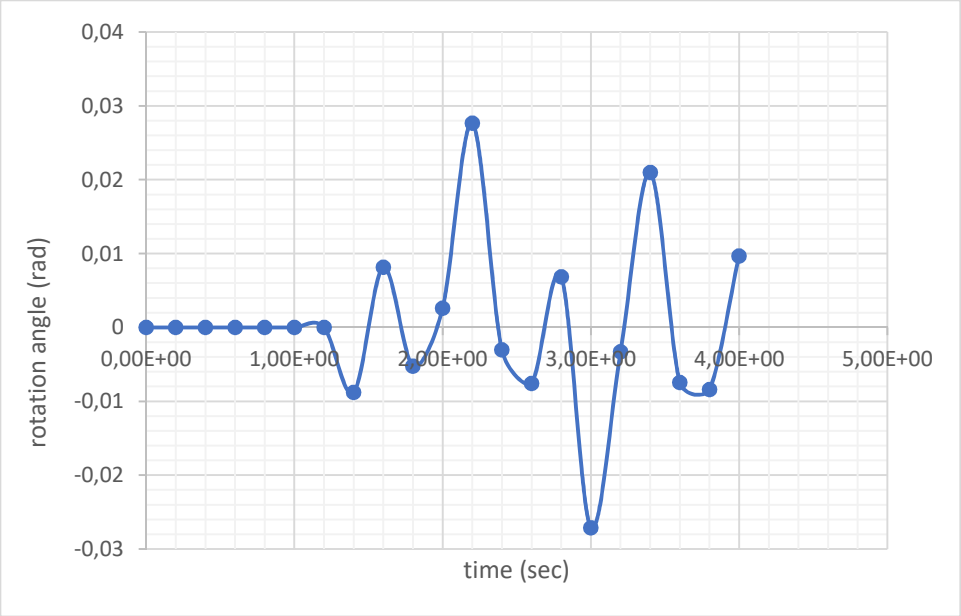

Figure 127 : Rotation angle for base-isolated model (T=2s , a =0.15g)

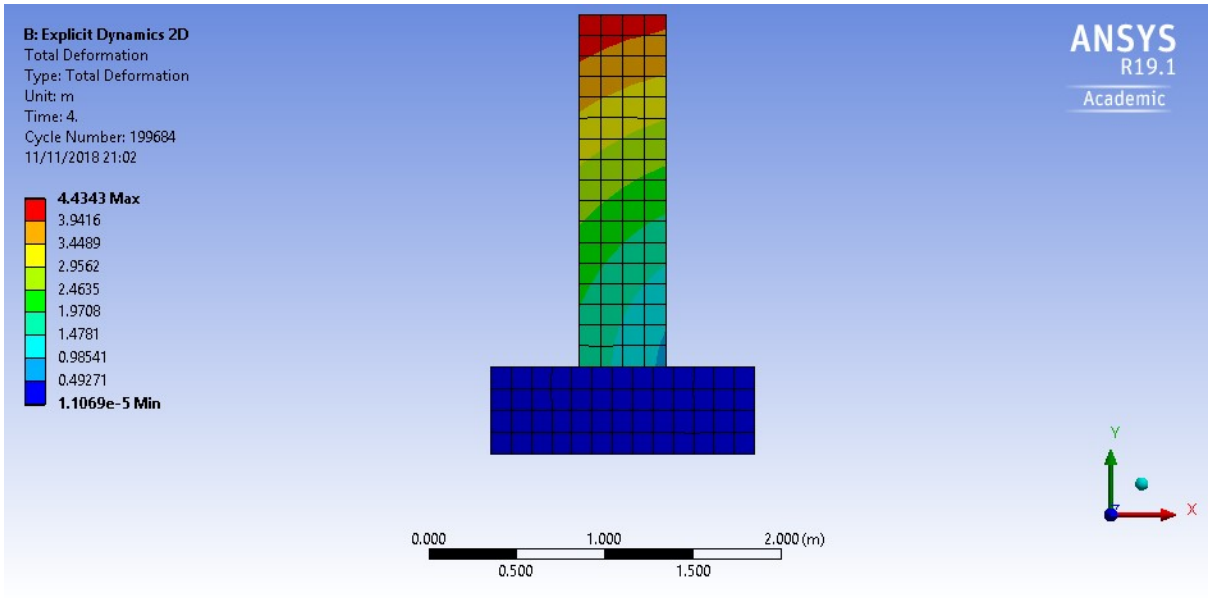

Figure 128: Deformation (simple column T=2s , a =0.3 g)

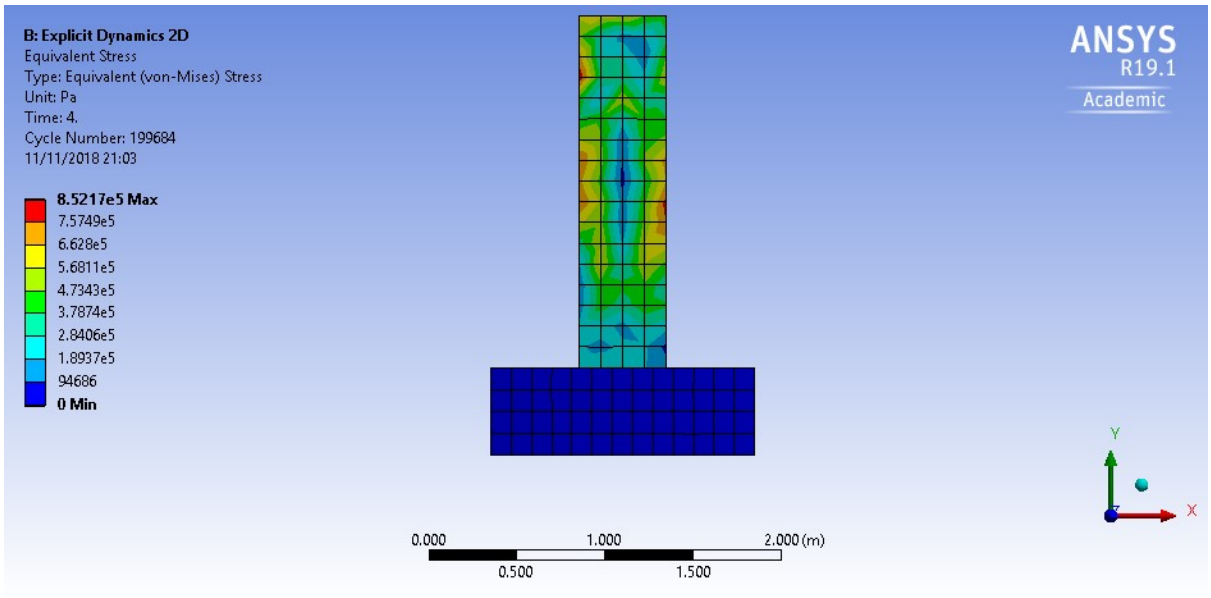

Figure 129: Stress distribution (simple column T=2s , a =0.3 g)

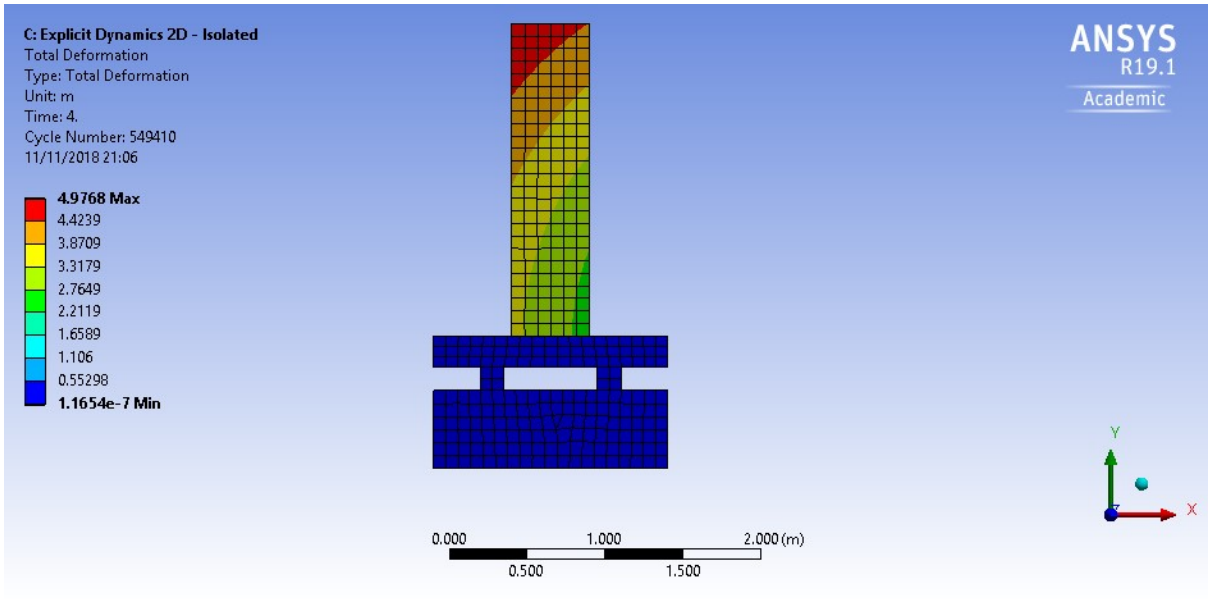

Figure 130 : Deformation (base-isolated T=2s , a =0.3 g)

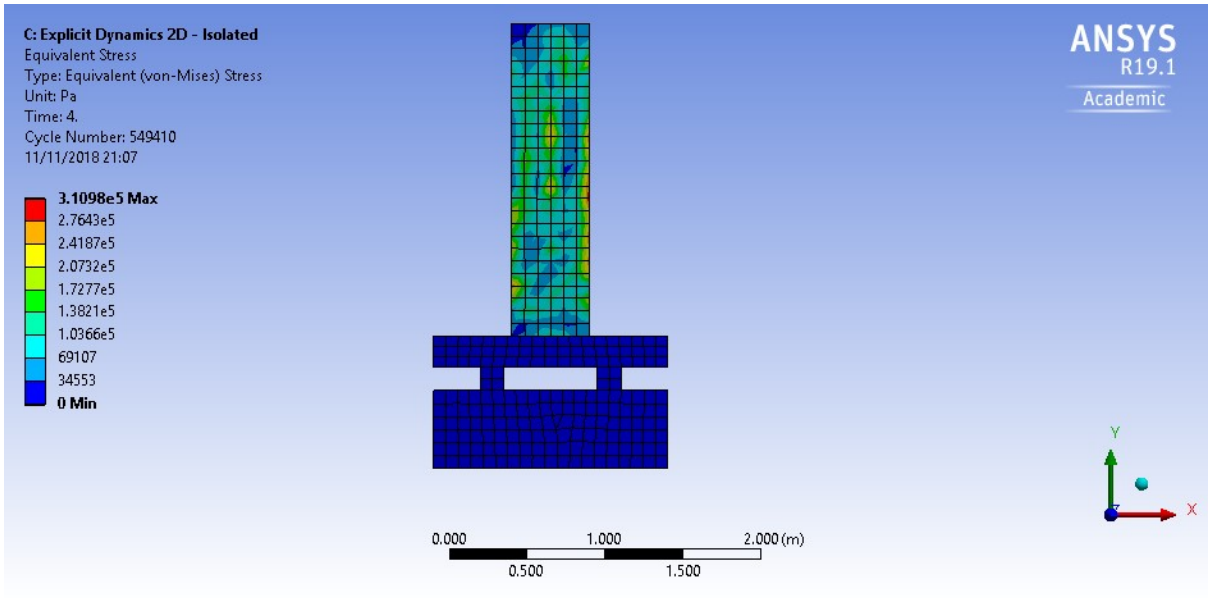

Figure 131 : Stress distribution (base-isolated T=2s , a =0.3 g)

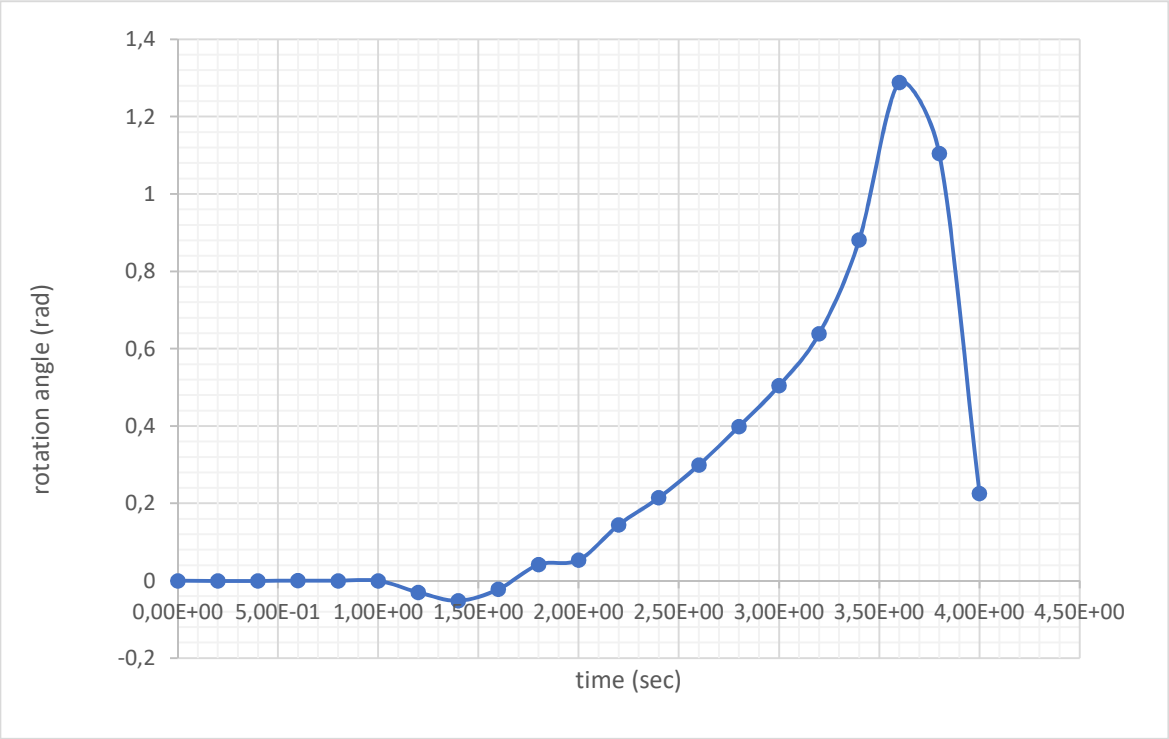

Figure 132: Rotation angle for simple column model (T=2s , a =0.3g)

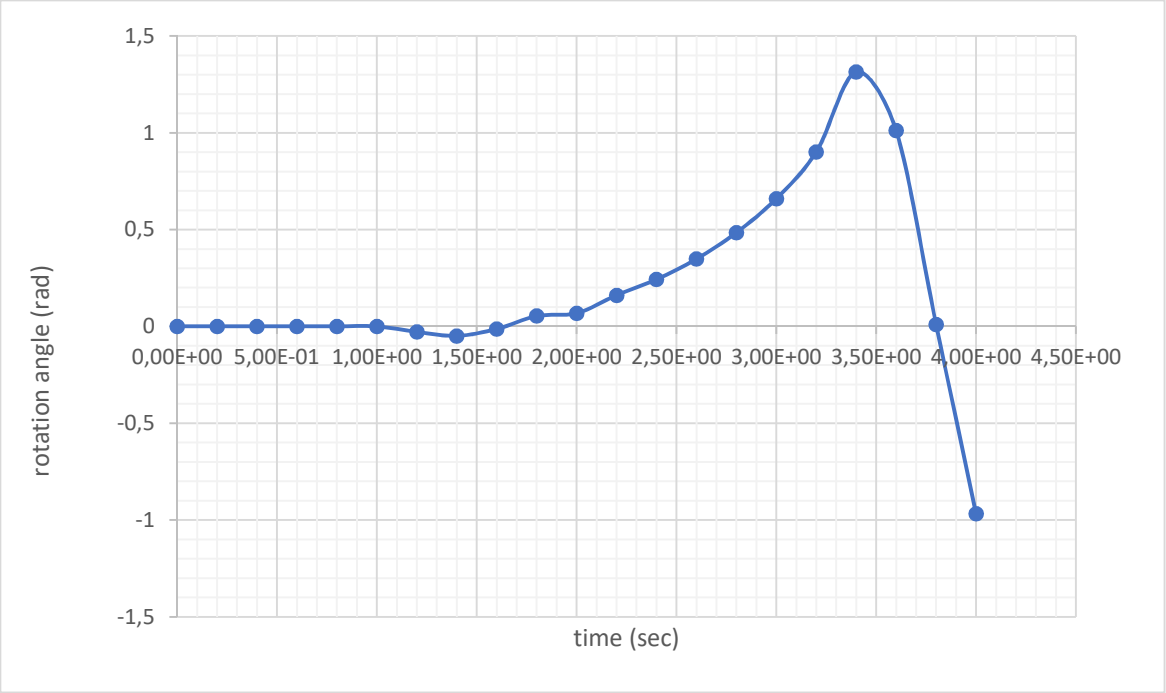

Figure 133: Rotation angle for base-isolated model (T=2s , a =0.3g)

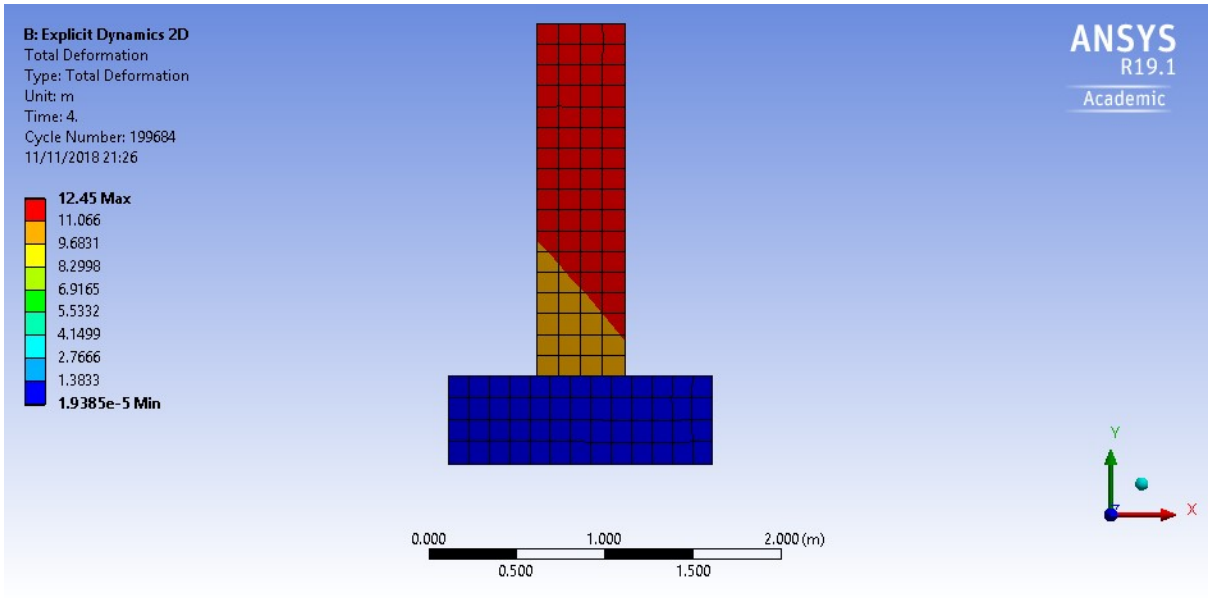

Figure 134 : Deformation (simple column T=2s , a =0.5 g)

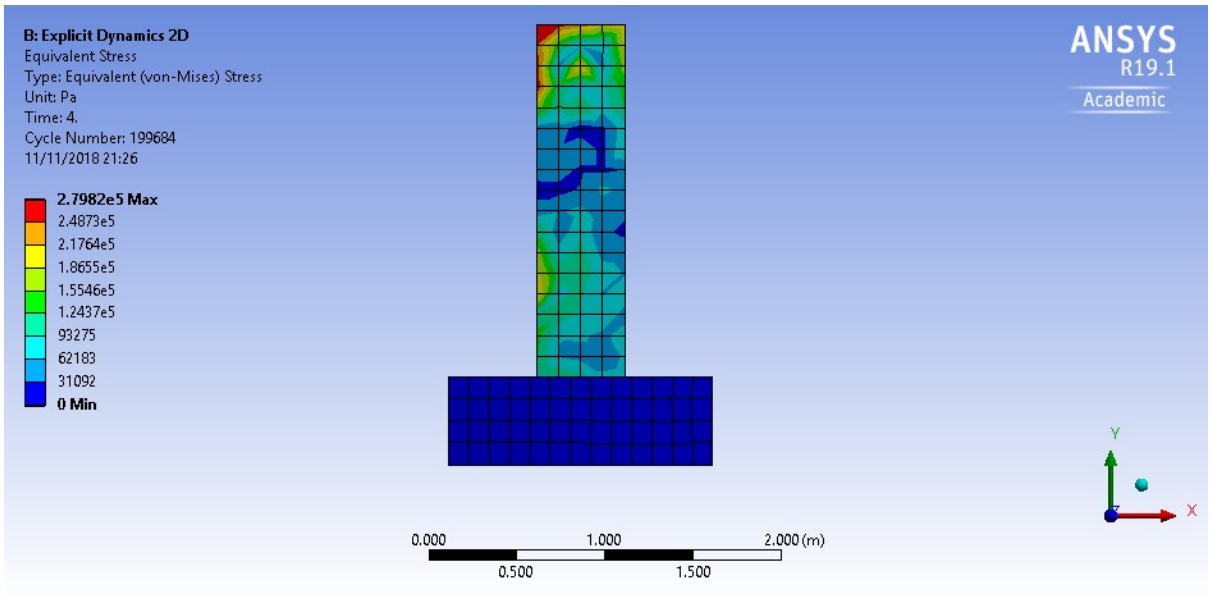

Figure 135 : Stress distribution (simple column T=2s , a =0.5 g)

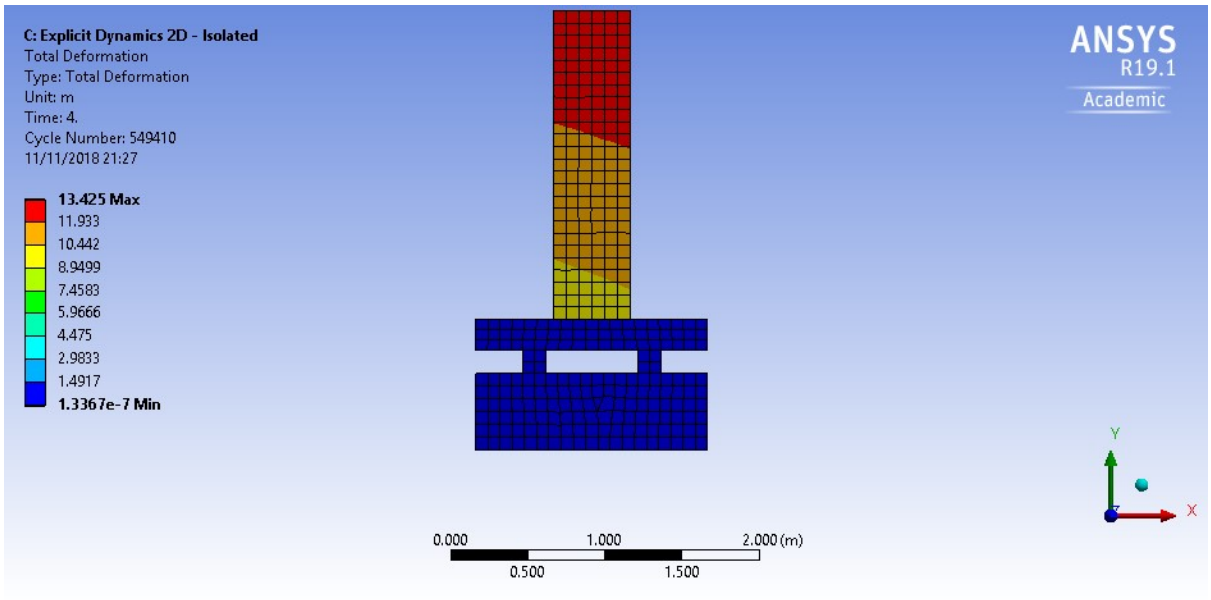

Figure 136 : Deformation (base-isolated T=2s , a =0.5 g)

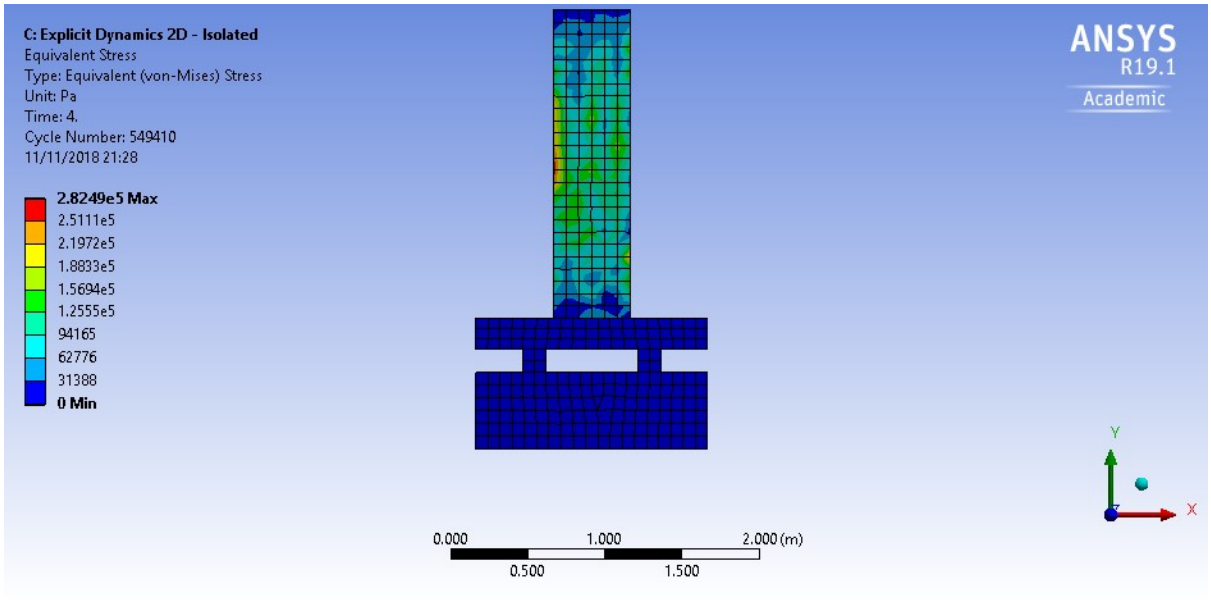

Figure 137 : Stress distribution (base-isolated T=2s , a =0.5 g)

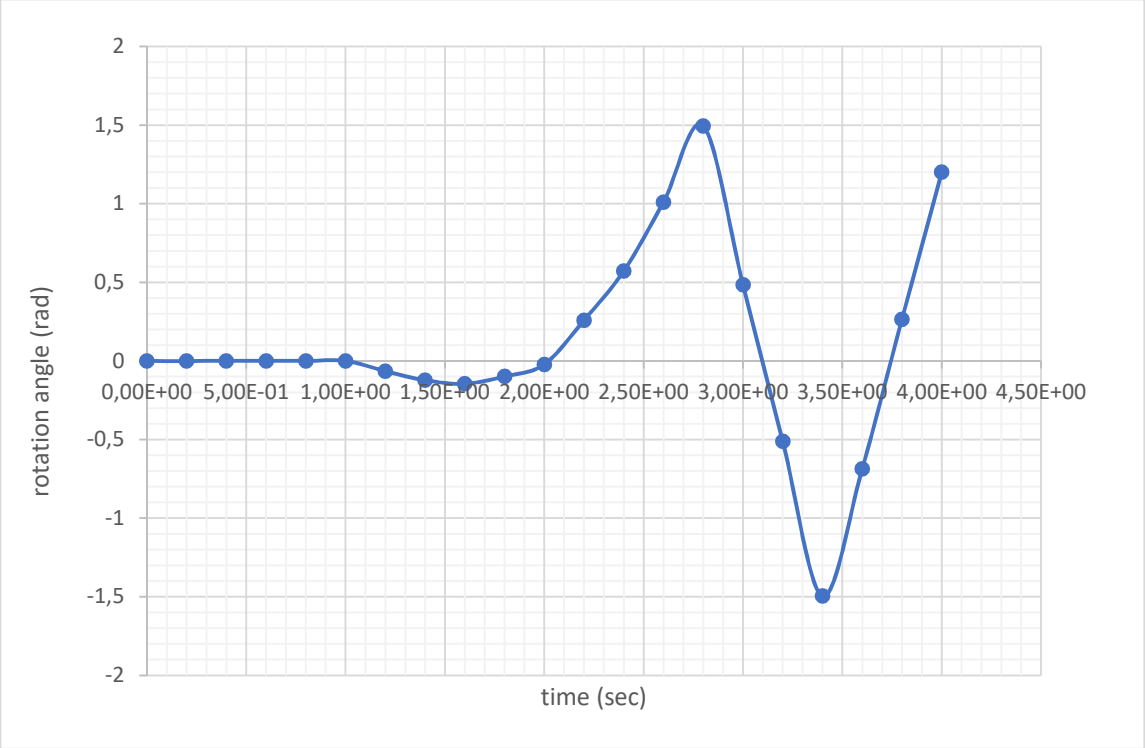

Figure 138 : Rotation angle for simple column model (T=2s , a =0.5g)

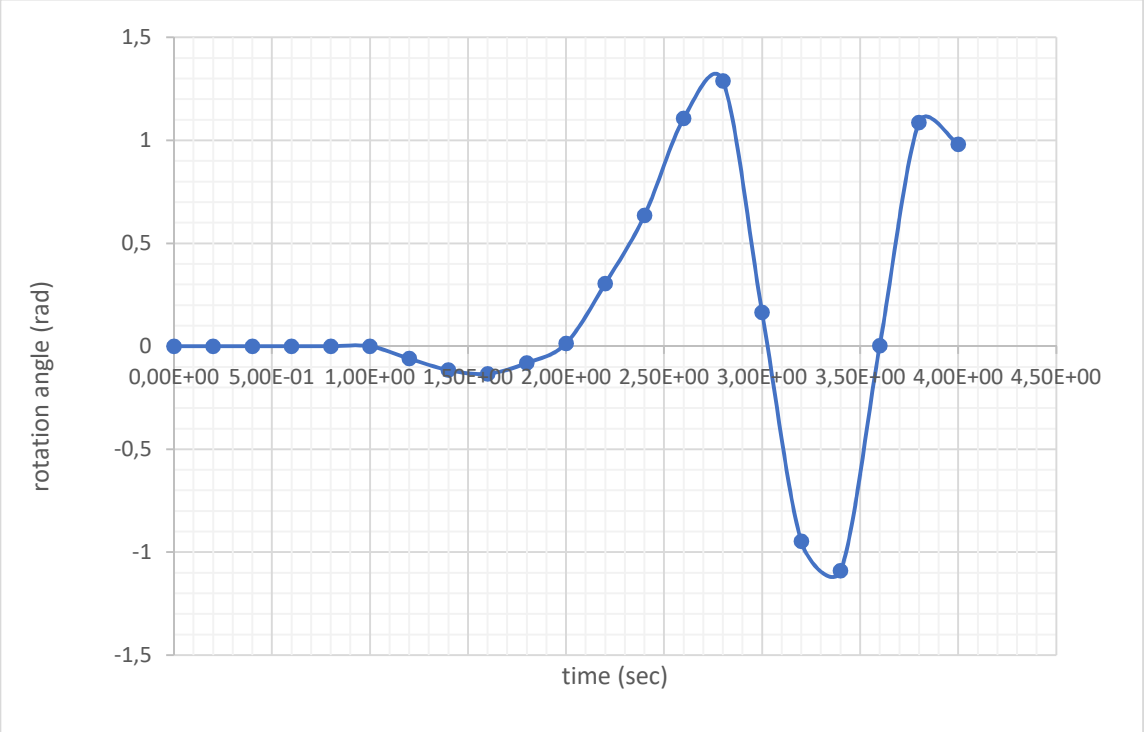

Figure 139 : Rotation angle for base-isolated model (T=2s , a =0.5g)

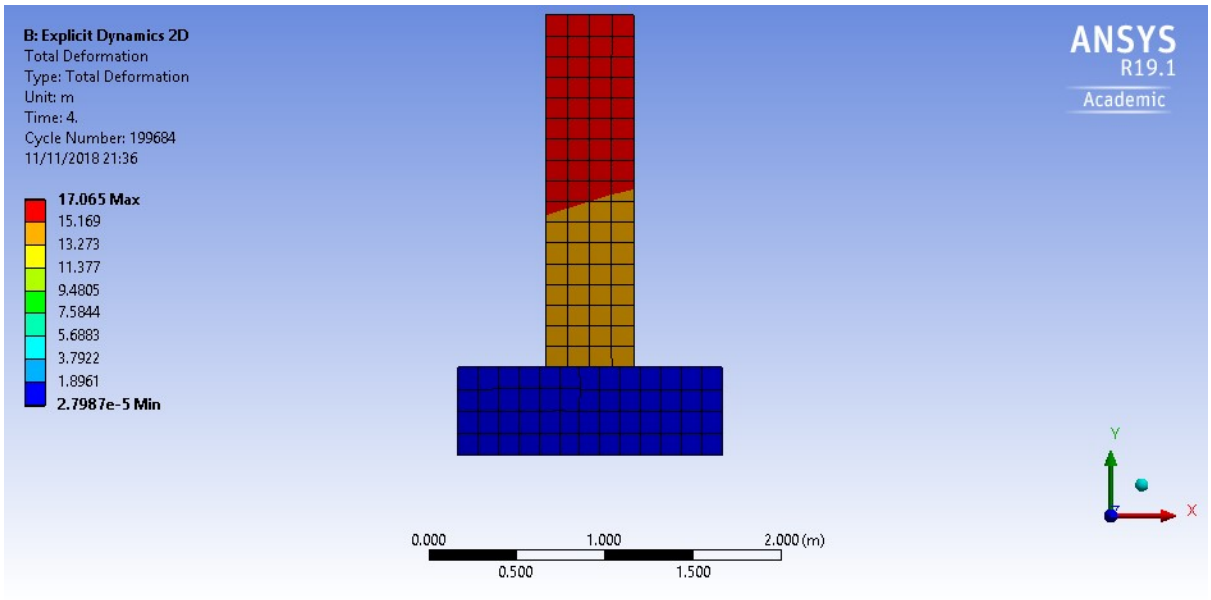

Figure 140 : Deformation (simple column T=2s , a =0.8 g)

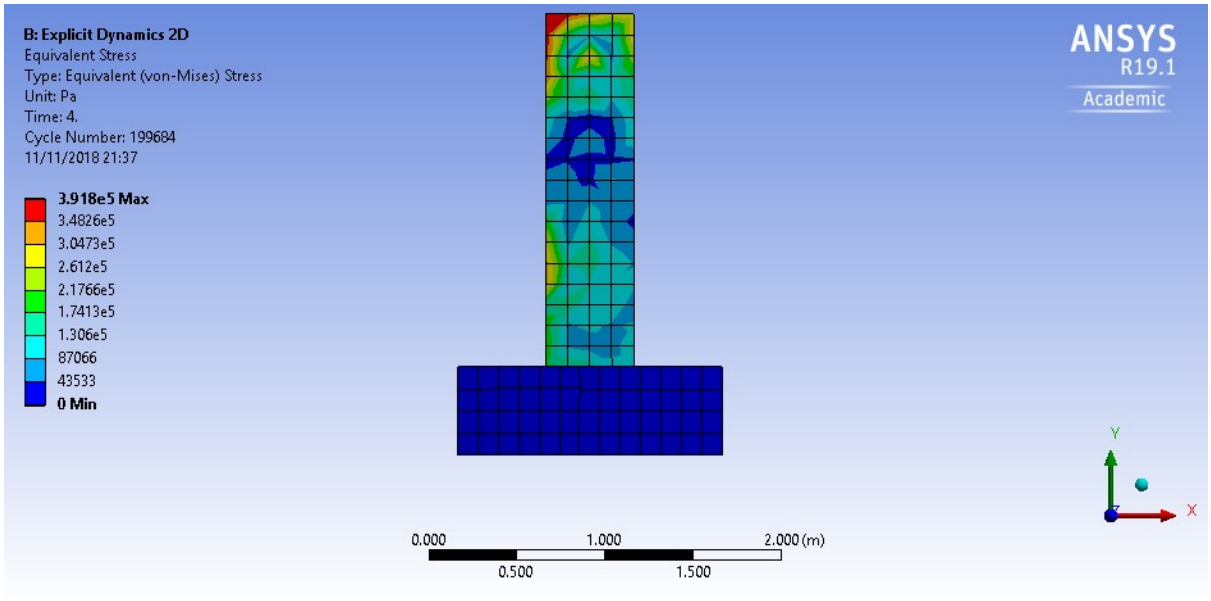

Figure 141 : Stress distribution (simple column T=2s , a =0.8 g)

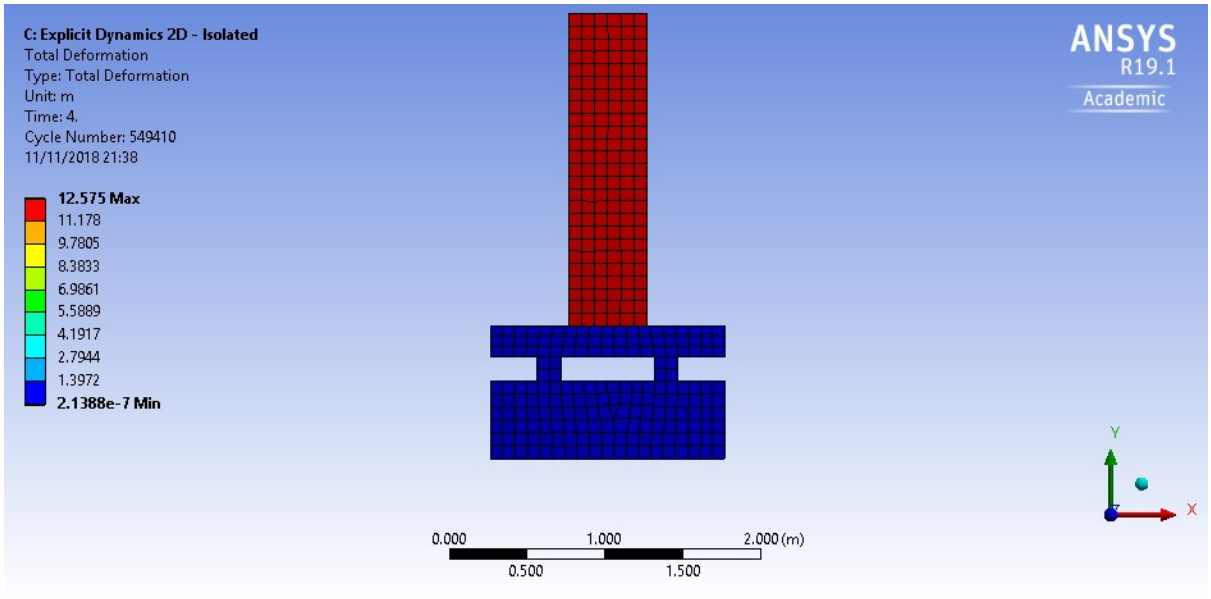

Figure 142 : Deformation (base-isolated T=2s , a =0.8 g)

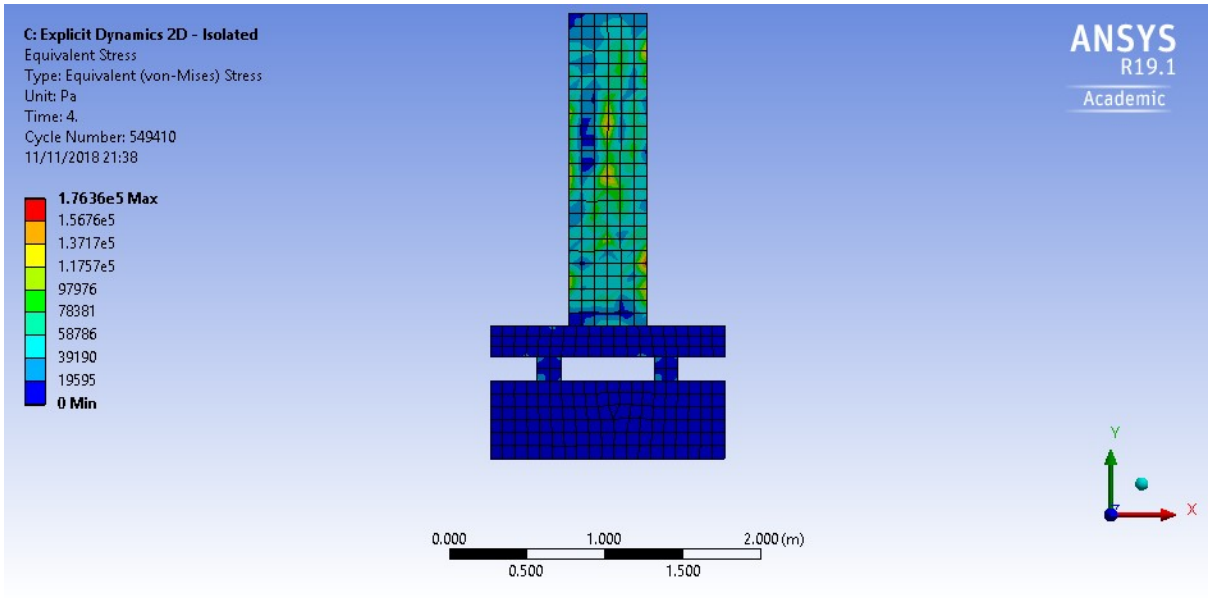

Figure 143 : Stress distribution (base-isolated T=2s , a =0.8 g)

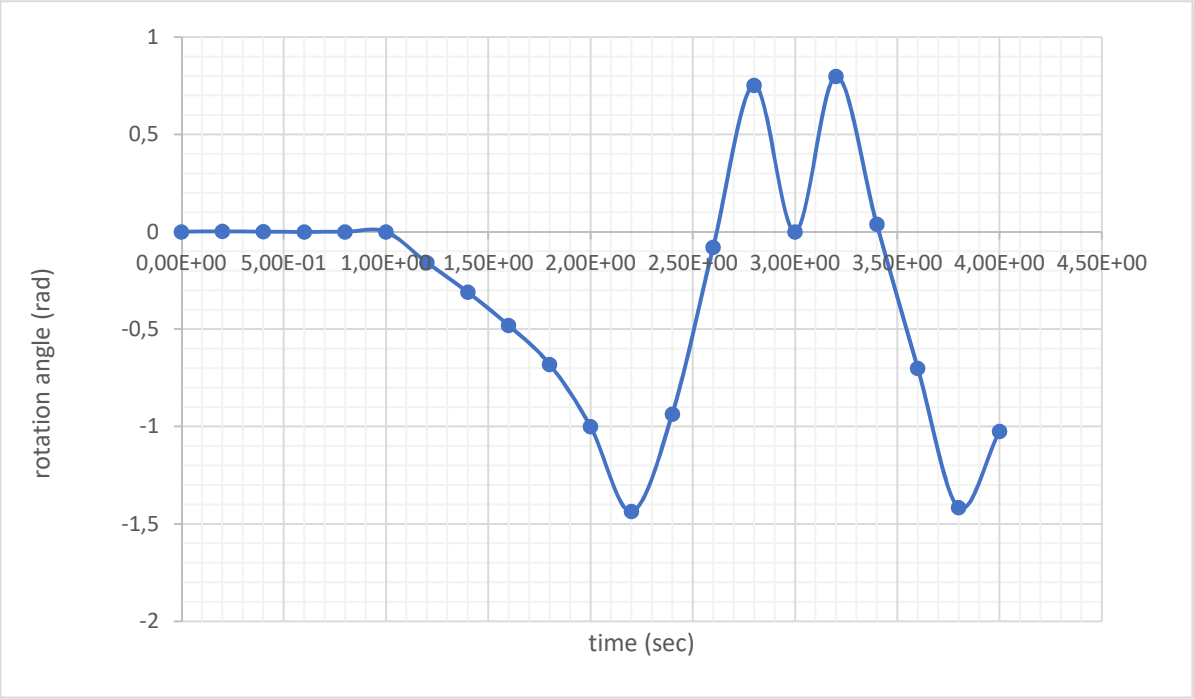

Figure 144: Rotation angle for simple column model (T=2s , a =0.8g)

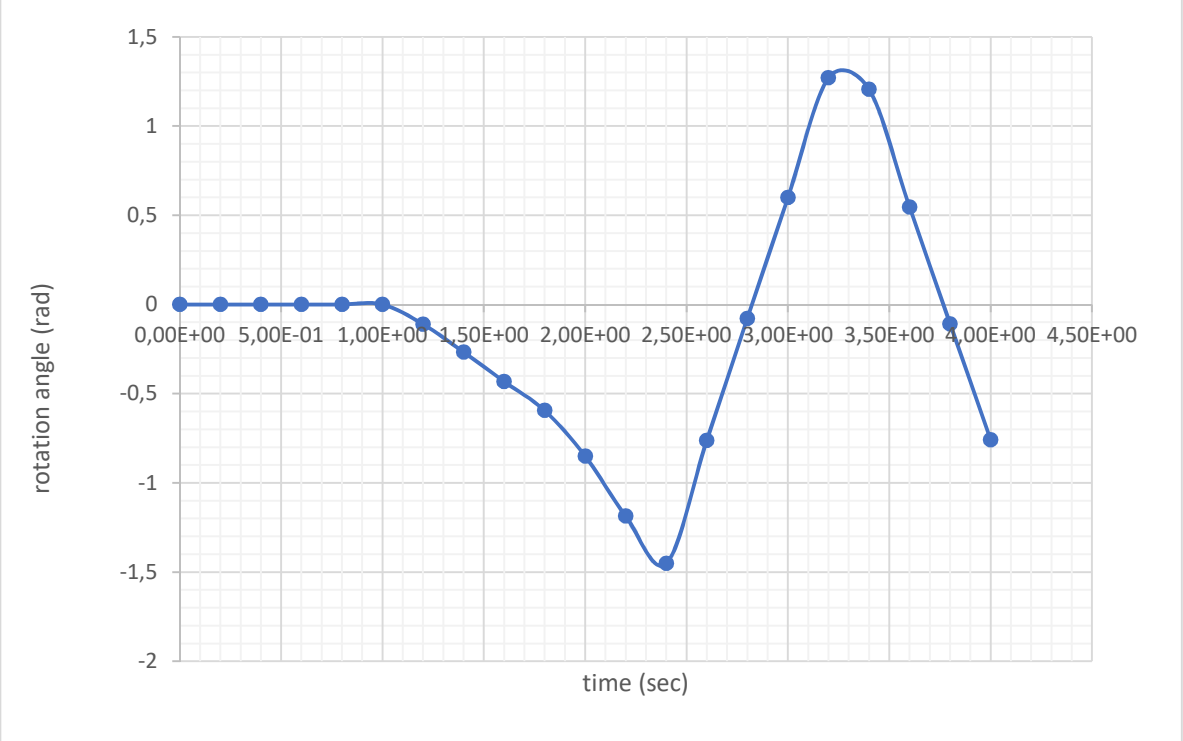

Figure 145: Rotation angle for base-isolated model (T=2s , a =0.8g)

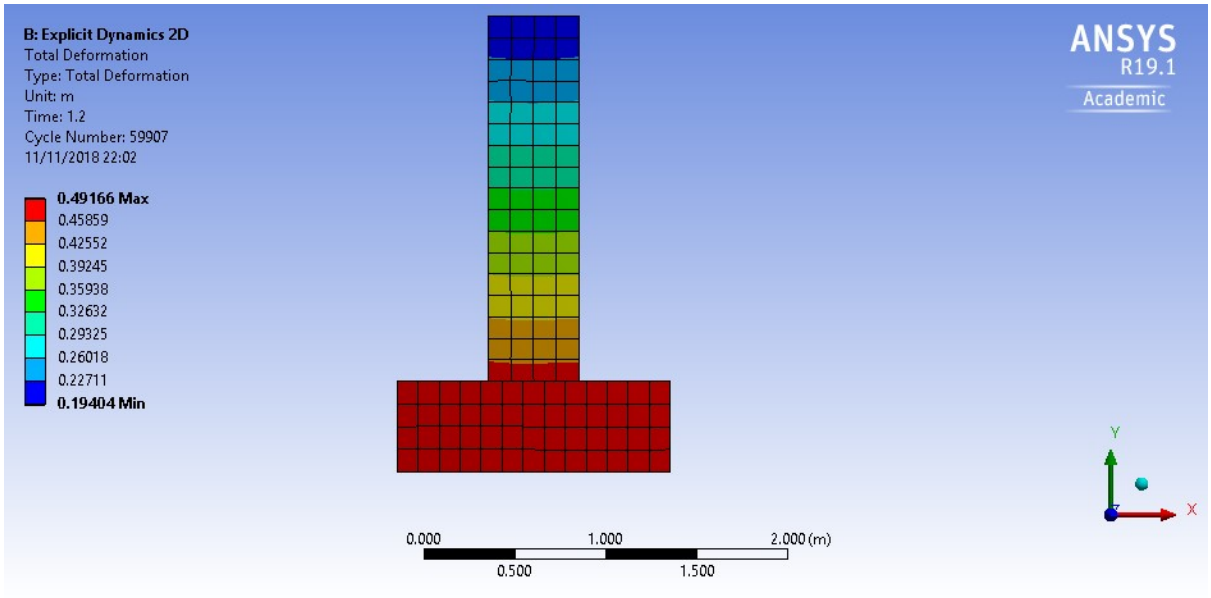

Figure 146 : Deformation (simple column T=2s , a =1.2 g)

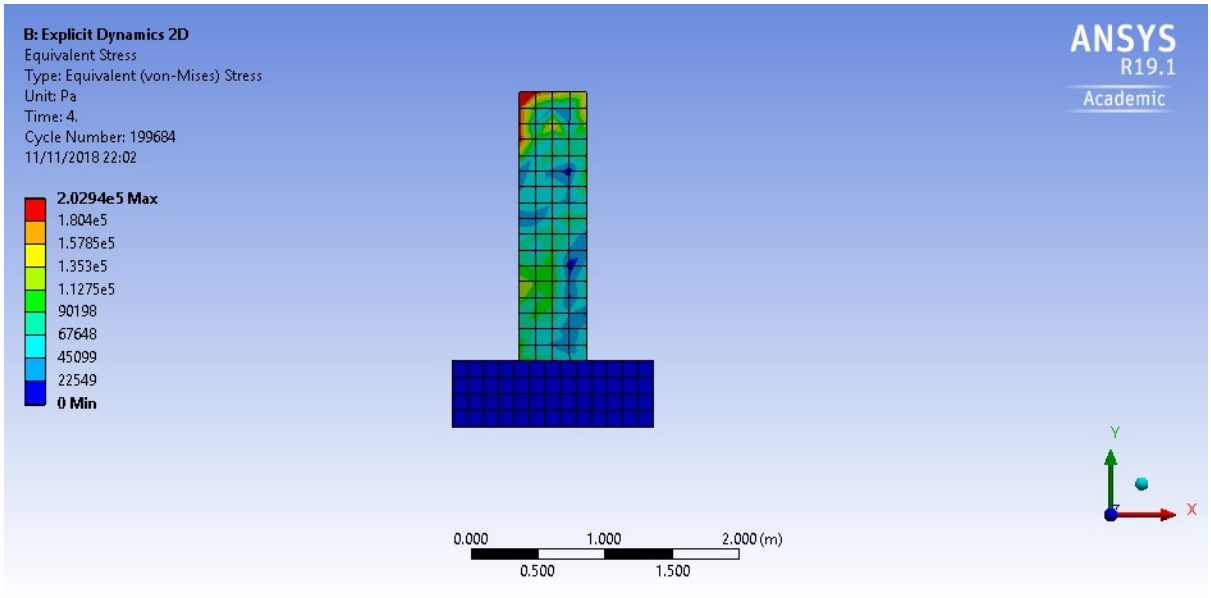

Figure 147: Stress distribution (simple column T=2s , a =1.2 g)

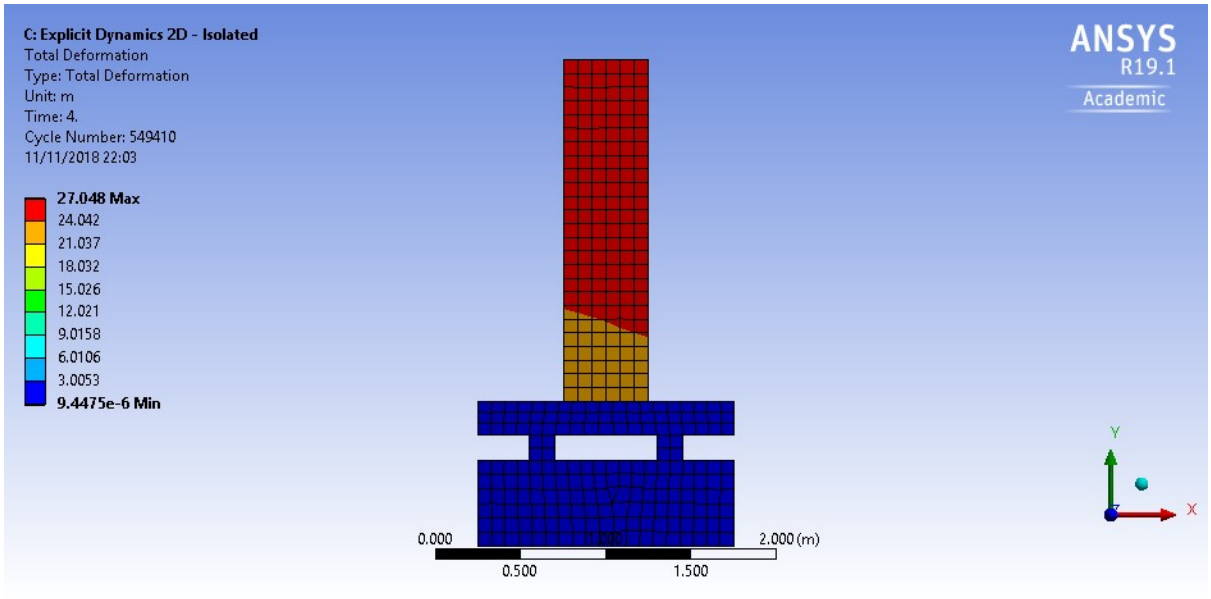

Figure 148: Deformation (base-isolated T=2s , a =1.2 g)

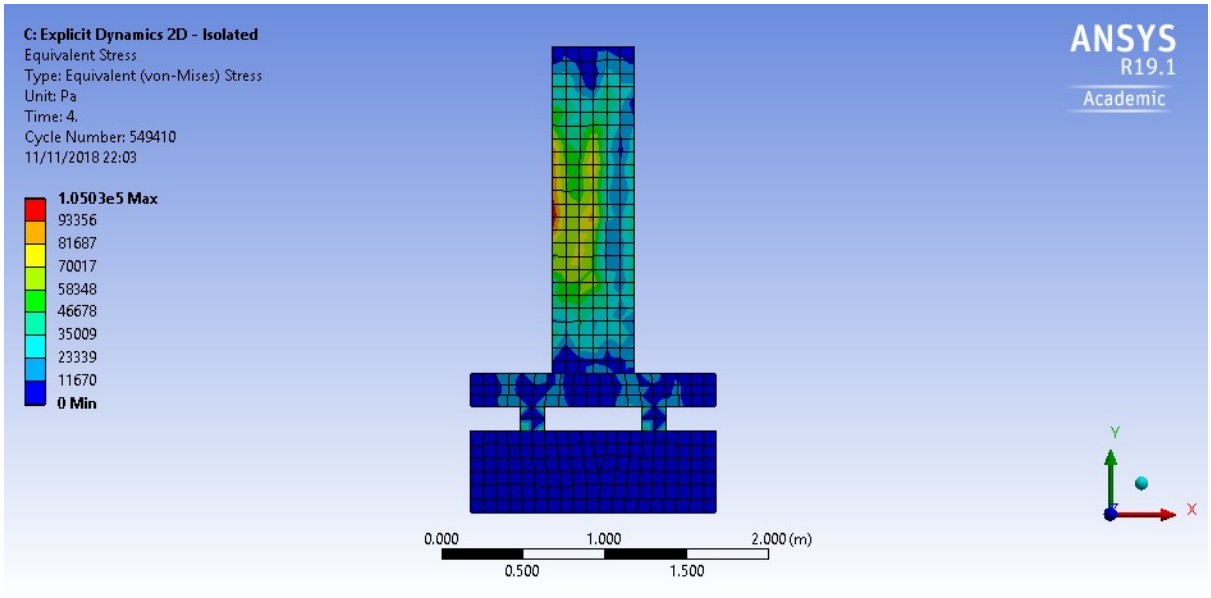

Figure 149: Stress distribution (base-isolated T=2s , a =1.2 g)

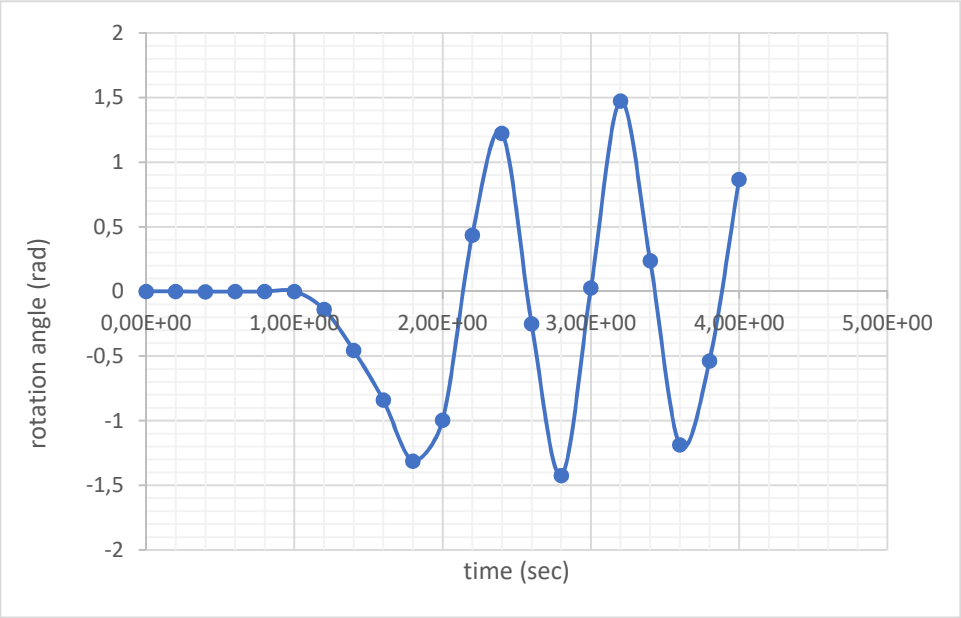

Figure 150 : Rotation angle for simple column model (T=2s , a =1.2g)

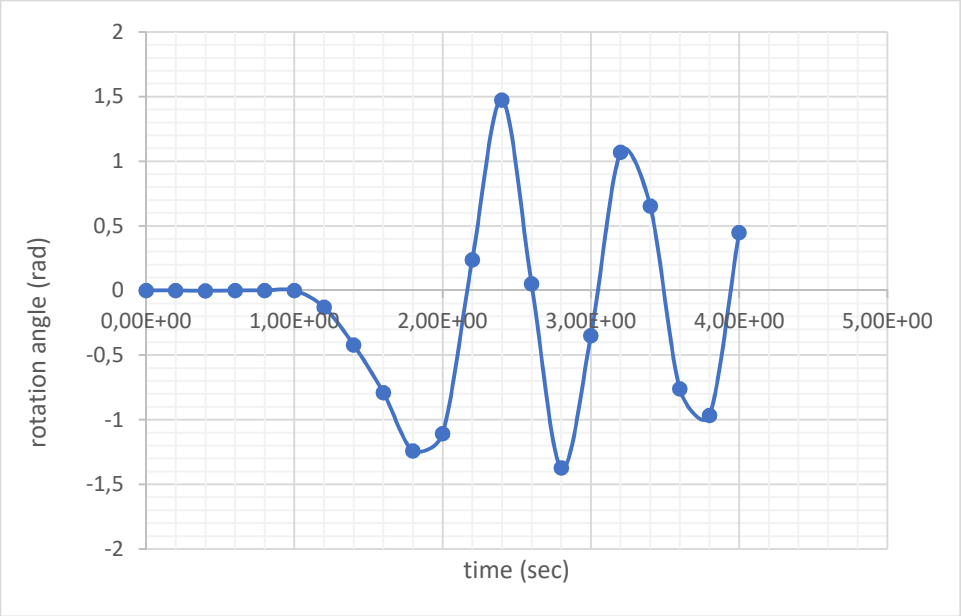

Figure 151: Rotation angle for base-isolated model (T=2s , a =1.2g)

1.4 Conclusion

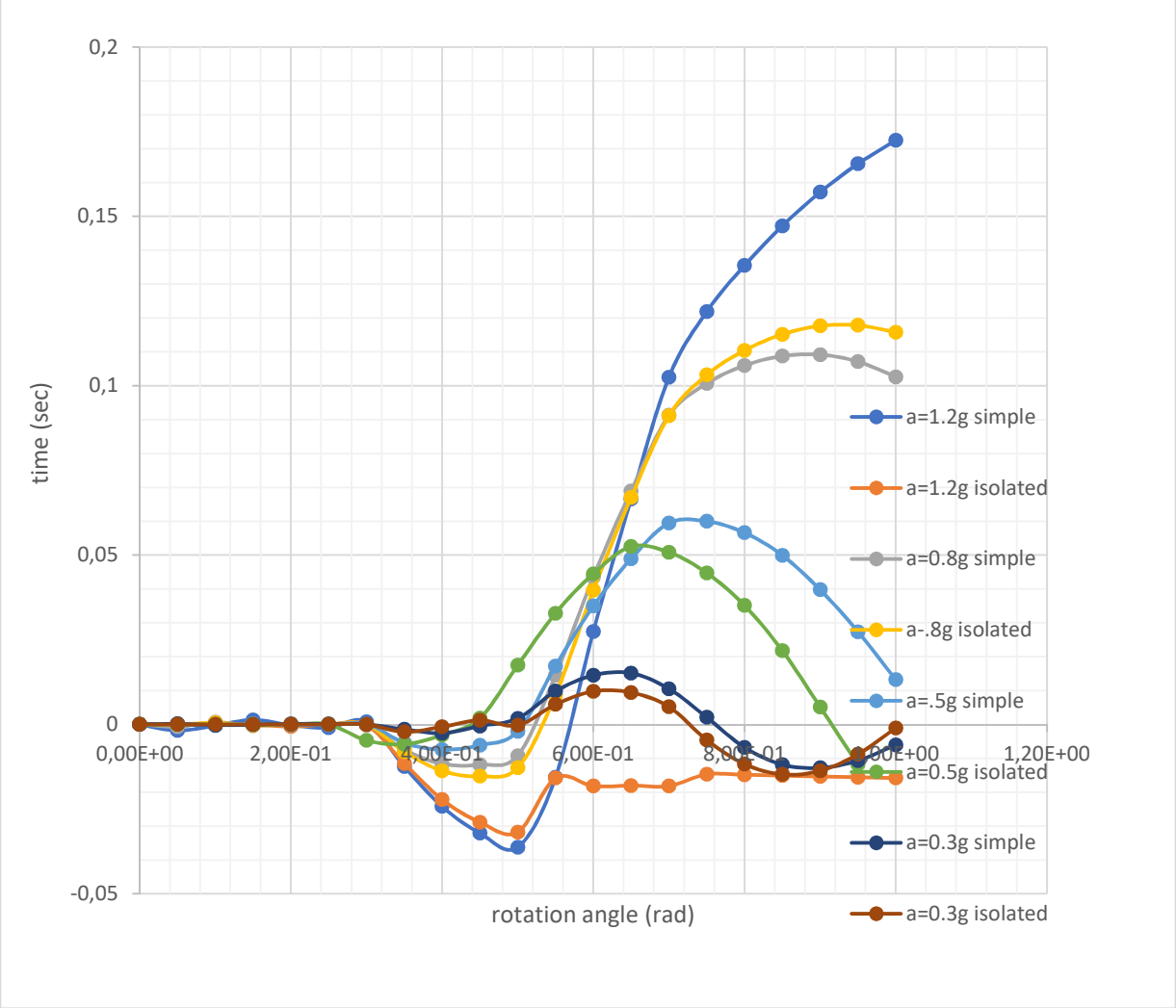

Figure 152: Rotation angles for T=0.5sec

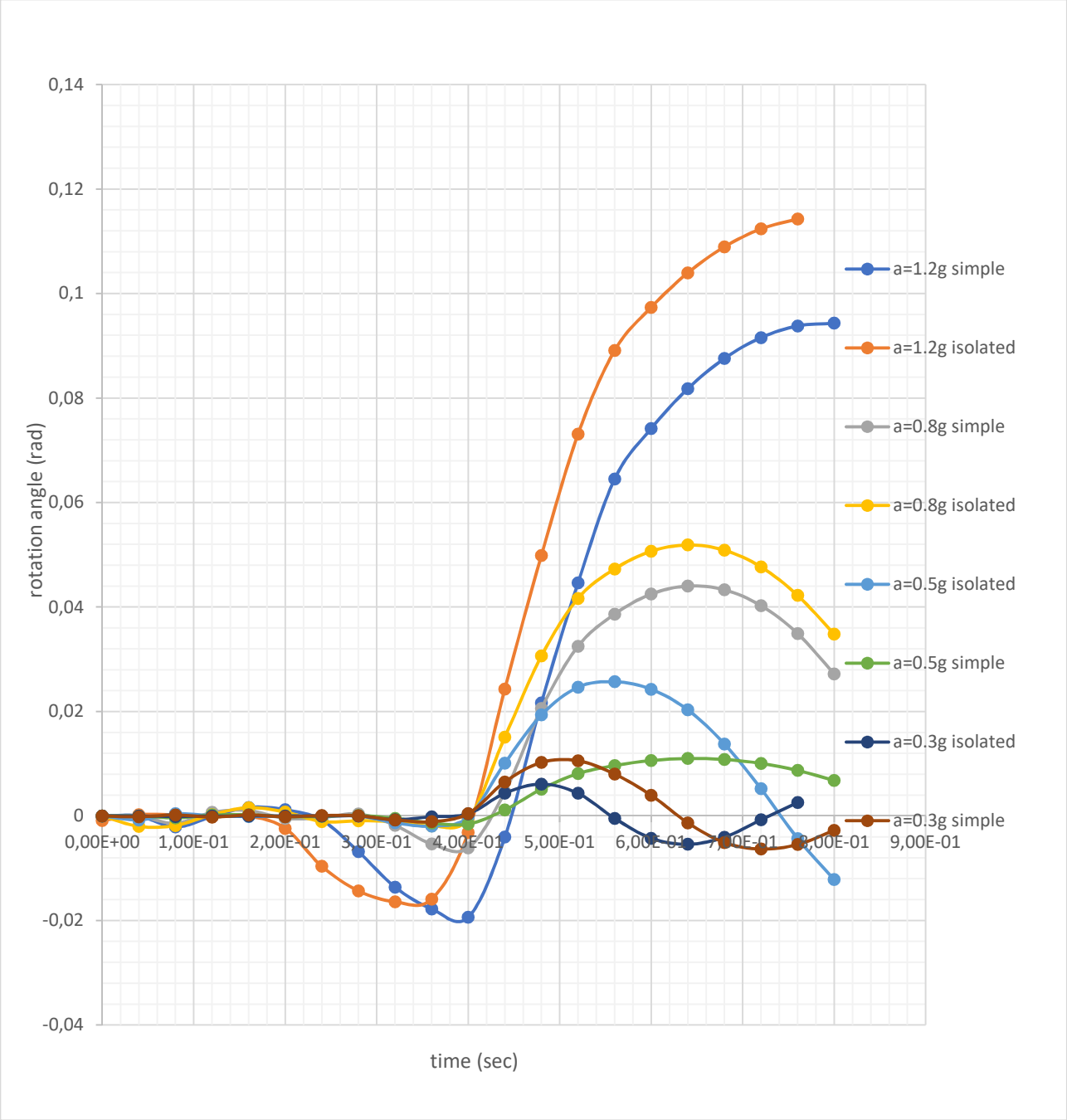

Figure 153: Rotation angles for T=0.4sec

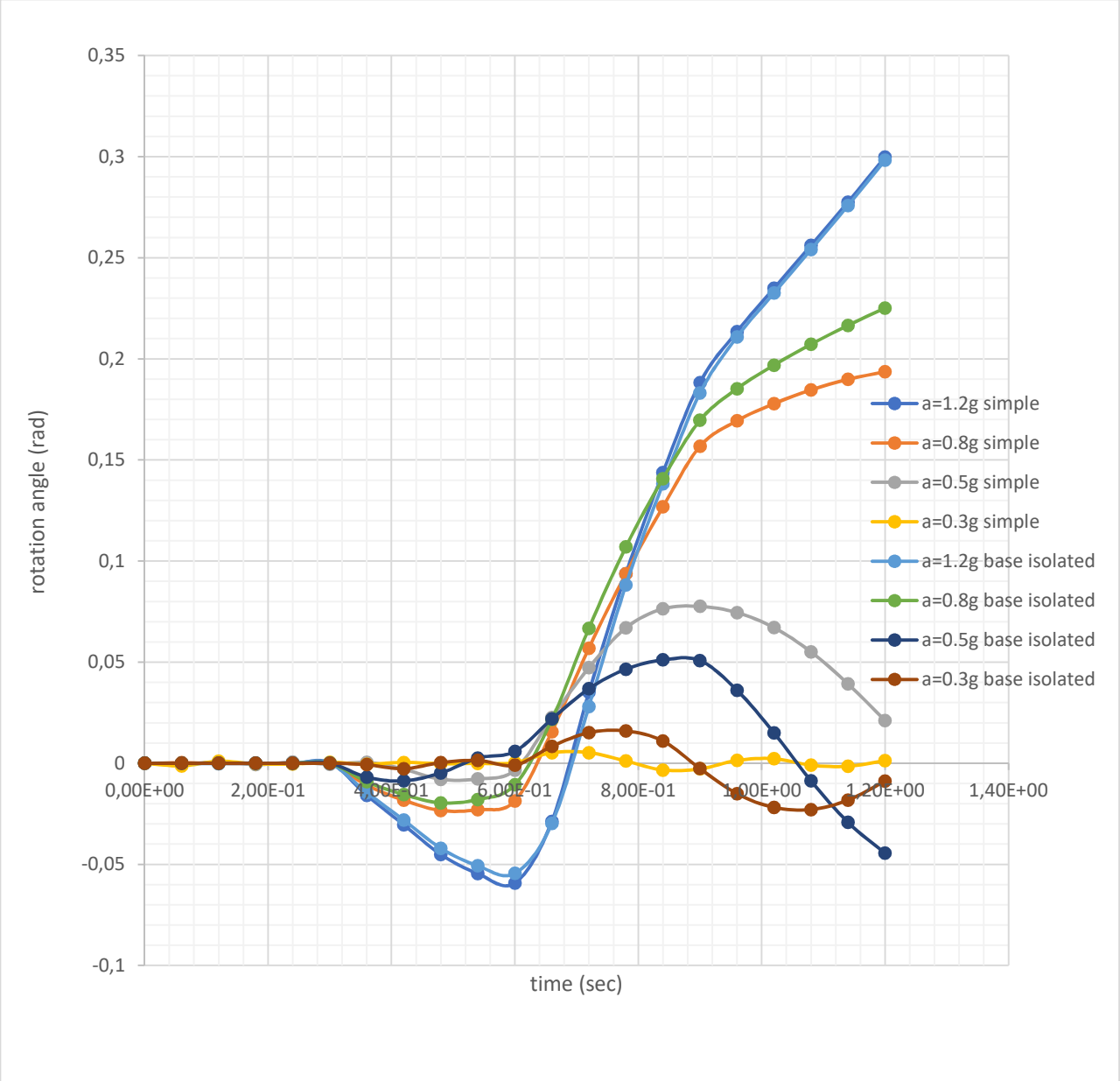

Figure 154: Rotation angles for T=0.6 sec

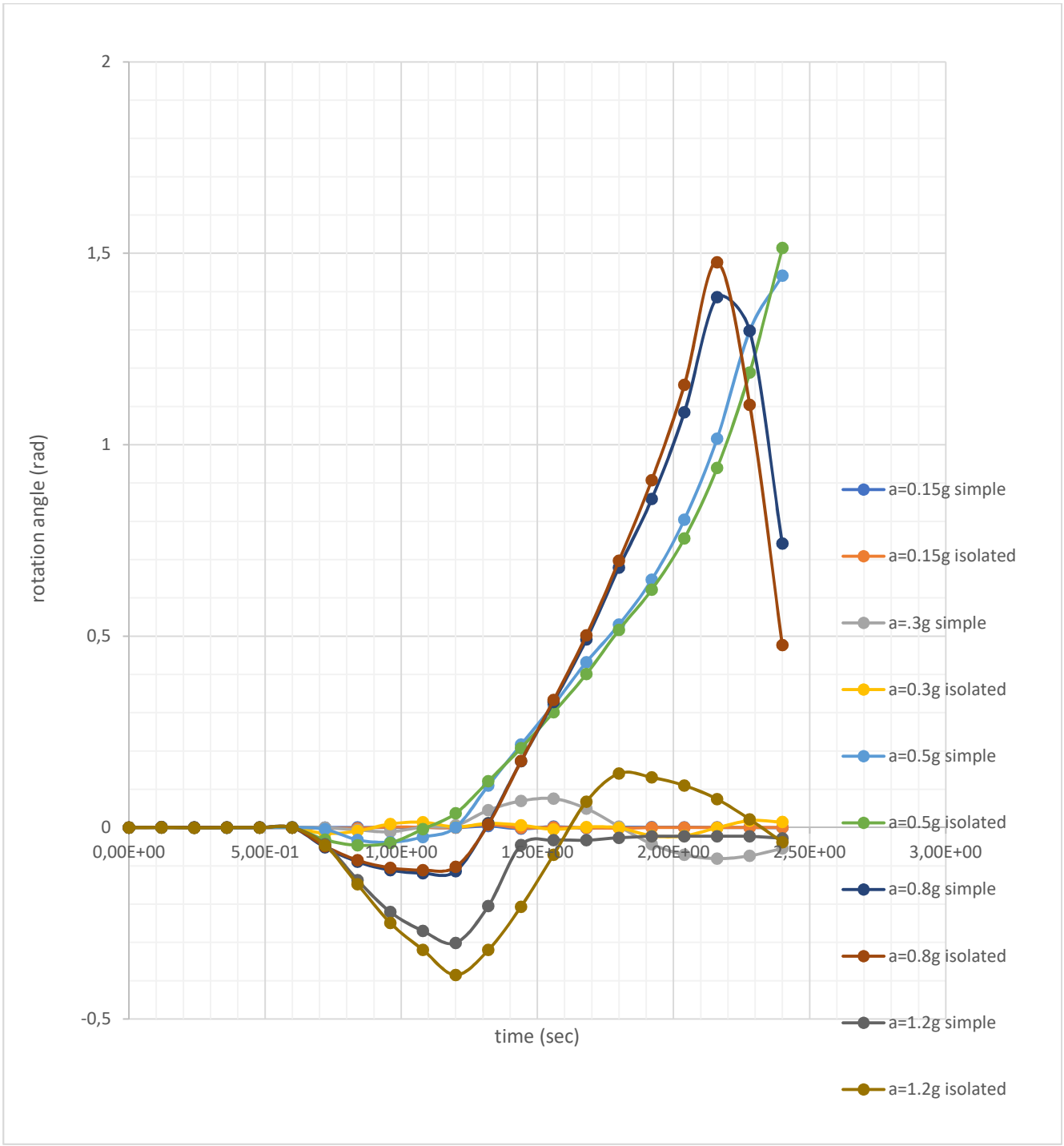

Figure 155: Rotation angles for T=1.2 sec

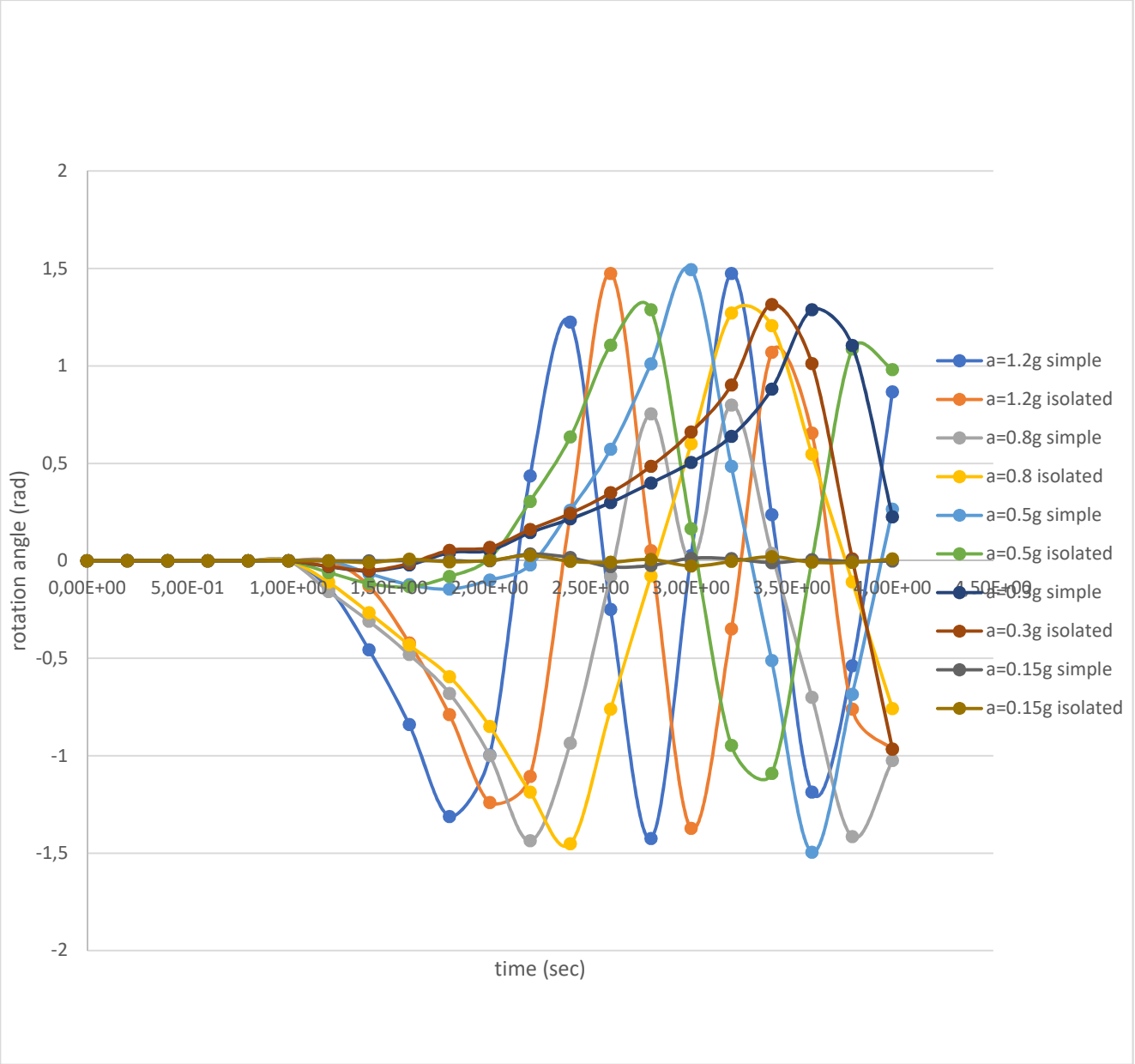

Figure 156: Rotation angles for T=2 sec

To conclude, the base isolated model had better response and smaller displacement for small values of acceleration. As it concerns higher values of acceleration the response of the two models did not show significant difference. Depending on the period T, for smaller values of T, the base isolated model showed higher angle of rotation (figure 153) while the base isolated model for the same values of base acceleration and higher values of T, showed smaller angle of rotation (figure 154).The simple column model showed better response for very high acceleration values while for very small values of acceleration the two models showed similar response. In the meantime, for high base acceleration and period values the response of model with the isolators is sifted forward (figure 156).

Overall, the simple column model displays better response for high acceleration rates while the base isolated model responds better in low acceleration rates. As the period increases the model with the base isolators shows smaller rotation angles for a broader range of base acceleration. Furthermore, the base isolators absorb most of the vibration at small acceleration rates as it is illustrated in the stress contour figures. The higher the base acceleration, the lower the stress at the isolators. When the base acceleration increases, maximum stress rates sift in the upper structure indicating that the excitation pulse was too tense that did not let the isolators absorb the shock. The longer the time period of the excitation, the better the response of the base isolated model at low acceleration rates.